LEVEL II

RADC-TR-79-149
Final Technical Report
June 1979

INFRARED LASER WINDOW COATING BY PLASMA POLYMERIZATION

University of California

AD A075008

DDC
RECEIVED
OCT 12 1979
E

Sponsored by
Defense Advanced Research Projects Agency (DoD)
ARPA Order No. 2415

APPROVED FOR PUBLIC RELEASE; DISTRIBUTION UNLIMITED

The views and conclusions contained in this document are those of the authors and should not be interpreted as necessarily representing the official policies, either expressed or implied, of the Defense Advanced Research Projects Agency or the U.S. Government.

DDC FILE COPY

ROME AIR DEVELOPMENT CENTER
Air Force Systems Command
Griffiss Air Force Base, New York 13441

79 10 12 007

This report has been reviewed by the RADC Information Office (OI) and is releasable to the National Technical Information Service (NTIS). At NTIS it will be releasable to the general public, including foreign nations.

RADC-TR-79-149 has been reviewed and is approved for publication.

APPROVED: Alexandar Golubovic

ALEXANDAR GOLUBOVIC
Project Engineer

If your address has changed or if you wish to be removed from the RADC mailing list, or if the addressee is not longer employed by your organization, please notify RADC (ESE), Hanscom AFB MA 01731. This will assist us in maintaining a current mailing list.

Do not return this copy. Retain or destroy.

(12)

INFRARED LASER WINDOW COATING BY PLASMA POLYMERIZATION

M. Shen

Contractor: Regents of the University of California
Contract Number: F19628-75-C-0097
Effective Date of Contract: 1 May 75
Contract Expiration Date: 31 Nov 78
Short Title of Work: Infrared Laser Window Coating by Plasma Polymerization
Program Code Number: 7D10
Period of Work Covered: Mar 75 - Aug 78

Principal Investigator: M. Shen
Phone: 415 642-2111

Project Engineer: Dr. Alexandar Golubovic
Phone: 617 861-2326

DDC
RECEIVED
OCT 15 1979
E

Approved for public release; distribution unlimited.

This research was supported by the Defense Advanced Research Projects Agency of the Department of Defense and was monitored by Dr. Alexandar Golubovic, ESE, Hanscom AFB MA 01731 under Contract F19628-75-C-0097.

UNCLASSIFIED

SECURITY CLASSIFICATION OF THIS PAGE (When Data Entered)

REPORT DOCUMENTATION PAGE

READ INSTRUCTIONS BEFORE COMPLETING FORM

1. REPORT NUMBER: RADC-TR-79-149	2. GOVT ACCESSION NO.
3. RECIPIENT'S CATALOG NUMBER	
4. TITLE (and Subtitle): INFRARED LASER WINDOW COATING BY PLASMA POLYMERIZATION,	5. TYPE OF REPORT & PERIOD COVERED: Final Technical Report. 1 Mar 75 — 31 Aug 78.
6. PERFORMING ORG. REPORT NUMBER: N/A	
7. AUTHOR(s): M. Shen	8. CONTRACT OR GRANT NUMBER(s): F19628-75-C-0097, ARPA Order-2415
9. PERFORMING ORGANIZATION NAME AND ADDRESS: The Regents of the University of California, Campus Research Office, M-11 Wheeler Hall, Berkeley, Alameda County CA 94720	10. PROGRAM ELEMENT, PROJECT, TASK AREA & WORK UNIT NUMBERS: 61101E, 2415ARAF, AK
11. CONTROLLING OFFICE NAME AND ADDRESS: Defense Advanced Research Projects Agency, 1400 Wilson Blvd, Arlington VA 22209	12. REPORT DATE: June 1979
	13. NUMBER OF PAGES: 117
14. MONITORING AGENCY NAME & ADDRESS (if different from Controlling Office): Deputy for Electronic Technology (RADC/ESE), Hanscom AFB MA 01731	15. SECURITY CLASS. (of this report): UNCLASSIFIED
	15a. DECLASSIFICATION/DOWNGRADING SCHEDULE: N/A

16. DISTRIBUTION STATEMENT (of this Report)

Approved for public release; distribution unlimited.

17. DISTRIBUTION STATEMENT (of the abstract entered in Block 20, if different from Report)

Same

18. SUPPLEMENTARY NOTES

RADC Project Engineer: Dr. Alexandar Golubovic (RADC/ESE)

19. KEY WORDS (Continue on reverse side if necessary and identify by block number)

The objective of the program on

20. ABSTRACT (Continue on reverse side if necessary and identify by block number)

This is the final report on the DARPA contract No. 19628-75-C-0097 on Infrared Laser Window Coating by Plasma Polymerization terminated on August 31, 1978. The objective of this program was to prepare protective and anti-reflection coatings for infrared laser windows by depositing a thin film from the hydrocarbon plasma. ~~In the Introduction Section of this report, we have outlined~~ outlines the state-of-the-art knowledge of plasma polymerization and the rationale of ~~our~~ this approach. ~~In the next section,~~ the details of plasma polymerization of (Cont'd)

DD FORM 1 JAN 73 1473

UNCLASSIFIED

SECURITY CLASSIFICATION OF THIS PAGE (When Data Entered)

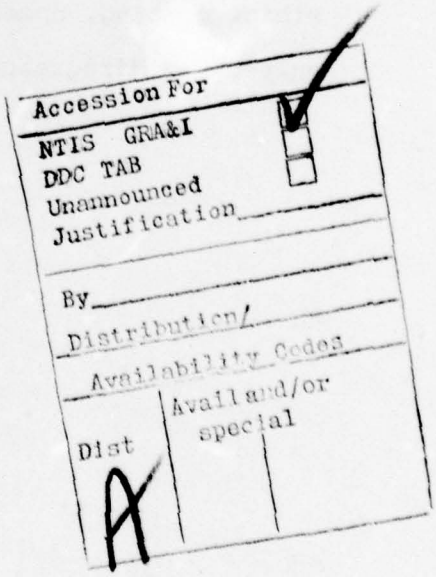
071850

Item 20 (Cont'd)

several simple saturated hydrocarbons were investigated. Here the radio-frequency glow discharge method was used as the method of generating plasma. We then investigate the effect of changing the frequency of the plasma on one of the most promising monomers, i.e., ethane. Finally, the preferred method of preparing laser window coating, namely the plasma polymerization of ethane using pulsed radiofrequency plasma.

TABLE OF CONTENTS

Section		Page
I.	Program Summary	4
II.	Introduction	5
III.	Plasma Polymerization of Saturated Hydrocarbons	22
IV.	Effect of Frequency on the Plasma Polymerization of Ethane	42
V.	Plasma Polymerization in Pulsed Discharge	61



Program Summary

This is the final report on the DARPA contract No. F19628-25-0097 on Infrared Laser Window Coating by Plasma Polymerization terminated on August 31, 1978. The objective of this program was to prepare protective and anti-reflection coatings for infrared laser windows by depositing a thin film from the hydrocarbon plasma. In the Introduction Section of this report, we have outlined the state-of-the-art knowledge of plasma polymerization and the rationale of our approach. In the next section, the details of plasma polymerization of several simple saturated hydrocarbons were investigated. Here the radiofrequency glow discharge method was used as the method of generating plasma. We then investigate the effect of changing the frequency of the plasma on one of the most promising monomers, i.e., ethane. Finally, the preferred method of preparing laser window coating, namely the plasma polymerization of ethane using pulsed radiofrequency plasma.

SECTION II

Introduction

Introduction

Polymerization in a low pressure electric discharge has been known for over a century(1-8). A variety of organic and organometallic compounds have been prepared in this way since then(9,10). A gaseous monomer at low pressure subjected to an alternating electric field at high frequency and with sufficient energy produces a glow discharge plasma. The active species in the plasma deposit on the substrate a highly cross-linked(11) polymer film that retains an abundance of radical sites(12) in a film matrix structure(13). Thus, the name plasma-polymerization.

The mechanisms for the formation of glow discharge polymers are complex, and many have discussed this topic (14-23). Some of the more important possible reaction mechanisms are shown in Figure 1. Basically, bond scission via the electric field occurs, and monomer molecules are variously dissociated into free radicals, ions and atoms. Excited nondissociated species are also produced that may indirectly contribute to the polymerization. Free radicals are considered to be the predominant active species in the plasma. The bond scission is essentially the initiation step in the overall polymerization, and produces the active species reacting among themselves and with monomer molecules to produce oligomers and oligomeric free radicals. Nucleation of the oligomers in the gas phase or on the substrate results in continuing polymerization. Termination is not complete since the trapped free radical species formed (24-26) are scattered throughout

Gas Phase Reactions

(Initiation)

1.) $e + M \longrightarrow M' + H_2 + e$

2.) $e + M \longrightarrow M' + 2H\cdot + e$

3.) $e + M \longrightarrow 2R + e$

4.) $e + H_2 \longrightarrow 2H\cdot + e$

M = saturated monomer

M'= unsaturated monomer

(Propagation)

5.) $H\cdot + M' \longrightarrow R$

6.) $H\cdot + M \longrightarrow R + H_2$

7.) $R_n + M \longrightarrow P + R$

8.) $R_n + M' \longrightarrow R_{n+1}$

R = free radical

R can contain unsaturation.

P = polymer molecule

n = integer

Surface Reactions

(Adsorption)

9.) $S + M \longrightarrow M\text{----}S$

10.) $S + M' \longrightarrow M'\text{---}S$

11.) $S + H\cdot \longrightarrow H\cdot\text{---}S$

12.) $S + R_n \longrightarrow R_n\text{---}S$

S = surface site

(Propagation)

13.) $R_n\text{---}S + M \longrightarrow P\text{---}S + R$

14.) $R_n\text{---}S + M' \longrightarrow R_{n+1}\text{---}S$

15.) $R_n\text{---}S + M\text{---}S \longrightarrow P\text{---}S + R\text{---}S$

16.) $R_n\text{---}S + M'\text{---}S \longrightarrow R_{n+1}\text{---}S$

17.) $H\cdot\text{---}S + H\cdot \longrightarrow H_2$

Figure 1. Some of the important possible reaction mechanisms in plasma-polymerization. (Termination reactions not shown).

the highly crosslinked, tight film matrix structure, and cannot migrate easily to terminate each other. In principle, any monomer, saturated or unsaturated, can be polymerized by this method. This is the unique feature of plasma-polymerization.

Some of the system variables (27) to consider in plasma polymerization are:

1. Monomer flow rate;
2. Total system pressure;
3. Electrode gap;
4. Power delivered to the electrodes;
5. Frequency;
6. Electrode surface temperature during polymerization; and
7. Composition of gas entering the reaction zone.

The system variables are either determined arbitrarily, by the design of the reactor and electrode temperature control system, or by the supporting equipment.

There are, of course, numerous applications (28) for these films. Dielectrics in thin film capacitors used in micro-electronic devices, the production and improvement of hyper-filtration membranes (29), laser lightguides, and protective coatings for such things as prosthetic devices, implantable biosensors, and alkali halide optics.

These films can be made uniform and extremely thin, and at the same time are pinhole free, which results from increased deposition at a hole or thin spot in the film. The increased deposition results from a smaller capacitive effect at that point, producing a stronger electric field, and subsequently,

increased deposition via increased polymerization rate.

The motivation for this research is to produce a uniform, moisture resistant, plasma-polymerized film that has high infrared transparency at designated wavelengths. The films are to protect alkali halide crystals from attack by atmospheric moisture. Good film adhesion and a matched refractive index with the crystal are also desired. The alkali halide optical crystals are to be used as cell windows on laser equipment.

In order to produce a highly uniform film a tubular plasma-polymerization flow reactor was designed and built that would produce a laminar flow proceeding into the reaction zone where the deposition occurs (see Figure 8). The laminar flow should produce a more uniform film than a non-laminar flow such as exists in a bell jar reactor with a more complex flow configuration. The design and construction of the flow reactor is discussed more completely later. The requirement that the film has a thickness variation no greater than one-quarter of the wavelength of the infrared (IR) radiation being transmitted is fulfilled by this flow reactor as shown later when the film thickness variation studies are discussed. The IR spectra of various polymers formed from hydrocarbon vapors has been discussed by others (30,31). Since the flow reactor is a new design, and not made of glass as are most plasma-polymerization reactors, a large part of the research is dedicated to its characterization.

The preparation of inorganic thin films by glow discharge deposition for various purposes has been investigated (32-35).

These films do not exhibit the IR transparency at the wavelengths of interest, and therefore were not considered in this research.

The film must provide the high IR transparency at 10.6μ and anywhere in the 3μ to 5μ region. Transmittance must exceed 99.99% at 10.6μ. The minimum thickness variation from the specification given earlier to provide the desired film uniformity can be calculated at the shortest wavelength radiation (3μ) to be used. The calculation (3μ x 1/4 = 0.75μ) shows that three-quarters of a micron is the minimum film thickness variation permitted. A similar calculation (10.6μ x 1/4 = 2.65μ) at the longest wavelength radiation (10.6μ) to be used shows that 2.65μ is the maximum film thickness variation permitted.

In order to fulfill the IR transparency requirement, ethane was chosen as the monomer that was to be used to deposit the films in the flow reactor. Ethane represents one of the simplest saturated molecules that had previously been plasma-polymerized to form good films (36). Ethylene monomer, which has a higher deposition rate because of its unsaturation, yields a film with stronger IR absorption at 10.6μ as shown in Figure 3 (37), compared to ethane as shown in Figure 2. Also, atmospheric exposure of films produced from ethylene increases the absorption at 10.6μ as shown in Figure 4 (37), compared to results of atmospheric exposure of ethane films done in studies by Akovali (38). Ethane provides the better IR transparency at 10.6μ (compare Figure 2 and 3).

Hollahan, Wydeven, and Johnson (39) deposited films from the monomers chlorotrifluoroethylene (CFTE) and tetrafluoro-

ethylene (TFE) on alkali halide crystal optics using a bell jar plasma-polymerization system as shown in Figure 5. This was one of the first successful uses of plasma polymerized films as protective coatings for crystal optics. Their choice of a fluorocarbon monomer arises from the known moisture resistance of fluorinated polymers. Their film provided a high degree of IR transparency in the 3μ to 5μ region as shown in Figure 6. But, their film showed strong IR absorption at 10.6μ from CF_2 stretching. The absorption near 6μ is probably from unsaturation produced in their film during deposition, and it is common to plasma-polymerized films. Plasma-polymerized ethane films also exhibit some absorption near 6μ as a result of unsaturation produced in the film during deposition (see Figure 2).

Hollahan, et al (39) found that a film about 1μ thick produced from fluorocarbon monomer provided good moisture protection for the crystals they employed when the film coated crystal was exposed to an environment of 88% relative humidity (RH) for a little more than 100 hours. Moisture resistance of optical films has been investigated and discussed by others (40-44). The moisture resistance of plasma-polymerized ethane films using similar exposure conditions is investigated and discussed later in this work.

A film with a refractive index intermediate between air and the substrate material will provide increased transmittance for radiation passing from the substrate through the film into the air. Proper matching of refractive indices will reduce

energy loss due to reflection. The optimum refractive index for an antireflection coating on a cell window to be used in an air environment is given by the equation,

$$n_{film} = (n_{air} \quad n_{substrate})^{1/2},$$

where n = refractive index. The fluorinated polymer film discussed above was found to have a refractive index of 1.478 (39). The refractive indices of sodium chloride (NaCl), cesium iodide (CsI), and potassium chloride (KCl) are 1.544 1.787, and 1.490 respectively. The fluorinated polymer film is, therefore, antireflective on any of these three substrates. All these refractive indices were measured with the 5893Å sodium D-line as a source. Hiratsuka (45) found that the refractive index for plasma-polymerized ethane films was 1.51 using the 5893Å sodium D-line source, and is presently attempting to determine its value at the infrared wavelengths of interest. Ethane films are antireflecting for the NaCl and CsI crystals, but slightly reflecting for KCl crystals when using the sodium D-line as the source. At the infrared wavelengths this may not be the case, and the ethane films may exhibit stronger or weaker antireflection characteristics on these crystals.

Film adhesion is a complex subject that has been thoroughly studied and discussed (46-57). Adhesion of the plasma-polymerized ethane films to the alkali halide crystal surfaces is discussed later in this research.

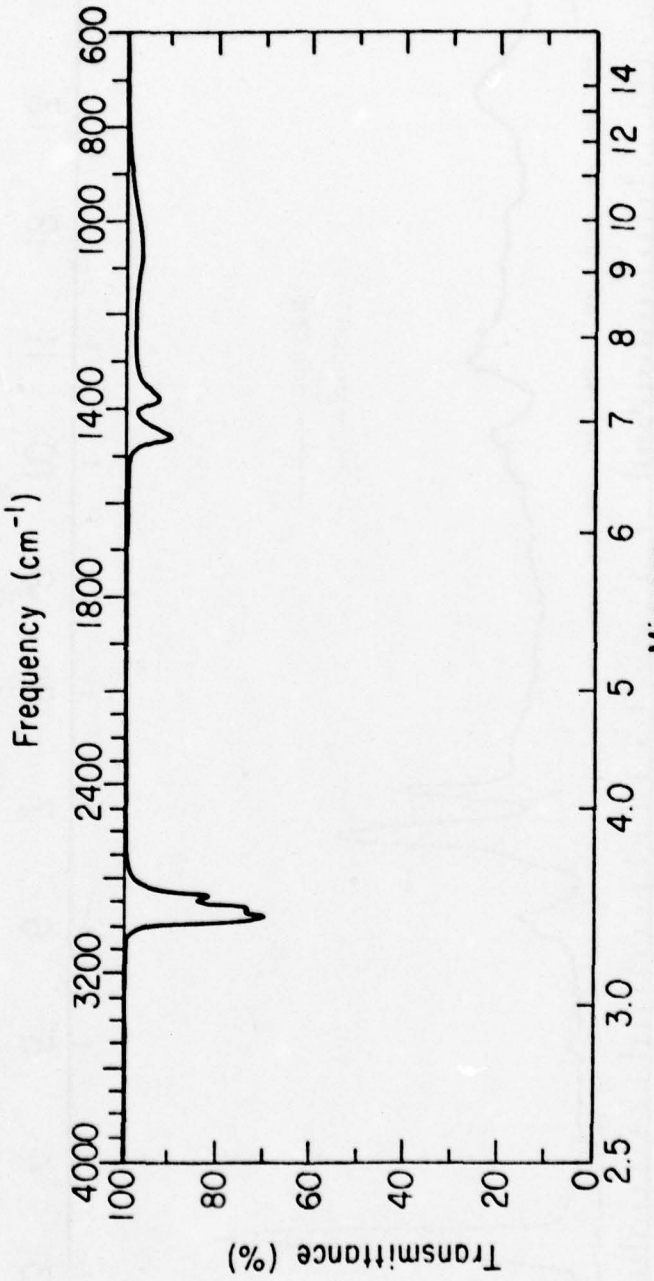


Figure 2. IR spectrum of plasma-polymerized ethane.

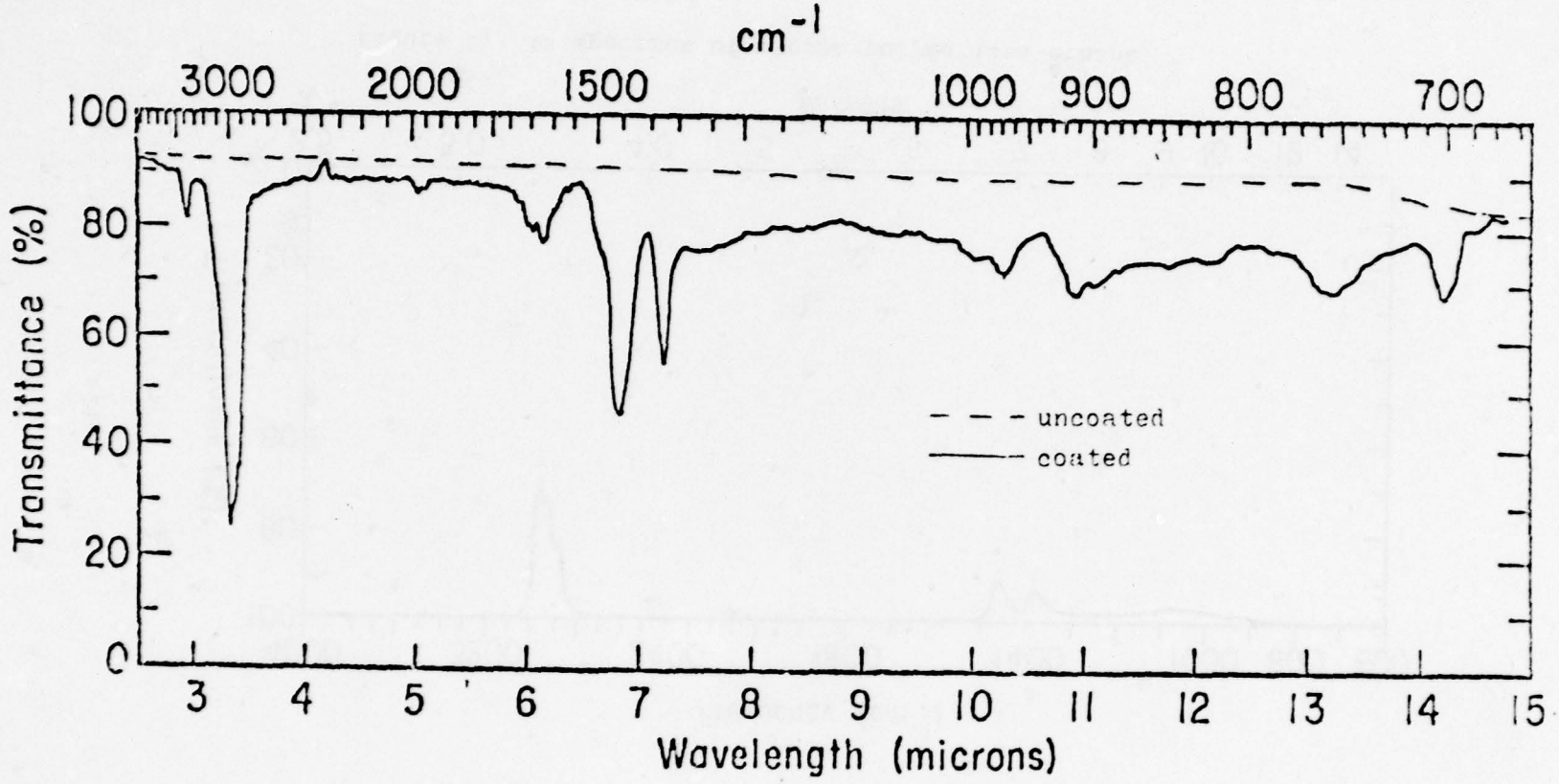


Figure 3. IR spectrum of plasma-polymerized ethylene on NaCl (37).

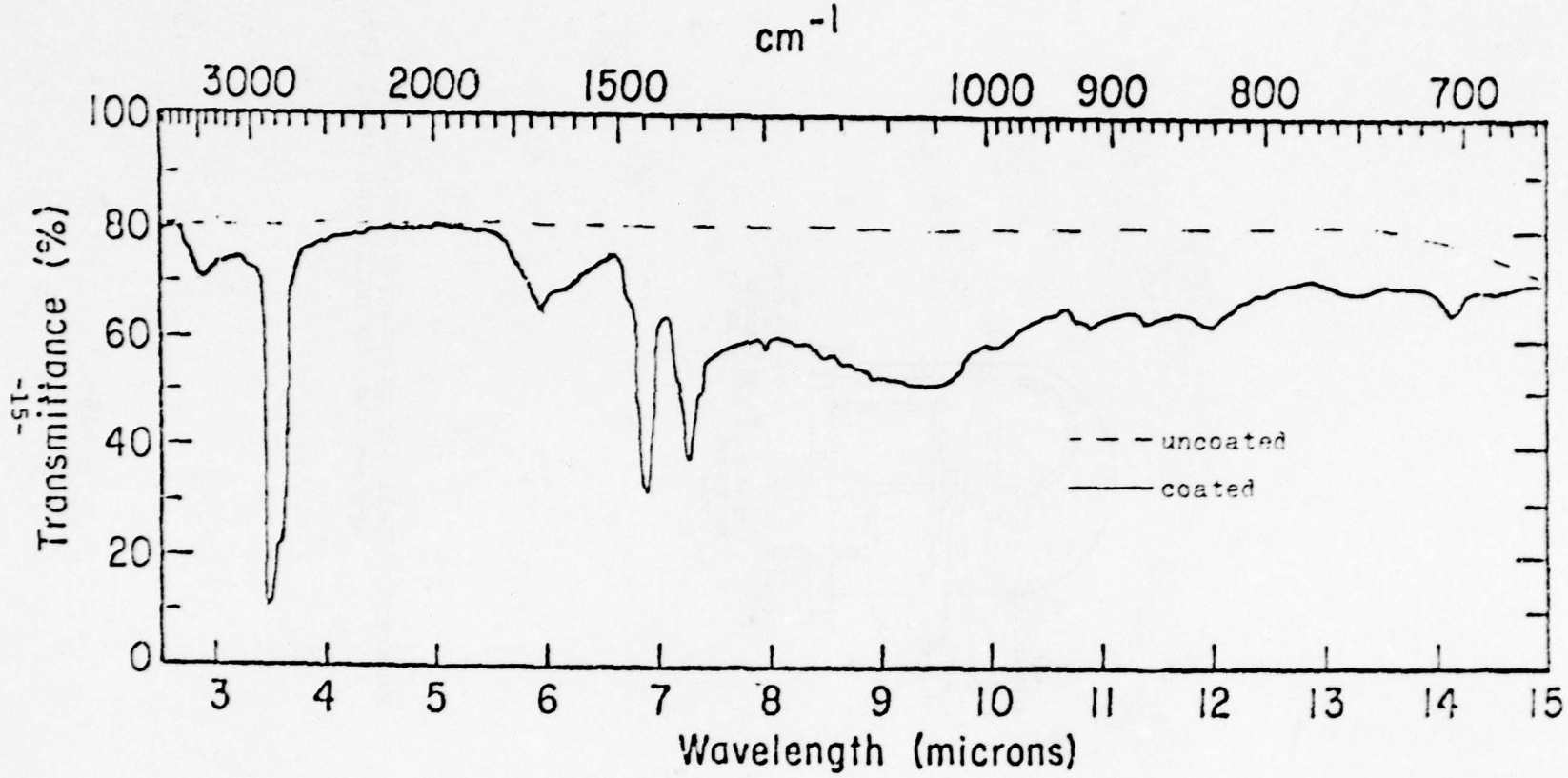


Figure 4. IR spectrum of plasma-polymerized ethylene coated NaCl after exposure to atmosphere for 30 days (37).

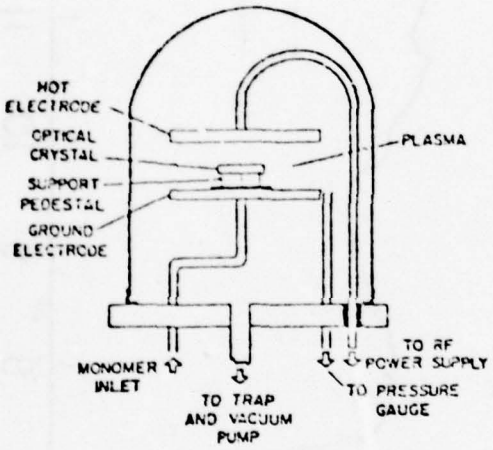


Figure 5. Bell jar plasma-polymerization system used by Hollahan, et al (39).

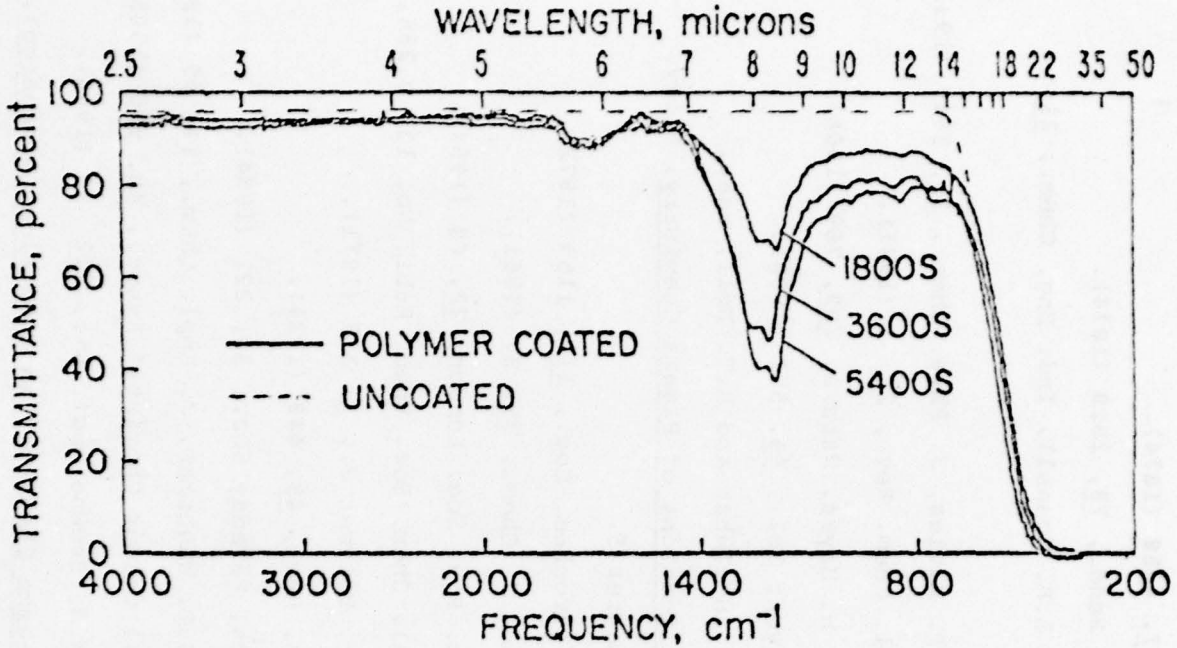


Figure 6. IR spectrum of plasma-polymerized CFTE obtained by Hollahan, et al (39).

Bibliography

1. P. DeWilde, Ber., 7, 4658 (1874).
2. A. Thenard, Compt. Rend., 78, 2919 (1874).
3. C.S. Schoepfle and L.H. Connell, Ind. Eng. Chem., 21, 529 (1929).
4. E.G. Linder and A.P. Davies, J. Phys. Chem., 35, 3649 (1931).
5. C.L. Thomas, et al, Chem. Rev., 28, 1 (1941).
6. T. Williams and M. W. Hayes, Nature, 209, 769 (1966).
7. J. Goodman, J. Polymer Sci., 44, 551 (1960).
8. M. Millard, in J.R. Hollahan and A.T. Bell, eds., Techniques and Applications of Plasma Chemistry, Wiley, New York, 1974, Chapter 5.
9. A. Bradley, J. Electrochem. Soc., 119, 1153 (1972).
10. A.W. Tickner, Canad. J. Chem., 39, 87 (1961).
11. A. Charlesby, Proc. Roy. Soc. London, 22, 60 (1954).
12. C.M. Bamford, et al, Chem. Soc. Spec. Publ. No. 15, p.284.
13. A.R. Westwood, Eur. Polymer J., 7, 377 (1971).
14. R.L. Stewart, Phys. Rev., 45, 448 (1934).
15. W.D. Harkins, Trans. Faraday Soc., 30, 221 (1934).
16. F.J. Vastola and J.P. Wightman, J. Appl. Chem., 14, 69 (1964).
17. T. Williams, J. Oil Colour Chemists' Assoc., 48, 936 (1965).
18. J.A. Coffman and W.R. Browne, Sci. Am., 212, 96 (1965).
19. F.K. McTaggert, Plasma Chemistry in Electrical Discharges, Elsevier, New York, 1967, p. 197.
20. L.V. Gregor, IBM J. Res. Dev., 12, 145 (1968).
21. A.R. Westwood, Eur. Polymer J., 7, 363 (1971).

22. K.C. Brown, Eur. Polymer J., 8, 117 (1972).

23. A.R. Denaro, P.A. Owens, and A. Crawshaw, Eur. Polymer J., 4, 93 (1968).

24. L.A. Wall and D.W. Brown, J. Research Natl. Bur. Standards, 57, 131 (1956).

25. G.K. Fraenkel, et al, J. Am. Chem. Soc., 76, 3606 (1954).

26. J.C. Bevington and D.E. Eaves, Nature, 178, 1112 (1956).

27. R.M. Brick and J.R. Knox, Modern Packaging, 123 (1965).

28. A. Bradley, Ind. Eng. Chem. Prod. Res. Dev., 9, 101 (1970).

29. T. Wydeven and J.R. Hollahan, in J.R. Hollahan and A.T. Bell, eds., Techniques and Applications of Plasma Chemistry, Wiley, New York, 1974, Chapter 6.

30. K. Jesch, J.E. Bloor, and P.L. Kronick, J. Polym. Sci., A1, 4, 1487 (1966).

31. P.L. Kronick, K. Jesch, and J.E. Bloor, J. Polym. Sci., A1, 7, 767 (1966).

32. P.K. Tien, G. Smolinsky, and R.J. Martin, Appl. Opt., 11, 637 (1972).

33. L.L. Alt, S.W. Ing, and K.W. Laendle, J. Electrochem. Soc., 110, 465 (1963).

34. H.F. Sterling and R.C.G. Swann, Solid State Electronics, 8, 653 (1965).

35. H. Kato and Y. Koga, J. Electrochem. Soc., 118, 1619 (1971).

36. H. Kobayashi, Ph.D. Thesis, University of California, Berkeley, California (1974).

37. J.M. Tibbitt, A.T. Bell, and M. Shen, Proc. of the 5th Annual Conference on IR Laser Windows Materials, Air Force Cambridge Research Labs, Bedford, Massachusetts, 1976, p. 205.

38. G. Akovali, Personal Communication.

39. J.R. Hollahan, T. Wydeven, and C.C. Johnson, Appl. Opt., 13, 1844 (1974).

40. R.H. Hopkins, R.A. Hoffman, and W.E. Kramer, Appl. Opt., 14, 2631 (1975).

41. P.A. Young, Thin Solid Films, 6, 423 (1970).

42. C.A. Pitha, A. Armington, H. Posen, and B. Bendow, eds., Third Conference on High Power IR Laser Window Materials, Air Force Cambridge Research Labs, Bedford, Mass., 1974, AFCRL-TR-74-0085, I, II, III.

43. C.A. Pitha, ed., Proc. of the Conference on High Power IR Laser Window Materials, Air Force Cambridge Research Labs, Bedford, Mass., 1973, AFCRL-TR-73-0372, I, II.

44. C.S. Sahagian and C.A. Pitha, Eds., Proc. of the Conference on High Power IR Laser Window Materials, Air Force Cambridge Research Labs, Bedford, Mass., 1971, AFCRL-TR-71-0592.

45. H. Hiratsuka, Personal Communication.

46. J. Strong, Rev. Sci. Instru., 6, 97 (1935).

47. O.S. Heavens, J. de Physique et Radium, 11, 355 (1950).

48. P. Benjamin and C. Weaver, Proc. Roy. Soc., A254, 163 (1960).

49. P. Benjamin and C. Weaver, Proc. Roy. Soc., A254, 177 (1960).

50. P. Benjamin and C. Weaver, Proc. Roy. Soc., 261, 516 (1961).

51. P. Benjamin and C. Weaver, Proc. Roy. Soc., 263, 267 (1963).

52. D.S. Campbell, in Handbook of Thin Film Technology, L.I. Maissel and R. Glang, eds., McGraw-Hill, New York, 1969.

53. B.N. Chapman, Proc. of the 7th Conference on Adhesion and Adhesives, D.J. Alner, ed., Univ. London Press, 1969.

54. D.W. Butler, C.T.H. Stoddart, and P.R. Stuart, J. Phys., D3, 877 (1970).

55. J. Greene, J. Woodhouse, and M. Pestes, Rev. Sci. Instru., 45, 747 (1974).

56. M.L. Williams, J. Adhesion, 4, 307 (1972).

57. K. Kendall, J. Phys. D. Appl. Phys., 6, 1782 (1973).

SECTION III

Plasma Polymerization of Saturated Hydrocarbons

INTRODUCTION

In conventional polymerization reactions, the presence of some kind of functional groups such as double bonds is generally required of the chemical structure of monomers. However, in the case of formation of polymers in the plasma created by a low pressure electric discharge, virtually any organic or organometallic vapor with or without functional groups can be polymerized[1,2]. In plasma polymerizations, the process is initiated by the collisions between energetic free electrons in the plasma with the monomer molecules to form active species. These active species may be ions or excited molecules, but more predominantly free radicals[3,6]. They then react either with themselves or with virgin monomers to form polymers both in the gas phase and on adjacent surfaces in the reactor. In previous publications from this laboratory, preliminary data on the plasma polymerization of saturated hydrocarbons were reported[6,7]. In this work further investigations in this regard will be carried out in an effort to shed some light on the kinetics and mechanism of these unique reactions.

EXPERIMENTAL

CP grade methane, ethane, propane and n-butane were purchased from the Matheson Gas Products Company, and were used as received. A tubular plasma polymerization reactor was employed throughout this study[8]. The schematic diagram for the reactor is shown in Figure 1. Essentially it consists of two parallel electrodes in a glass tube. The bottom electrode is cooled by circulating water. Monomer gas is supplied through a circular

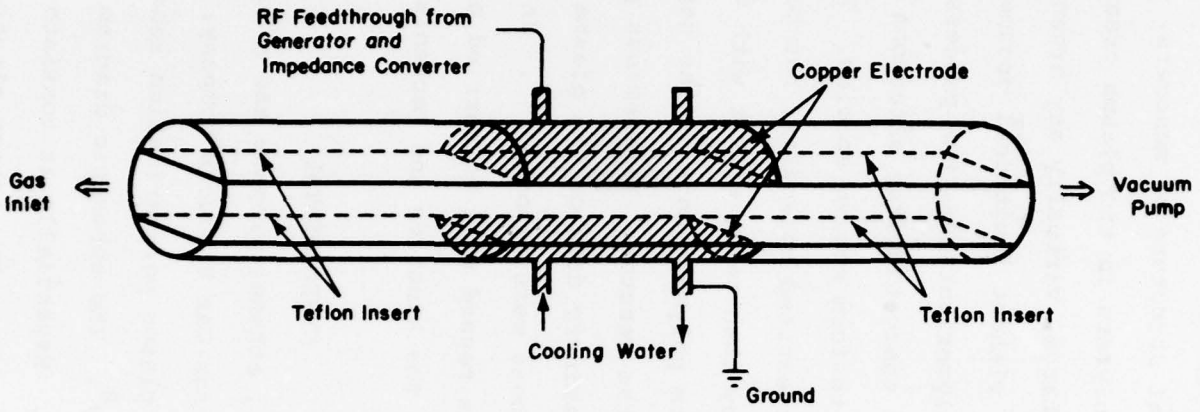


Figure 1. Schematic diagram of the tubular flow plasma reactor.

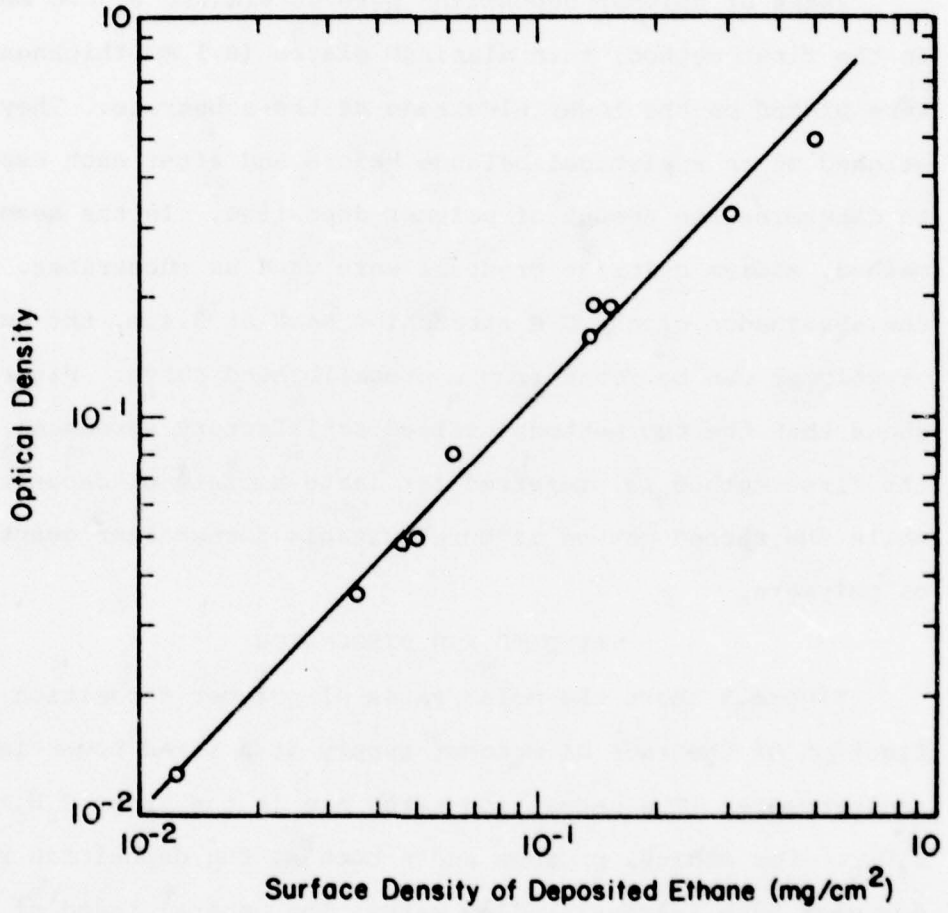


Figure 2. Optical density of plasma polymerized ethane determined at 3.4 μ m (C-H stretching frequency) plotted against surface density determined by weighing method.

frittered distributor on one end of the reactor. Evacuation is effected by a mechanical pump from the other end. Power is supplied by an International Plasma Corporation Model PM401 radiofrequency generator at 13.56 MHz with a maximum output of 150 watts.

Rates of polymer deposition were determined by two methods. In the first method, thin aluminum plates (0.1 mm thickness) were placed on the lower electrode as the substrate. They were weighed on an analytical balance before and after each experiment to determine the amount of polymer deposited. In the second method, sodium chloride crystals were used as substrates. From the absorbance of the C-H stretching peak at 3.4μm, the amount of polymer can be found from a precalibrated curve. Figure 2 shows that the two methods yielded satisfactory agreement. Usually the first method is preferred for large amounts of deposition, while the second method is more suitable for smaller quantities of polymers.

RESULTS AND DISCUSSION

Figure 3 shows the molar rates of polymer deposition as a function of the rate of monomer supply at a fixed power level and pressure. The deposition rates are in the order $C_2H_6 > C_3H_8 > C_4H_{10}$. For ethane, propane and n-butane, the deposition rates decrease with increasing flow rate. The general trend of rates creasing rates deposition with increasing monomer feed rate is consistent with that observed in the plasma polymerization of other monomers[6-8]. The interpretation is that the residence time of the reactive species are decreased by increased flow rate,

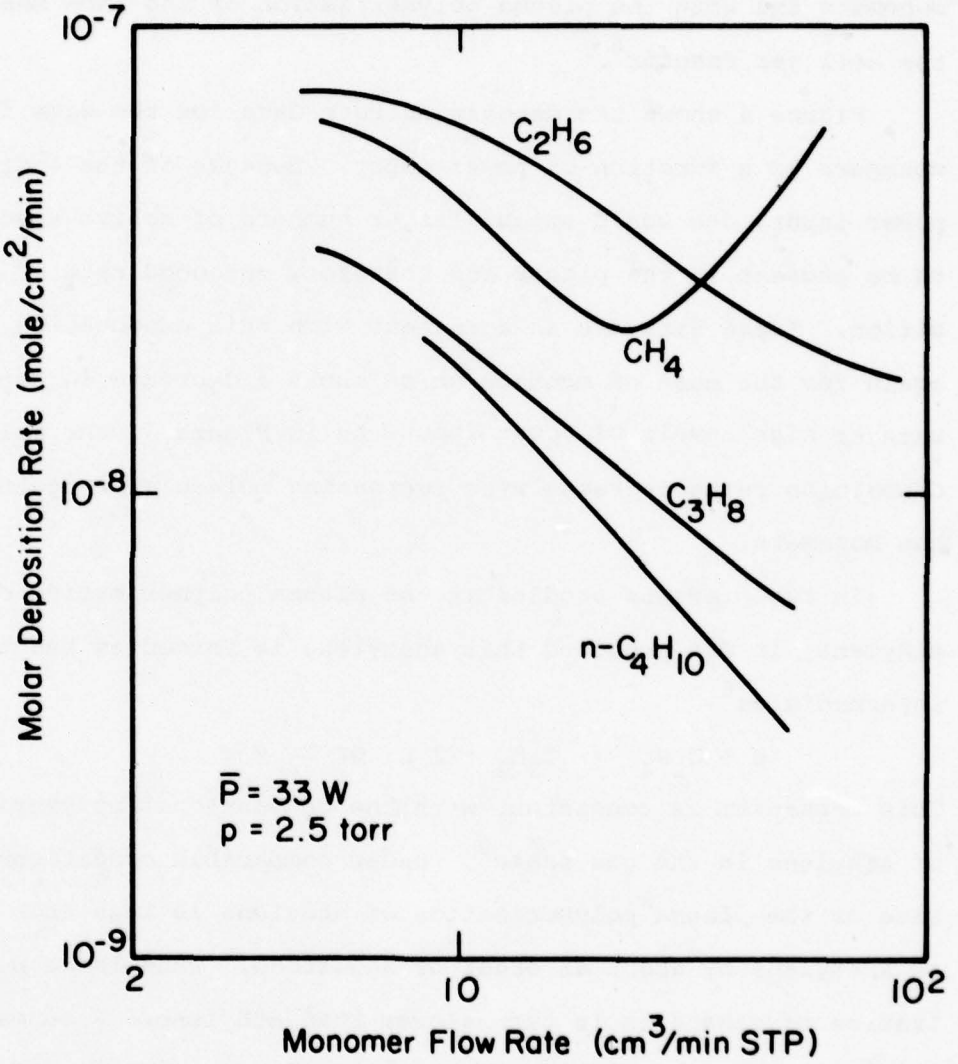


Figure 3. Molar deposition rates for the plasma polymerization of methane, ethane, propane and n-butane at power of 33 watts and pressure of 2.5 torrs plotted as a function of monomer flow rate.

and that some of them were swept away before polymerization can take place. The anomalous case is that of methane, which first decreased in deposition rate to a minimum and then increased with flow rate. The observed behavior differs from that of other monomers and with the plasma polymerization of the same monomer in the bell jar reactor[6].

Figure 4 shows the deposition rate data for the same four monomers as a function of power input. Because of the increased power input, one would expect larger numbers of active species to be present in the plasma and therefore enhanced rate of deposition. These data are in agreement with this expectation, except again for the case of methane which shows a decrease in deposition rate at high levels of power input. As in Figure 3, the molar deposition rates decrease with increasing molecular weights of the monomers.

In our previous studies in the plasma polymerization of ethylene, it was proposed that acetylene is formed as reaction intermediates[6].

$$e + C_2H_4 = C_2H_2 + 2\ H\cdot \text{ or } H_2 + e \qquad (1)$$

This mechanism is consistent with the conventional polymerization of ethylene in the gas phase[9]. Under comparable conditions, the rate of the plasma polymerization of ethylene is less than that of acetylene by about an order of magnitude. The plasma polymerization of ethane is in turn slower than ethylene. Presumably an extra step is required for the initial decomposition of ethane by electron impact to form ethylene first[6]:

$$e + C_2H_6 = C_2H_4 + H_2 + e \qquad (2)$$

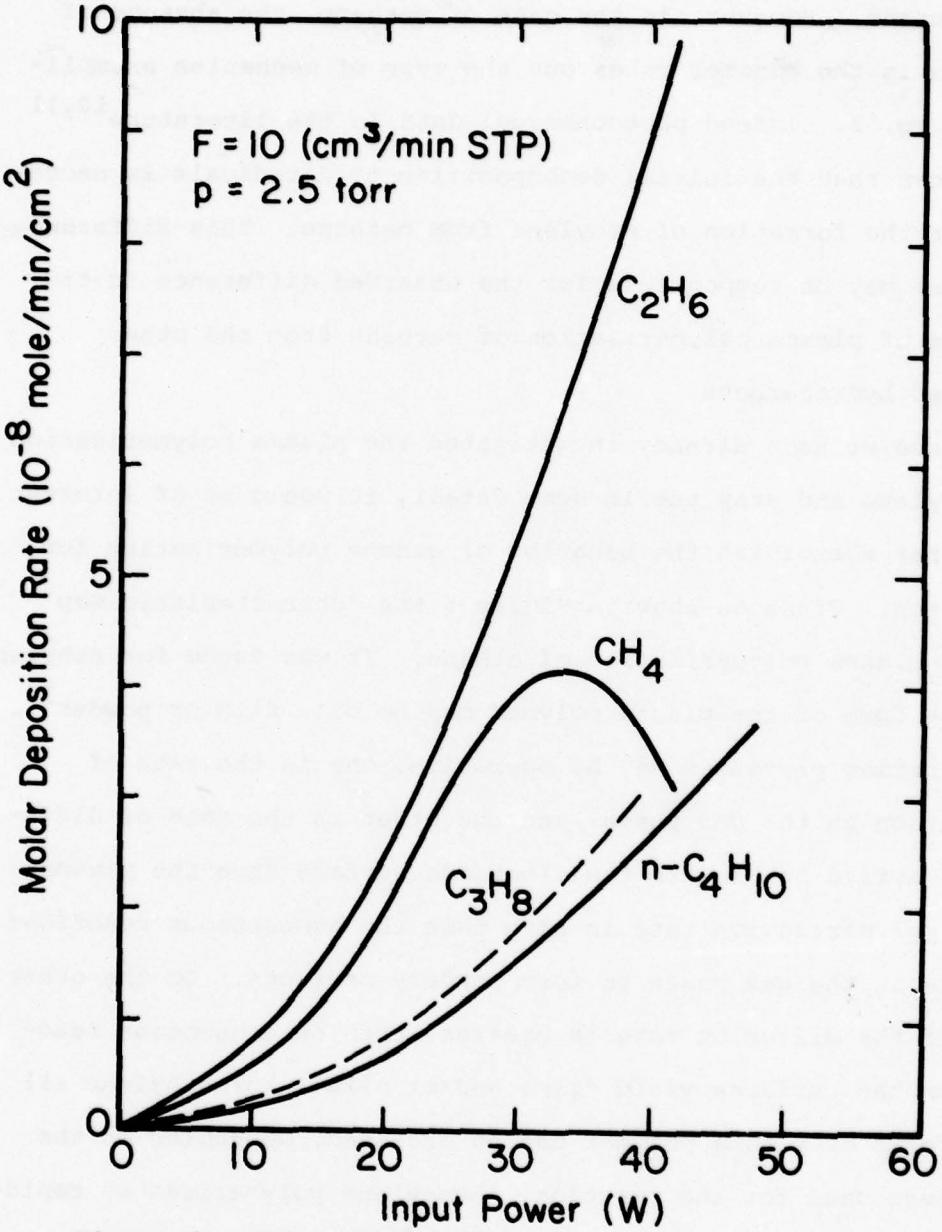


Figure 4. Molar deposition rate for the plasma polymerization of methane, ethane, propane and n-butane at the flow rate of 10 c.c./min STP and the pressure of 2.5 torrs plotted as a function of input power level.

which then eventually form acetylene to undergo polymerization as in eq. 1. Similar mechanism may also be responsible for propane and n-butane. However, in the case of methane, the absence of C-C bond in the monomer rules out the type of mechanism exemplified by eq. 2. Indeed photochemical data in the literature[10,11] have shown that the initial decomposition to diradicals is necessary for the formation of ethylene from methane. This difference in mechanism may be responsible for the observed difference in the kinetics of plasma polymerization of methane from the other saturated hydrocarbons.

Since we have already investigated the plasma polymerization of acetylene and ethylene in some detail, it would be of interest to further scrutinize the behavior of ethane polymerization for comparison. First we show in Figure 5 the "characteristic map" for the plasma polymerization of ethane. It was found for ethylene that the form of the plasma polymer may be oil, film or powder[12]. Two competing processes may be operative, one is the rate of propagation in the gas phase, and the other is the rate of diffusion of active species to the electrode surface from the plasma. If the polymerization rate is high then the homogeneous reactions dominate in the gas phase to form powdery products. On the other hand, if the diffusion rate is greater, then heterogeneous reactions on the surfaces yield films and/or oils. For ethylene all three forms of plasma polymer can be obtained, depending on the parameters used for the reaction. Acetylene polymerizes so rapidly that only powder can be obtained[6]. In the case of ethane, which polymerizes slowly in the plasma, films are formed under most conditions. Only at very low pressures and low flow rates

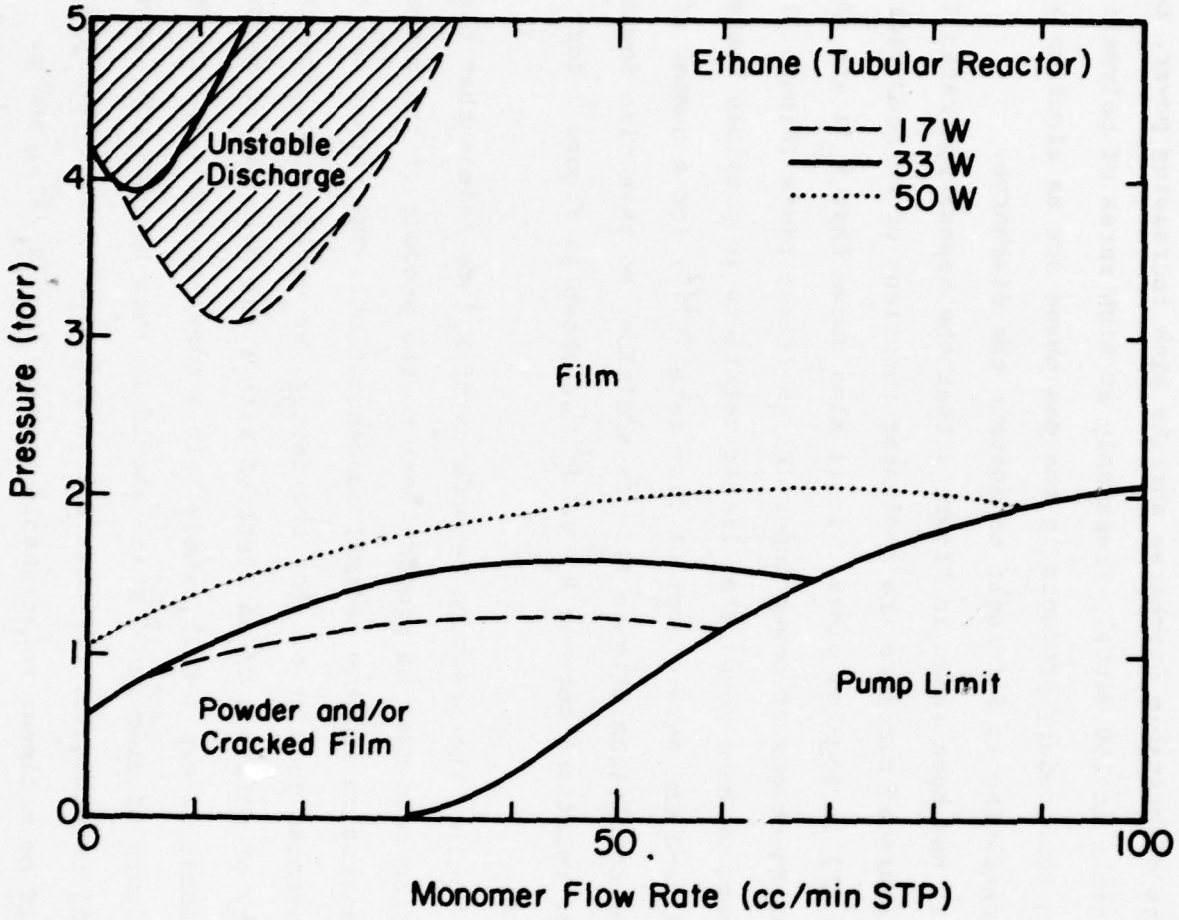


Figure 5. Characteristic map for the plasma polymerization of ethane in the tubular reactor.

can partial formation of powder be observed. The regions of powder formation are enlarged with increasing power input because of the enhanced population of active species. On the other hand, the regions of unstable discharge shrinks with increasing power, being negligible at 150 watts. Presumably at high rates of polymerization the powdery products in the gas phase act as electron sinks, thus rendering it difficult to sustain the discharge.

It has been shown in Figure 3 that the deposition rates (R_p) for saturated monomers are nonlinear functions of monomer flow rates (F) in log-log plots. It is also shown that R_p's are nonlinear functions of power input ($\bar{P}$) in linear plots (Figure 4). However, we have found that linear relations is possible between log R_p and the square root of flow rate ($F^{1/2}$) for a number of plasma conditions (Figure 6). In addition, we have also found linear relations between R_p and $\bar{P}^2$, as shown in Figure 7 for ethane.

To find the pressure dependence of R_p' we reason that the reaction rate must be proportional to the product of the monomer concentration and the radical concentration. The former can be represented just by p. For the latter, we would expect the probability of collison of an electron with a gas molecule to be proportional to exp $(-K/\lambda)$, where K is a constant and λ is the mean free path of electron[13] which should in turn be inversely proportional to pressure. If this rationalization is correct, then there should be a linear relationship between log $(R_p/\bar{P}^2 p)$ and p. Here we have incorporated the $\bar{P}^2$ dependence in order to use the data obtained at different power levels. Figure 8 shows in fact

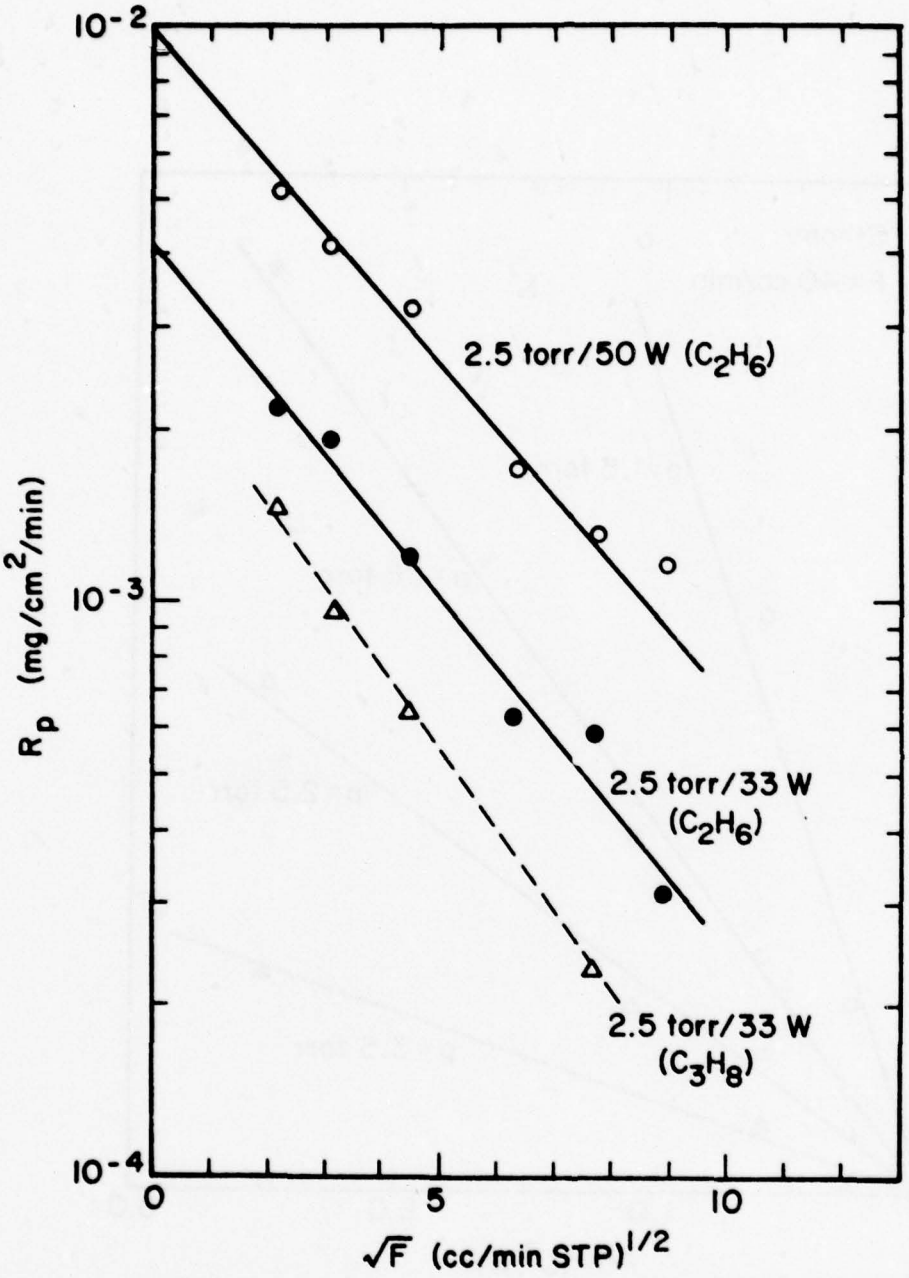


Figure 6. Rates of deposition for the plasma polymerization of ethane and propane plotted against the square root of monomer flow rate.

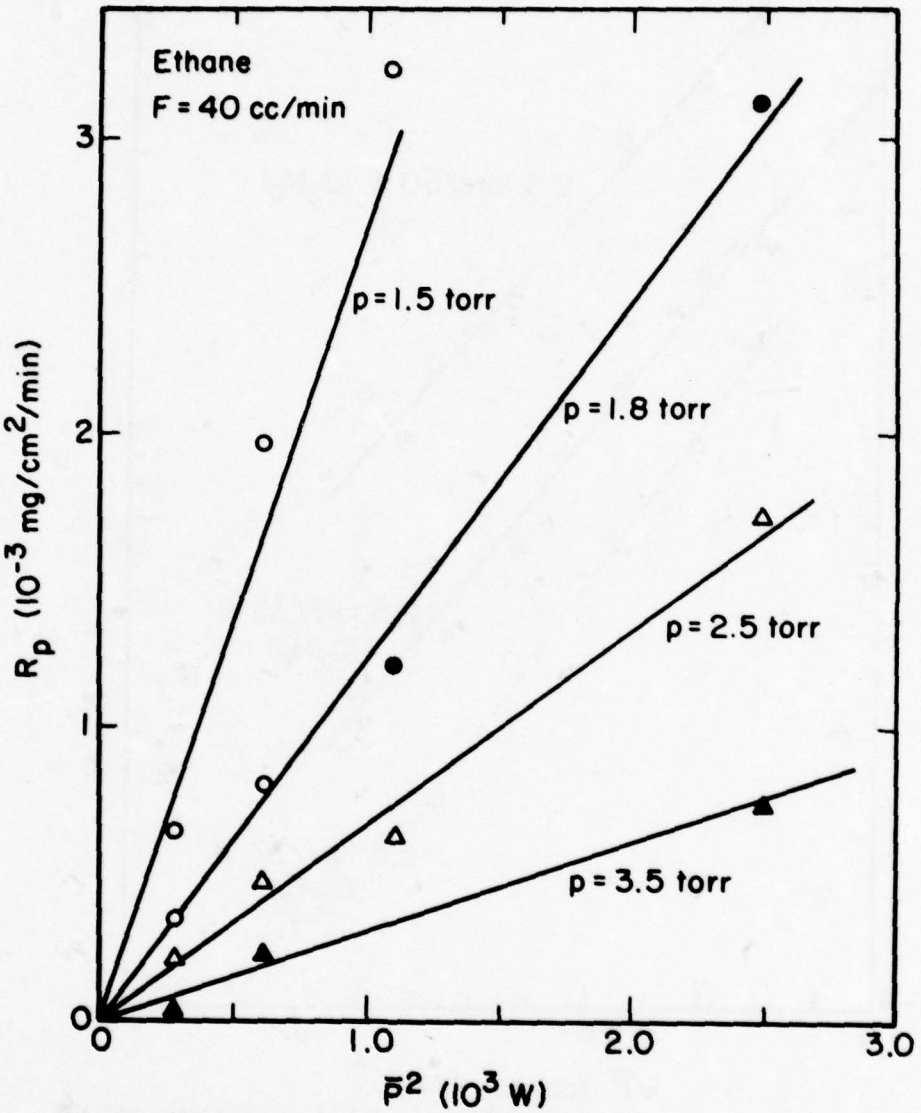


Figure 7. Rate of deposition for the plasma polymerization of ethane plotted against the square of power input at a series of pressures.

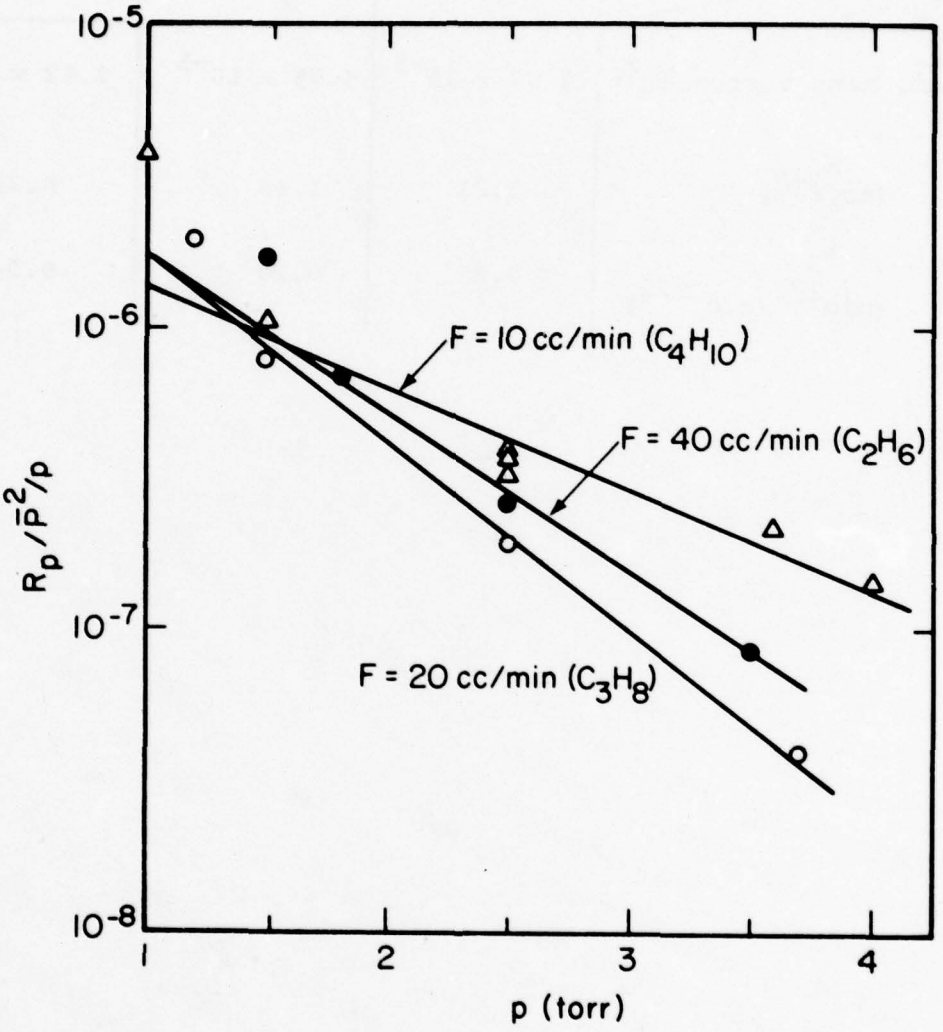


Figure 8. $R_p/\bar{P}^2_p$ plotted against pressure for the plasma polymerization of ethane, propane and n-butane.

Table 1. Kinetic Constants for Plasma Polymerization of Simple Saturated Hydrocarbons

Constant \ Monomer	Ethane	Propane	n-Butane
k_1 (mg/cm. min. torr.watt^2)	2.97×10^{-5}	3.05×10^{-5}	1.62×10^{-5}
k_{2-1} (torr^{-1})	1.23	1.45	0.77
k_3 (min$^{1/2}$/c.c.$^{1/2}$)	0.25	0.29	0.54

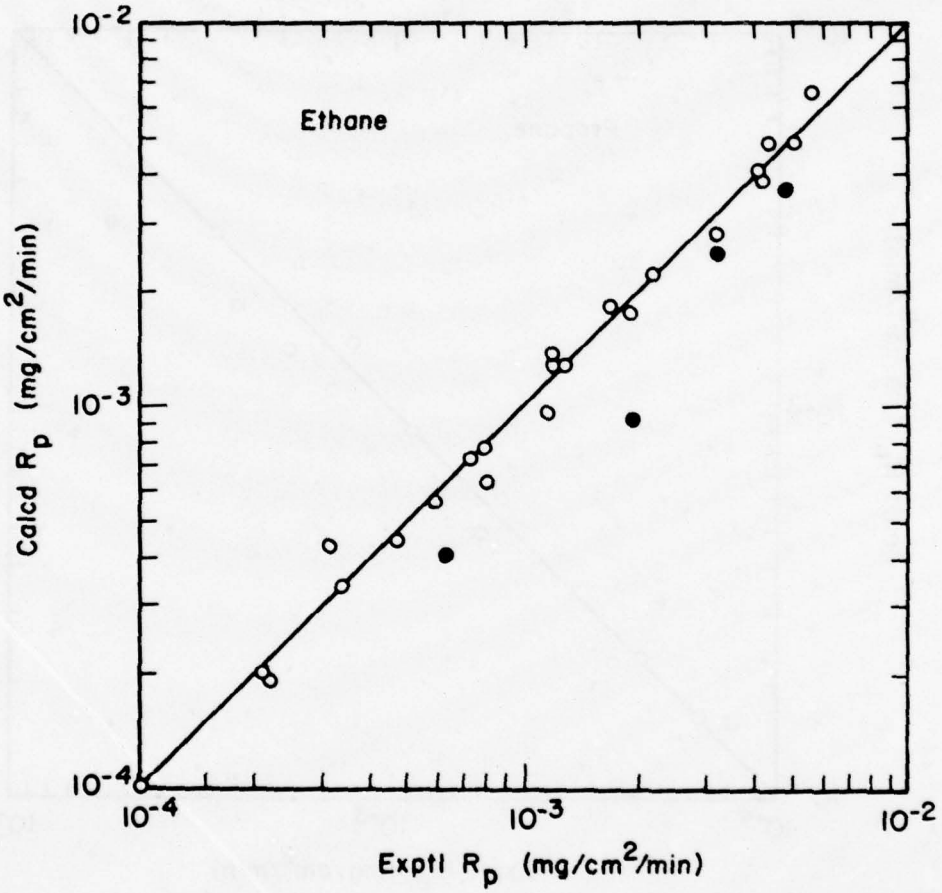


Figure 9a. Comparison of experimental and calculated rates of deposition for the plasma polymerization of ethane. Open circles are data taken from the film regions, closed circles are from powder regions.

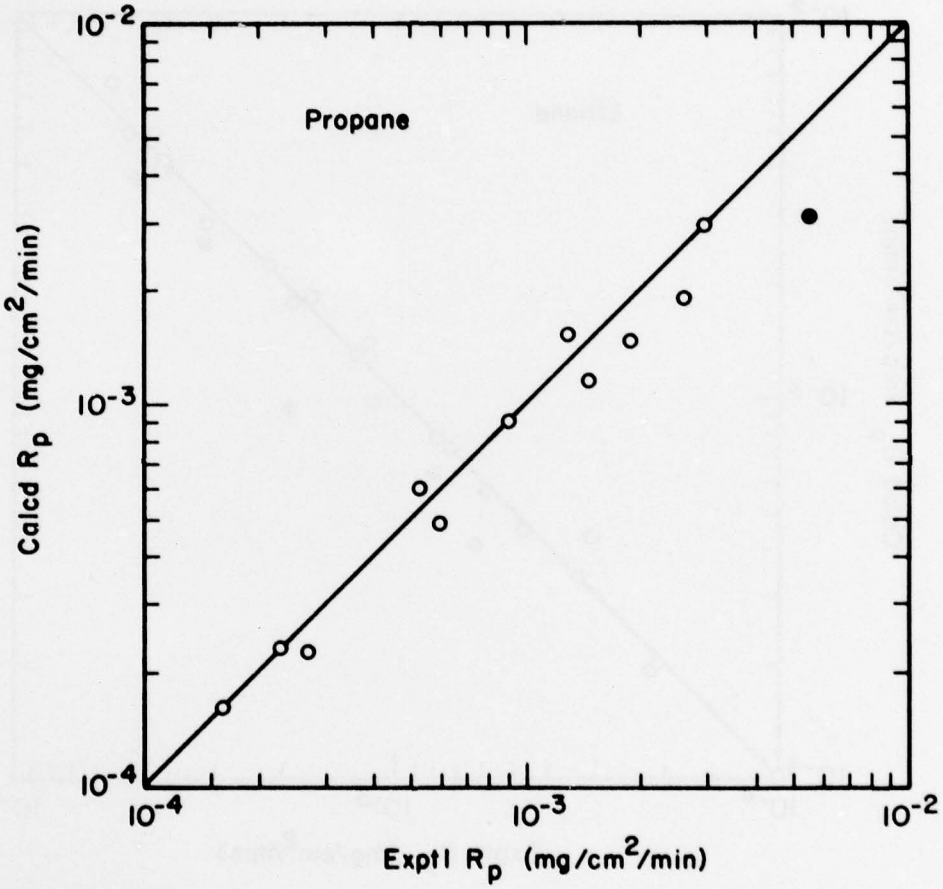


Figure 9b. Comparison of experimental and calculated rates of deposition for the plasma polymerization of propane. Open circles are data taken from the film regions, closed circles are from powder regions.

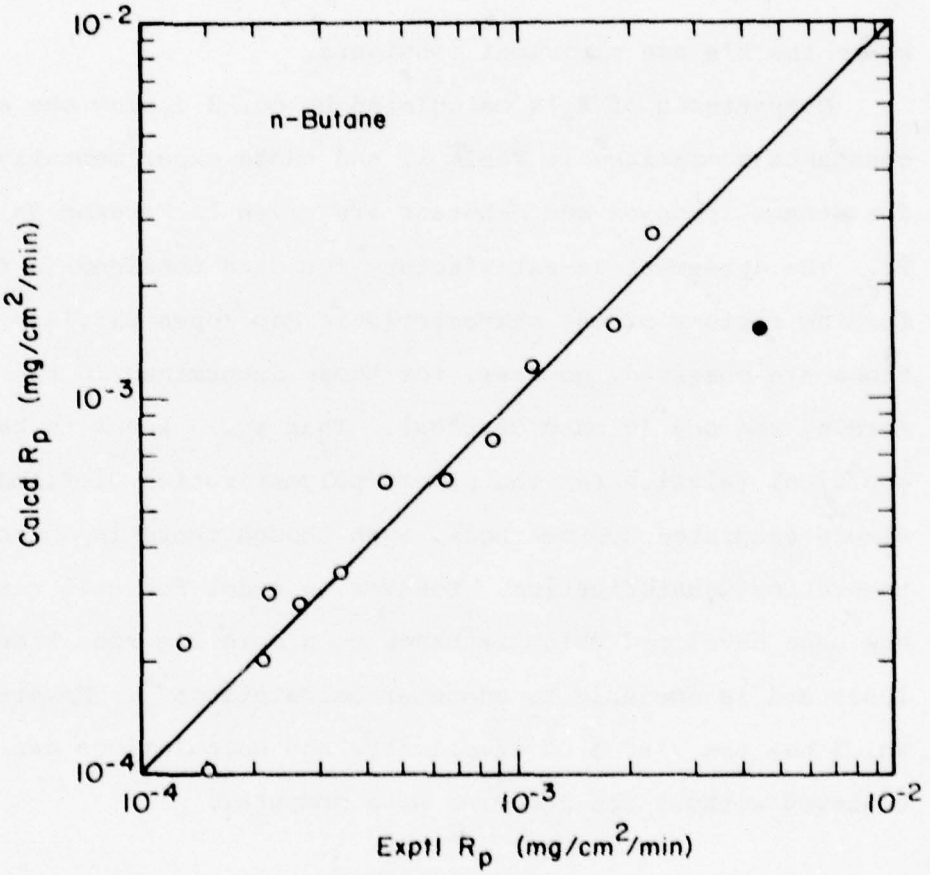


Figure 9c. Comparison of experimental and calculated rates of deposition for the plasma polymerization of n-butane. Open circles are data taken from the film regions, closed circles are from powder regions.

that the data seem to bear out this expectation. Thus on the basis of these observations, we can write the following empirical equation for the plasma polymerization of saturated hydrocarbons:

$$R_p = k_1 \bar{P}^2 p \exp \left[- (k_2 p + k_3 F^{1/2}) \right] \quad (3)$$

where the k's are empirical constants.

Comparisons of R_p's calculated by eq. 3 (using the empirical constants summarized in Table 1) and those experimentally observed for ethane, propane and n-butane are given in Figures 9a through 9c. The agreement is satisfactory for data obtained in film-forming regions of the characteristic map (open circles). Deviations are observed, however, for those determined in the powder-forming regions (closed circles). Thus eq. 3 seems to be a useful empirical relation for the plasma polymerization of films from simple saturated hydrocarbons, even though there is a lack of theoretical justification. However, a model for this reaction has now been developed which is based on a more rigorous kinetic analysis and is amenable to computer calculations[14]. Nevertheless eq. 3 has the virtue of simplicity, and calculations can be readily achieved without the recourse of a computer.

ACKNOWLEDGEMENT

This work is supported by the Defense Advanced Research Projects Agency, monitored by the Air Force Cambridge Research Laboratory.

REFERENCES

1. A. T. Bell and J. R. Hollahan, eds., "Techniques and Applications of Plasma Chemistry," Wiley, New York, 1974.
2. M. Shen, ed., "Plasma Chemistry of Polymers," Dekker, New York, 1976.
3. H. Yasuda and C. E. Lamaze, J. Appl. Polymer Sci., 15, 2277 (1971).
4. M. Duval and A. Theoret, J. Appl. Polymer Sci., 17, 527 (1973).
5. H. Carchano, J. Chem. Phys., 61, 3634 (1974).
6. H. Kobayashi, A. T. Bell and M. Shen, Macromol., 7, 277 (1974).
7. T. Reis, H. Hiratsuka, A. T. Bell and M. Shen, Nat'l Bur. Stds. Special Publication, in press.
8. H. Kobayashi, A. T. Bell and M. Shen, J. Macromol. Sci.-Chem., A10, 123 (1976).
9. G. M. Burnett, "Mechanism of Polymer Reactions," Interscience, New York, 1954.
10. W. Braun, K. H. Welge and J. R. McNesby, J. Chem. Phys., 45, 2650 (1960).
11. C. A. Jensen and W. F. Libby, J. Chem. Phys., 49, 2831 (1968).
12. H. Kobayashi, A. T. Bell and M. Shen, J. Appl. Polymer Sci., 18, 885 (1973).
13. E. Nasser, "Fundamentals of Gaseous Ionization and Plasma Electronics," Wiley-Interscience, New York, 1971.
14. H. J. M. Tibbitt, A. T. Bell and M. Shen, Macromol., in press.

SECTION IV

Effect of Frequency on the Plasma Polymerization of Ethane

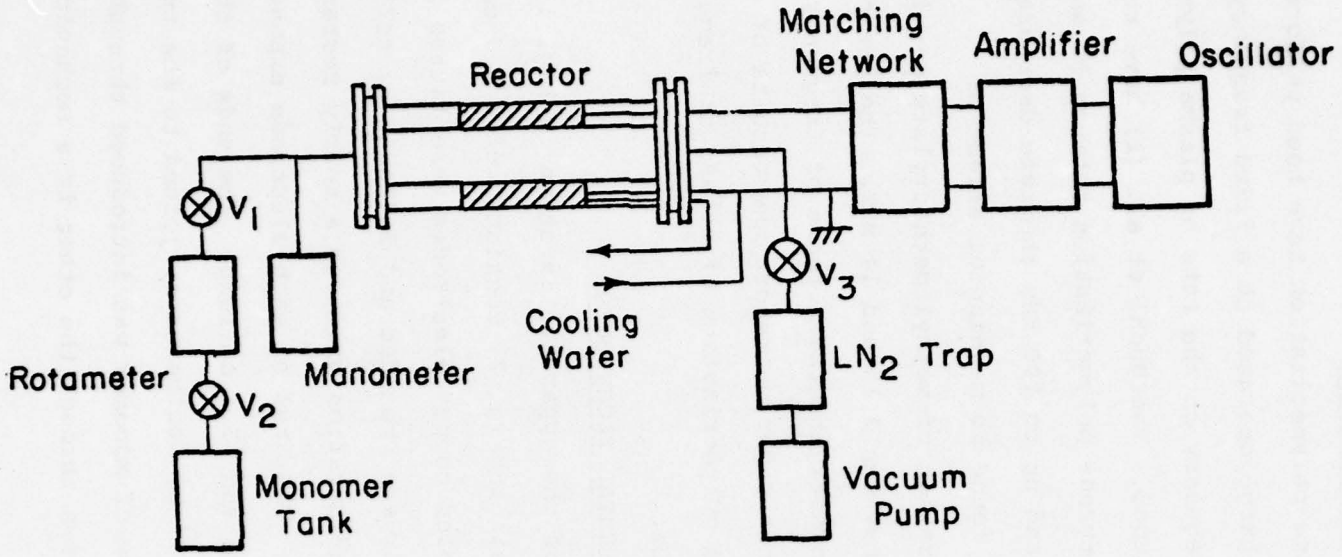
INTRODUCTION

Most studies of plasma polymerization have been performed using a low pressure discharge operated at a fixed frequency. As a result the effect of frequency on the rate of plasma polymerization is not well understood. Taniguchi et al. (1) have reported an increase in the rate of styrene polymerization between 50 and 500 Hz, but above 500 Hz and up to 100 KHz the rate decreased. However, Brown et al. (2) found no meaningful effect of frequency on the polymerization of methyl methacrylate or vinyl chloride for frequencies between 3.15 and 14 MHz. The present study was undertaken to investigate the effects of frequency over a broad range. In this paper we report the results of our observations on the plasma polymerization of ethane at frequencies between 50 Hz and 13.56 MHz.

EXPERIMENTAL TECHNIQUES

A schematic diagram of the apparatus is shown in Fig. 1. The reactor, shown in detail in Fig. 2, consisted of a 3.7 cm I.D. Pyrex tube. Two water-cooled copper electrodes were fitted into the center of the tube and were preceded and followed by Teflon blocks. The resulting configuration produced a nearly rectangular flow channel, 3.5 cm high. The area of each electrode exposed to the channel was 6.5 cm wide and 15.4 cm long. The ends of the reactor tube were closed off by Lucite caps, joined to the tube by O-rings. A metered flow of monomer was introduced through one of the end caps and withdrawn through the other to a mechanical vacuum pump.

Power for the discharge was supplied by one of four power



f = 50 Hz to 20 KHz — OSC: IEC-F33, AMP: Bogen-MT125A

f = 20 KHz to 10 MHz — OSC: HP-651A, AMP: ENI-240L

f = 13.56 Mz — OSC/AMP: IPC-PM104B

Figure 1. Schematic of experimental apparatus.

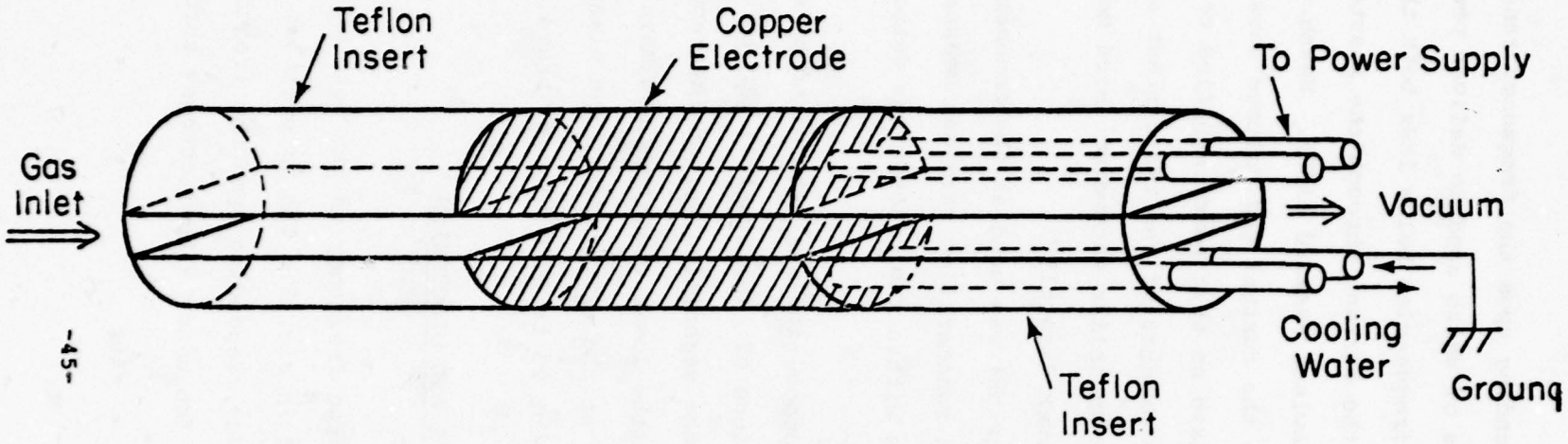


Figure 2. Schematic of reactor intervals.

supply configurations, depending upon the frequency range of interest. The combinations of units used to deliver power are indicated in Fig. 1. For frequencies below 2MHz both the voltage across the electrodes and the current through the reactor were determined using a VTVM (Hewlett Packard 410B). Measurements of the phase angle between the current and voltage showed that the two were essentially in phase so that power supplied to the reactor could be determined as the product of the rms current and voltage. For frequencies above 2MHz an inline wattmeter (Bird Model 43) was used to measure the power directly.

CP grade ethane (Matheson) was used as the monomer without further purification. The monomer flow rate was measured with a rotameter. The pressure within the reactor was determined with a McLeod gauge.

The rate of polymer deposition was determined by measuring the gain in weight of a piece of luminum foil placed over the lower electrode. During the deposition period the temperature of the water exiting from the lower electrode was maintained at 19°C. The temperature at the electrode at the plasma-electrode interface was probably about 25 to 30°C higher, based upon previous measurements (3).

RESULTS AND DISCUSSION

Results

The effect of discharge frequency on the rate of polymer deposition is illustrated in Fig. 3. The rate either increases or decreases with frequency, depending upon the frequency range, and the direction of the frequency effect changes abruptly at

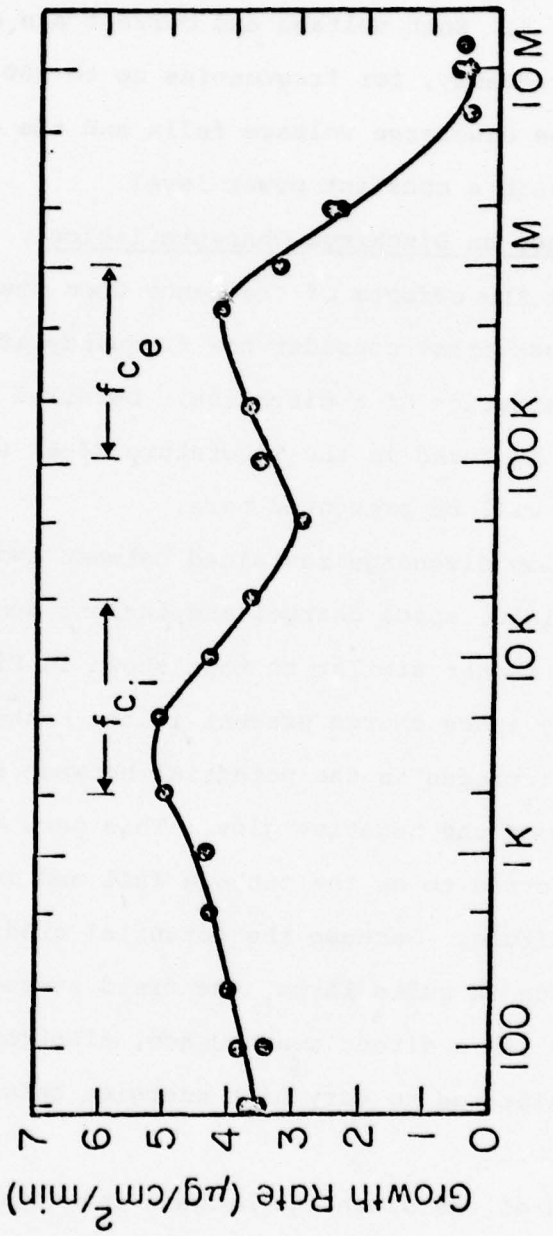


Figure 3. Effect of frequency on the rate of polymer deposition.

5KHz, 50KHz, 600 KHz, 6 MHz.

The voltage across the discharge and the current through it are shown in Fig. 4. Both voltage and current are essentially independent of frequency, for frequencies up to 200 KHz. Above this frequency the discharge voltage falls and the current rises in order to maintain a constant power level.

Effect of Frequency on Discharge Characteristics

To interpret the effects of frequency upon the rate of polymer deposition, we must first consider how frequency affects the physical characteristics of a discharge. Detailed treatments of this subject may be found in the literature (4-6) so that only a brief overview will be presented here.

In a d.c. glow discharge sustained between two electrodes, the potential, field, space charge, and current density are distributed in a manner similar to that shown in Fig. 5. The high net positive space charge present in the cathode dark space causes a sudden increase in the potential between the cathode and the leading edge of the negative glow. This part of the potential is referred to as the cathode fall and is typically 100 to 200 V in magnitude. Because the potential gradient in the cathode dark space is quite large, the field strength in this region is large. As a direct consequence, electrons leaving the cathode are accelerated to very high energies before they enter the negative glow.

The portion of the discharge between the negative glow and the end of the positive column is characterized by a small potential increase and nearly equivalent concentrations of ions and

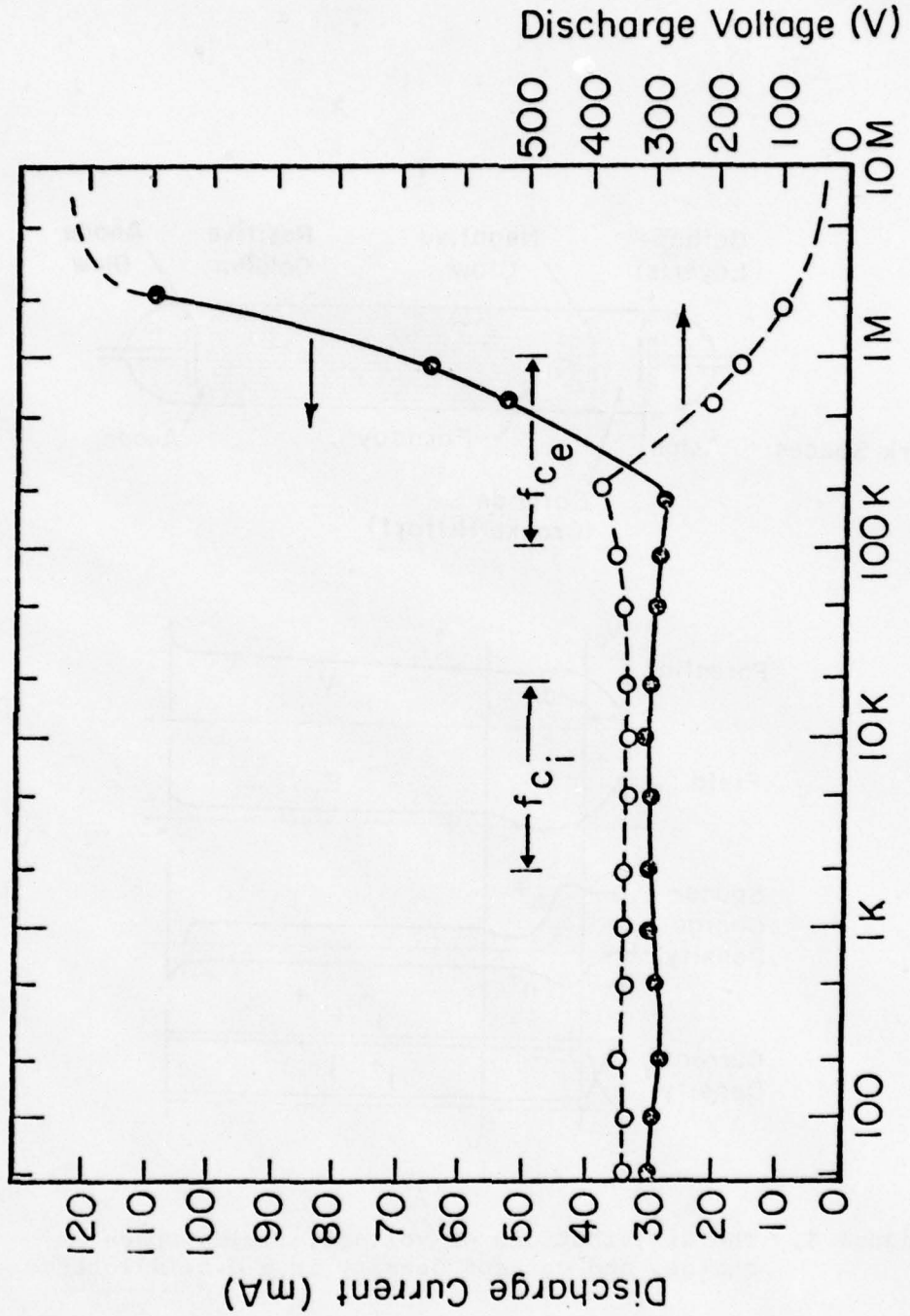


Figure 4. Effect of frequency on the discharge voltage and current.

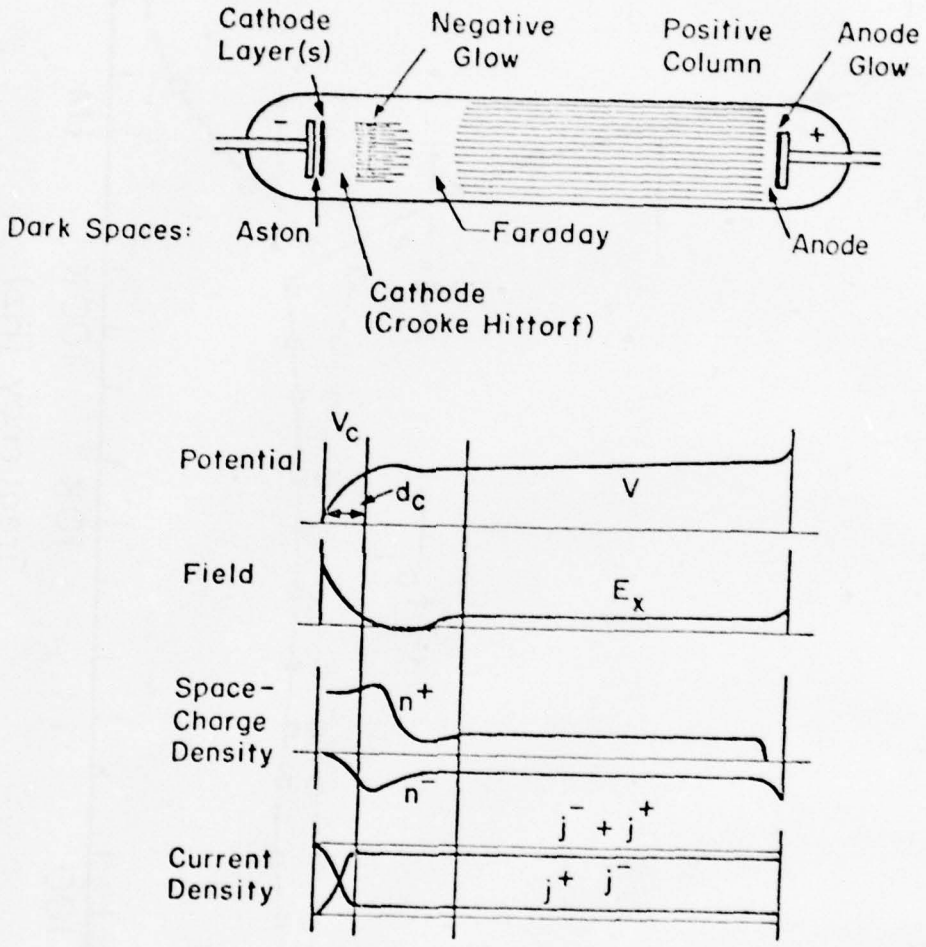


Figure 5. The distributions of voltage, field, space charge, and current density in a d.c. discharge.

electrons. Because the potential gradient in these regions is considerably smaller than in the cathode dark space, the electron energies are also smaller. Finally, in the space between the positive column and the anode a third potential increase is observed. This component is referred to as the anode fall and is typically 10 to 20 V in magnitude. It arises due to the excess negative space charge present in the anode dark space.

Since electrons and ions are swept out of the discharge by the imposed field, they must be replaced continuously. New electrons are created at the cathode by the impingement of ions accelerated through the cathode fall and by photons created in the negative glow. The majority of positive ions collected by the cathode are replaced by electron-impact ionization occurring in the negative glow.

When a low frequency (<100 Hz) field is used to create the discharge, each electrode alternately acts as cathode and anode. On each half cycle a dc-type discharge is established once the breakdown potential is surpassed. As long as the applied voltage remains above the maintenance potential, the discharge is sustained, but when the voltage falls below the maintenance potential, the discharge is extinguished, and the space charge is swept out of the volume. For sufficiently low frequencies all of the space charge is eliminated before the potential rises on the next half cycle to a point where a new discharge is initiated.

As the frequency of the applied field is increased, a point is reached at which the time taken by a positive ion to move

between the electrodes becomes equal to one half the period of the field. The corresponding frequency is defined by (5)

$$f_{c_i} = \frac{v_{d_i}}{2L} \qquad (1)$$

where v_{d_i} is the average ion drift velocity and L is the interelectrode distance. For frequencies above f_{c_i}, ions created near a momentary anode cannot transit to the cathode before the field is reversed. This leads to a partial retention of the positive space charge from one half cycle to the next and facilitates reinitiation of the discharge. For systems which do not depend upon secondary electron generation through ion bombardment, increasing the frequency above f_{c_i} has no significant effect on the starting or maintenance potential of the discharge (5). This situation prevails in the present experiments, as can be judged by the absence of any change in the discharge voltage in the vicinity of f_{c_i} (see Fig. 4).

Raising the frequency of the applied field above f_{c_i} leads to the observation of a second critical frequency f_{c_e}, corresponding to the condition that an electron makes the transit between electrodes in one half cycle of the field. The relationship defining f_{c_e} is (5)

$$f_{c_e} = \frac{v_{d_e}}{2L} \qquad (2)$$

where v_{d_e} is the average electron drift velocity. For frequencies above f_{c_e} both the positive and negative space charge are retained from one half cycle to the next, leading to a significant reduction in the loss of charged particles from the system. As

a result, the voltages required to both initiate and maintain the discharge decrease abruptly (4-6). As can be seen from Fig. 4, estimated values of f_{c_e} agree very closely with the frequency at which the maintenance potential shows a significant decrease (200 KHz).

The spatial distributions of electrons and ions in a discharge maintained at frequencies above f_{c_e} are governed by the processes controlling the formation and loss of these species. Since the ac field no longer causes significant displacement of either electrons or positive ions, the loss of charged species from the discharge is controlled by amibipolar diffusion and homogeneous recombination (4,5). Replacement of charged species occurs by electron-impact ionization of neutral gas molecules. Throughout the bulk of the discharge volume the concentrations of electrons and ions are essentially equal. The concentration profiles have a maximum at the midpoint between the electrodes and fall off monotomically towards each electrode. Within a Debye length of the electrode surface a space charge sheath is set up across which a potential of several volts may exist. The presence of the sheath accelerates the transport of ions but decelerates the transport of electrons.

For frequencies between f_{c_i} and f_{c_e}, the distribution of space charge and potential within the discharge is governed by the manner in which the applied field affects the motions of ions and electrons. Because of their low mobility the positive ions are unable to move significant distances during each half cycle of the field. This results in an essentially stationary spatial

distribution of ions which has a maximum value at the center of the discharge. In contrast to the behavior of the ions, the electrons are swept through the interelectrode gap by the field on each half cycle, causing the electron distribution to be a function of both position and time. During each half cycle, an excess of positive space charge will appear near the electrode near the electrode acting as cathode and an excess of negative space charge will appear near the electrode acting as the anode. The net effect of these charge imbalances is to create sharp potential increases in the vicinity of each electrode.

Effect of Frequency on Plasma Polymerization

We turn next to a consideration of the mechanism by which polymer deposition occurs. In recent studies conducted (7,8) in this laboratory it has been shown that a free radical mechanism of polymerization can successfully describe the rates of polymer deposition. Using this work as a basis, we propose the following simplified reaction sequence to explain the polymerization of ethane.

1. $e + M \rightarrow 2R_g^{\cdot} + e$

2. $P_s \xrightarrow{e,I,h\nu} 2R_s^{\cdot}$

3. $R_g^{\cdot} + P_s \rightarrow R_s^{\cdot}$

4. $R_g^{\cdot} + R_s^{\cdot} \rightarrow P_s$

Reaction 1 represents the dissociation of the monomer, M, to produce gas phase radicals, $R_g^{\cdot}$. Surface free radicals, $R_s^{\cdot}$, are produced by reaction 2 which involves the impact electrons, ions, and/or photons on the polymer surface, represented by P_s.

Additional surface radicals can be created by the adsorption of gas phase radicals, reaction 3. Finally, reaction 4 illustrates polymer chain growth through the recombination of surface and gas phase radicals. It is this last reaction which controls the rate at which new polymer is formed. The role of frequency in controlling the rate of polymer deposition can now be examined by considering the effects of frequency on the rate at which surface and gas phase free radicals are produced.

For frequencies below 5kHz the discharge has the characteristics of a pulsating dc discharge. On each half cycle the electrode acting as the cathode is subjected to a flux of energetic ions accelerated, through the cathode fall. The impact of these ions on the surface of the polymer film covering the momentary cathode will cause a disruption of the polymer film and the formation of surface free radicals (9). A similar phenomenon will occur at the opposite electrode, or anode, due to the impact of electrons. Based upon numerous observations of polymer deposition in d.c. discharges (10), we conclude that radical formation will be more effective at the cathode than at the anode, due to the higher energy carried by the ions.

The formation of gas phase radicals will occur throughout the discharge. However, due to the significantly higher field strength in the region of the cathode dark space, the rate of radical production will be maximized there. This is advantageous since it shortens the distance for radical diffusion from the gas phase to the cathode surface.

Because the discharge is initiated and extinguished on each

half cycle, the rate of radical production is not constant but, rather, occurs in pulses. The time averaged concentration of gas phase radicals will depend upon the frequency of the pulses and the kinetics of radical consumption. In studies of pulsed photopolymerization it has been observed that the time averaged radical concentration will increase from a low level plateau to a high level plateau as the pulse frequency is increased (11). This behavior causes the rate of polymerization to exhibit a similar response to increasing pulse frequency. A very similar trend has been observed in recent studies of ethylene and ethane polymerization using a pulsed rf discharge and a reactor nearly identical to that shown in Fig. 2 (12). The rate of polymerization was found to increase by about 50% as the pulse frequency was increased from 500 sec^{-1} to 5000 sec^{-1}. These observations suggest that the increase in polymer deposition rate between 50 Hz and 5 KHz, observed in Fig. 3, might be ascribed to an increasing time averaged concentration of gas phase free radicals.

As the frequency of the applied field becomes greater than f_{c_e}., ion bombardment of the electrodes will be reduced. However, complete suppression of the ion flux will not occur until frequencies considerably greater than f_{c_i} are attained, due to the fact that ions located near the electrodes will still be able to reach the electrode surfaces in times small compared to $2/f_{c_i}$. Over the same frequency range the effect of frequency on the gas phase concentration of free radicals is not expected to be large, since the time between individual discharge periods is too small for the radical population to collapse. As a result,

it is anticipated that the rate of ion impingement will control the rate of polymer deposition and that a reduction in the impingement rate will cause a reduction in the rate of polymer deposition. Inspection of Fig. 3 supports this contention since we note a sudden reduction in the polymer deposition rate for frequencies greater than f_{c_i}.

The increase in polymer deposition rate which occurs between 50 and 600 KHz is the most difficult feature of Fig. 3 to explain. It is conceivable that this increase is associated with an increase in the energy of the electrons striking the electrode acting as the anode. Such an increase could occur if the magnitude of the anode fall were to increase. Thus, here again we suggest that the effect of frequency is associated with the rate at which surface free radicals are produced.

Fianlly, we believe that the very low polymer deposition rates observed at frequencies near 10MHz can be ascribed to low rates of formation of both surface and gas phase free radicals. At frequencies in this range, charge transport to the electrode surfaces is governed totally by ambipolar diffusion. As noted earlier, this transport mechanism leads to substantially lower current densities than can be achieved by field driven transport. Furthermore, the energies of the species arriving at the electrodes are much lower than those characteristics of frequencies below f_{c_e}. Because of these effects it is expected that the rate of surface free radical generation by the impact of charged species will be low.

As was discussed earlier, the production of gas phase free

radicals occurs via electron-impact dissociation, reaction 1. For a given monomer concentration the rate of radical production will depend upon the magnitude of the rate coefficient for Reaction 1 and the electron density. The primary variable influencing the rate coefficient is the ratio of the electric field strength to the gas pressure, E/p (4-6,13). Since there is a strong dependence of the rate coefficient on E/p, we expect the rate coefficient to be substantially smaller for frequencies near 10 MHz than for frequencies below f_{c_e} (see Fig. 4). Conversely, the electron density is expected to be higher when the discharge is operated at frequencies near 10 MHz. Because it is anticipated that the decline in the magnitude of the dissocation rate coefficient will be much greater than the increase in electron density, the rate of radical production is expected to be low when the discharge is operated at frequencies significantly above f_{c_e}.

ACKNOWLEDGEMENT

This work was supported by a grant from the Defense Advanced Research Projects Agency, monitored by the Air Force Cambridge Research Laboratory.

LITERATURE REFERENCES

1. I. Taniguchi et al., IEE Japan, Report of Study Meeting on on Insulating Materials, EI-42-8 (1967).
2. K. C. Brown, Europ. Polym. J. 8, 117 (1972); and K. C. Brown and M. J. Copsey, Europ. Polym. J. 8, 129 (1972).
3. T. A. Reis, M.S. Thesis, Department of Chemical Engineering, University of California, Berkeley, California, 1976.
4. S. C. Brown, "Basic Data of Plasma Physics," M.I.T. Press, Cambridge, Mass., 1959.
5. G. Francis, "Ionization Phenomena in Gases," Butterworths, London, 1960.
6. E. Nasser, "Fundamentals of Gaseous Ionization and Plasma Electronics," Wiley, New York, 1971.
7. A. T. Bell, J. Macromol. Sci.-Chem. A10, 369 (1976).
8. J. M. Tibbitt, R. Jensen, A. T. Bell, and M. Shen, Macromol. 10, 647 (1977).
9. M. Hudis, "Plasma Treatment of Solid Materials," in "Techniques and Applications of Plasma Chemistry," ed. by J. R. Hollahan and A. T. Bell, Wiley, New York, 1974.
10. M. Millard, "Synthesis of Organic Polymer Films in Plasmas," in "Techniques and Applications of Plasma Chemistry," ed. by J. R. Hollahan and A. T. Bell, Wiley, New York, 1974.
11. G. M. Burnett and H. W. Melville, Proc. Roy. Soc. A189, 494 (1947).
12. H. Hiratsuka, J. W. Vinzant, A. T. Bell, and M. Shen, "Infrared Laser Window Coating by Plasma Polymerization of Ethane in Pulsed Flow Discharge" to be published in "Proceedings of the High Power Laser Optical Components and Component Materials Meeting," Boulder, Colorado, 1977.

13. A. T. Bell, "Fundamentals of Plasma Chemistry," in Techniques and Applications of Plasma Chemistry" ed. by J. R. Hollahan and A. T. Bell, Wiley, New York, 1974.

SECTION V

Plasma Polymerization in Pulsed Discharge

I. INTRODUCTION

The field fo plasma polymerization has recently generated considerable interest. It has been found that organic compounds that are not polymerizable by conventional means (i.e., saturated hydrocarbons) can be made to form high molecular weight products in a plasma. It has also been found that the products of conventional monomers in plasma polymerization are quite different from their chemically initiated or radiation initiated counterparts. The products of plasma polymerization are unique in character and have some very useful aspects. In this work a pulsed radio frequency potential is used to probe the chemical mechanism of plasma polymerization in the manner suggested by the theory of intermittent illumination. As a second objective, the effectiveness of using a pulsed plasma as a means of improving the optical characteristics of plasma polymerized ethane, as required for antireflection coatings of infrared laser windows, is tested.

The term plasma polymerization refers to the formation of high molecular weight solids and liquids from organic monomers in a low pressure electrical discharge. By imposing a sufficiently large electrical potential across parallel plate electrodes, the gas between them can be made to break down and conduct. The degree of ionization in such a plasma is 10^{-5} to 10^{-6} and the concentrations of free electrons and positive ions are approximately equal (1).

Collisions of free electrons and/or photons in the plasma with neutral species lead to the formation of metastables, radicals,

atoms and ions which are chemically active. For pressures below 10 torr the plasma will be in a non-equilibrium state characterized by an imbalance between electron temperature (T_e) and gas temperature (T_g). Values of T_g between 300 and 400°K and of T_e between 10^4 and 10^5°K are typical.

The phenomenon of plasma polymerization was first reported in 1796 when four Dutch chemists converted ethylene to an oily substance in a spark discharge (2). The formation of solid products was recorded by De Wilde (3) and by Thenard (4) in 1874. Similar observations were subsequently reported by many investigators and the solid product was considered to be nothing more than an undesired byproduct of plasma-induced organic reactions. Not until the early 1960's was it noted that plasma-deposited films possessed unique and useful properties. Plasma polymers are amorphous and in most cases do not bear a simple relation in stoichiometry to the monomer. It was found that solid, uniform films could be formed with thicknesses from several hundred angstroms to several microns. The films are highly cross-linked, pinhole free, insoluable in most organic solvents and adhere well to the substrate.

During the past decade many papers have appeared describing the plasma polymerization reaction and it's products. Still the mechanism of plasma polymerization and the microstructure of the polymer are not clearly understood. It is likely that the active species formed by collisions of electrons and photons with monomer are responsible for the polymer formation. The extent to which ions or free radicals participate is a subject of debate. Experiments

with radical scavengers and the application of a D.C. potential to the afterglow region of a radio frequency discharge have led to the assertion that cations are the major precursor to plasma polymers, (5,6). Anionic intermediates have been postulated from observations of the products of a microwave discharge with toluene vapor in a carrier gas and arguments concerning energy transfer processes (7). On the other hand, it is known that at pressures greater than 1.0 torr the concentration of free radicals is 10^3 to 10^5 greater than that of ions (8). Thus it can be shown that free radical-molecule reactions occur 10 to 100 times faster than ion-molecule reactions. ESR spectra show a high concentration of free radicals trapped within the polymer matrix in plasma polymerized materials (9). These sites are immobilized and unable to combine with each other, but tend to oxidize on contact with air (10). It has also been found that the addition of small amounts of halogens accelerates the rate of polymer formation while decreasing the hydrogen-to-carbon ratio in the product. This effect can be explained by assuming that halogen atoms formed in the plasma enhance the free radical population via hydrogen abstraction. Experiments with the tail flame section of a radio frequency discharge confirm the importance of radicals in plasma polymerization (11) Emission spectra of benzene, halo benzenes, and toluene in R.F. discharges have been recorded (12-18). These spectra indicate the presence of phenyl, methyl, and benzyl radicals. From the evidence gathered to date, it appears that while any reactive species formed in a gaseous

plasma can contribute to polymer formation, a free radical mechanism is dominant at high frequencies.

It is generally agreed that both homogeneous and heterogeneous reactions are involved in plasma polymerization, but the roles of each are not certain. Reaction schemes have been developed assuming various combinations of homogeneous and heterogeneous initiation, propagation, and termination (19). The effects of monomer pressure and electrode temperature indicate the importance of adsorption in film formation (20). An increase in the rate of film deposition occurs with a decrease in electrode temperature and, up to a certain limiting value, with an increase in monomer pressure. The increase in polymerization rate with pressure can be explained, in part, by the increase in monomer concentration, but the increased film formation rate with decreased electrode temperature is most easily explained by an increased adsorption of monomer and/or radicals.

Plasma polymerized materials can be produced in the form of a solid film, an oily film, or a powder. The type of product obtained is related to the polymerization rate and the relative extent of gas phase versus surface reactions. The product is usually a powder at low pressures and low flow rates, a rigid film at low pressures and high flow rates, and an oily film at high pressures and high flow rates. Conditions of high pressure and low flow rate tend to produce an unstable discharge. Figure 1 illustrates a "characteristic map." The exact form of this map varies with monomer, power and reactor configuration. The powder formation region generally is enlarged with increasing monomer

reactivity and with power, while the region of film formation decreases. The production of powder with long gas phase residence times indicates a predominance of gas phase reactions. Film formation with shorter residence times is probably the result of increased surface reaction.

The variables of importance in continuous wave plasma polymerization rates include:

1. monomer (M)
2. flow rate (Q)
3. system pressure (p)
4. power or field strength ($\bar{P}$ or E)
5. frequency (F)
6. electrode gap (d)

For hydrocarbons monomer reactivity increases with increased unsaturation. At very low flow rates the rate of polymer formation is limited by monomer supply. As flow is increased a maximum in the rate of polymerization (R_p) is reached and R_p becomes residence time limited. The pressure dependence of R_p also shows a maximum. As p is increased from a very low value R_p increases with monomer concentration and adsorption. Since in a plasma the electron energy increases with E/p, (21) at higher pressures the rate of polymerization decreases with decreasing electron energy. Frequency effects on R_p have been studied by Morita, et al. (22) in the region from 50 Hz to 13.56 MHz. R_p varies by an order of magnitude over this range with the maximum at 5 KHz and the minimum at 6 MHz. The report suggests a change in mechanism from ionic at low frequencies to free radical at

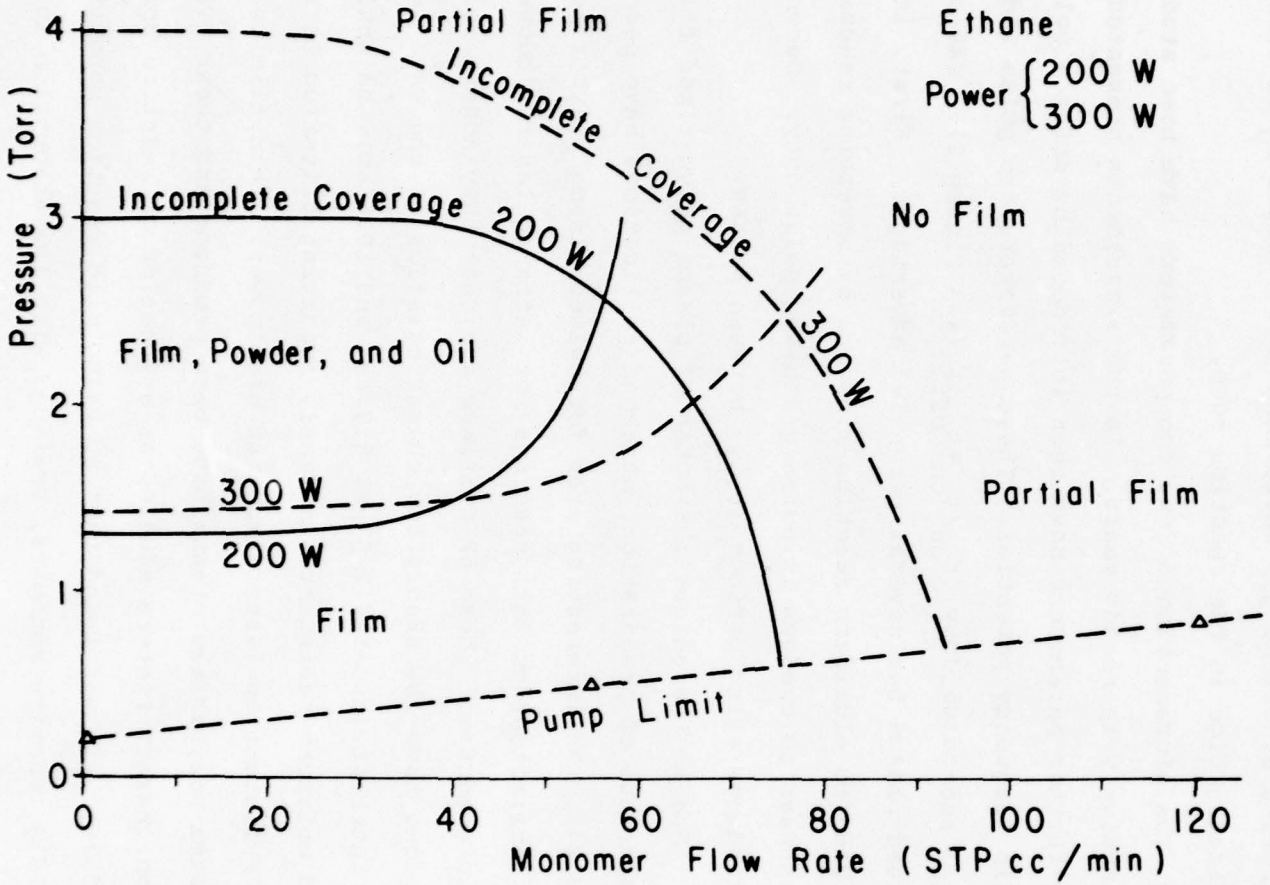
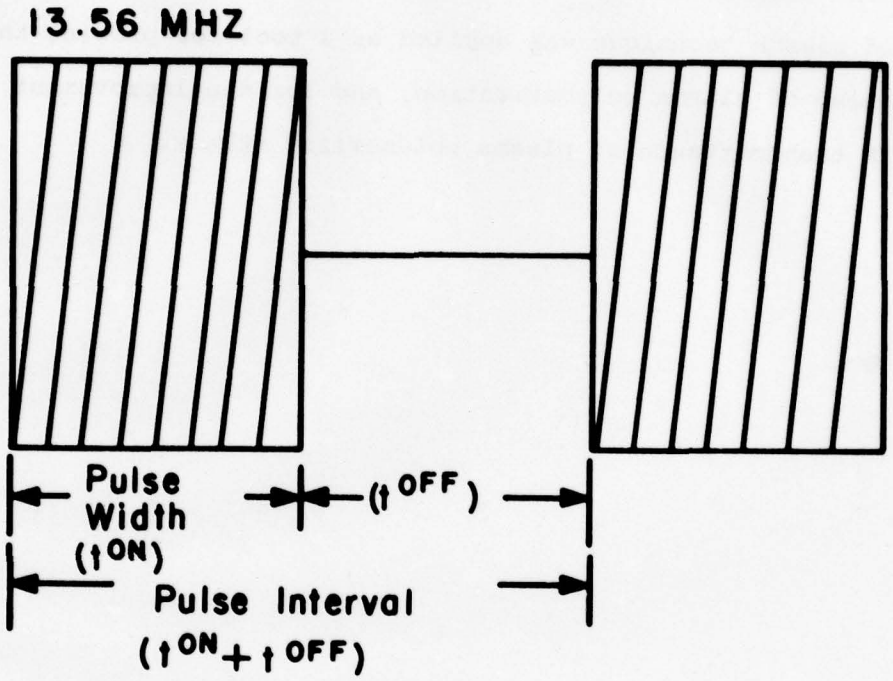


Figure 1. Characteristic Map.

high frequencies. Electrode gap is inversely proportional to power density (watts/cm^3) at constant delivered power. Thus a decreased electrode gap would lead to increased R_p at constant residence time in the reaction zone.

The aforementioned reaction parameters have been studied extensively in recent years. In the experiments presented here, two further parameters have been introduced by using a pulsed radio frequency potential. These parameters are pulse width (t_{on}) and pulse duty ($t_{on}/t_{on}+t_{off}$) (see Figure 2). Use of a pulsed plasma has several potential advantages. First, it can be used to elucidate reaction kinetics by observing reaction rate responses to changes in pulse width and pulse duty. Second, it introduces aging periods (t_{off}) between pulses.

Due to the unique character of plasma polymerized films and their ease of preparation, numerous applications have been proposed (23,24). An interesting area for pulsed plasma polymerization is an antireflection (AR) coatings for infrared laser windows. The requirements of these AR coatings are that they adhere well to the window, have low absorption characteristics at the wave lengths of interest (usually 2.5 μm, 5.9 μm, and 10.6 μm), be antireflective and moisture resistant. A final, important criterion is that they be resistant to laser damage at high power. Thin film coatings of plasma polymerized ethane have been produced and their I.R. absorption characteristics studied as a function of reaction conditions (25,26). It was found that by using mild reaction conditions and mildly reactive monomers, coatings with low absorption in much of the I.R. range can be produced. The refractive index of plasma



$$r = \frac{t^{OFF}}{t^{ON}}$$

$$\text{PULSE DUTY} = \frac{t^{ON}}{t^{ON} + t^{OFF}} = \frac{1}{r+1}$$

Figure 2. Definition of Pulse Variables.

polymerized ethane is 1.51 (at the sodium d line) (25) and therefore can, as a single layer AR coating, give zero reflectance only on a substrate with a refractive index of 2.28 (26).

The purpose of the research presented here is twofold. The pulsed plasma technique was applied as a tool for probing the mechanism of plasma polymerization, and for the improvement of the IR transmittance of plasma polymerized ethane.

II. APPARATUS AND EXPERIMENTAL METHODS

The films in this study were formed in a tubular flow reactor, shown schematically in Figure 3. The shell of this reactor is a glass tube 50 cm long with an 8 cm inside diameter. The end plates are lucite and are sealed with O-rings to the glass tube. All connections, including pressure gauge, electrode potential, electrode cooling, and monomer entrance and exit are made through the end plates. Two parallel plate electrodes, having exposed rectangular surfaces of 6.5 cm by 15 cm and a 3.5 cm gap between them, are located within the glass tube. These electrodes contain cooling coils for circulation of heat transfer fluids. Teflon inserts (see Figure 3) upstream and downstream of the electrodes create a smooth flow path across the electrodes and minimize boundary layer separation near the reaction zone. The electrodes are fixed to the teflon inserts, which are, in turn, fixed to the exit end plate. Thus, the entire electrode assembly can be pulled out for cleaning and sample retrieval. The lower electrode is grounded and cooled with water. The upper electrode is connected through an impedance matching network to a 13.56 MHz RF generator (Tegal Pulsed Plasma Generator). The RF generator can be operated in continuous wave (CW) or in pulsed mode.

C.P. grade monomer (Matheson Gas Prod.) was used as received in gas cylinders. The gas is fed through a pressure regulator at 5 psig to a glass float rotometer (Matheson Gas Prod., no. 610) and throtted with a micrometering valve (White & Co.). System pressure is measured with a McCleod gauge (Gilmont Instrument Co.)

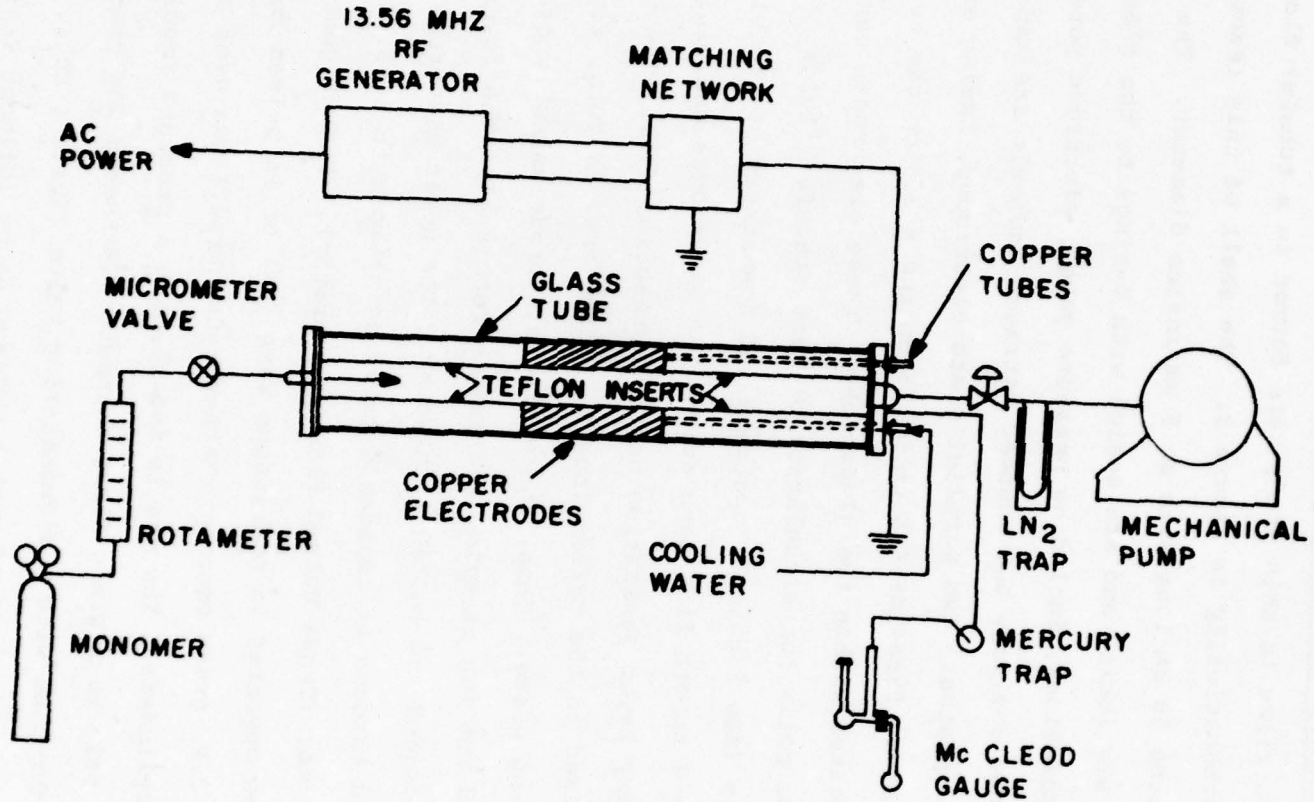


Figure 3. Tubular flow reactor schematic.

connected through the downstream end plate. Reactor pressure is maintained by an oil filled rotary vacuum pump (Kinney Model KC-5) which is protected by a liquid nitrogen cold trap.

For reaction rate measurements a ferrotype plate was cut into 6.5 cm x 6.5 cm squares. Prior to reactor assembly, this substrate is cleaned with acetone, weighed, and placed on the center of the lower electrode. The reactor is then assembled and the vacuum pump turned on. The system is flushed with monomer for 10 min. and monomer flow stopped. With no monomer flow the system is pumped down for one hour or until the pressure reaches 0.02 torr. When the system has been degassed, monomer flow is set to the desired rate and reactor pressure is adjusted to the operating level. Cooling water is introduced and the generator is allowed to warm up while the system equilibrates.

For continuous wave (CW) operation, after the system variables are steady, the RF power is turned on and set to the desired net power level (forward minus reflected power) with a watt meter (Bird Thruline 4314). The pressure must now be readjusted because of the change produced by the reaction (9). A glow can now be observed in the reaction zone where polymerization takes place. After a time long enough to negate startup effects or to gather several milligrams of polymer, whichever is longer, the generator is turned to standby. After allowing time for reaction intermediates to be pumped out, the monomer flow, vacuum pump, and cocling water are shut off. Air is allowed to enter the reactor until the pressure rises to atmospheric. The reactor is then disassembled and the substrate reweighed. The rate of

The rate of polymerization is determined and reported as mg/hr-cm^2.

For pulsed mode operation, prior to initiating the glow, the pulse width (t_{on}) and pulse interval ($t_{on}+t_{off}$) must be adjusted with an oscilloscope (Tektronix 531A). This can be done with the generator in the pulsed mode and in standby operation. Once the desired pulse variables are set, the glow is initiated in CW mode and net power set. Then the generator is switched to pulsed mode and the power read on the meter is maintained. The power shown on the meter is usually not proportional to the duty cycle (pulse width/pulse interval), because the power meter is designed for CW operation. While the reading on the meter does not give an accurate value for the delivered power, it can be used to maintain a steady valve in pulsed operation.

Samples for evaluation as antireflection (AR) coatings were made by placing the alkali halide crystal on the lower electrode. The crystals were recessed in copper electrode covers to avoid disturbance of the flow pattern. Potassium chloride crystals for IR analysis at this laboratory (Perkin-Elmer 467 Spectrophotometer) were obtained from Barnes Engineering and used as received. Alkali halide crystals were also obtained from Hughes Research Laboratory, Honeywell Systems and Research, and Honeywell Corporate Research Center. These substrates were coated with plasma polymerized ethane (PPE) and returned to the respective laboratory for evaluation by fourier transform IR spectroscopy and microcalorimetry. All samples produced were allowed to stand 12 hours in an ethylene atmosphere before exposure to air. This procedure

has been found to reduce the concentration of trapped free radicals in the polymer (27).

III. KINETICS AND MECHANISM OF PULSED PLASMA POLYMERIZATION

Prior to conducting pulsed plasma experiments, continuous wave studies were done with both ethane and ethylene. The purpose of these studies was to find a common set of reaction conditions under which solid films could be formed. In order to compare the effects of pulse variables on the plasma polymerization of saturated and unsaturated monomers, it was necessary to choose plasma conditions under which the monomer concentrations and the electron energies and densities are comparable. Equal pressures correspond to equal monomer concentrations. The initiation rate is related to electron energy and density, which are in turn related to the electromagnetic field strength divided by pressure (E/P). Since the ionization potentials for ethane and ethylene are similar (12.8 volts and 12.2 volts respectively), equal applied RF power would give similar electron densities and energies in plasmas of ethane and of ethylene. Thus, by using equal pressures and powers, comparable monomer concentrations and rates of initiation can be assumed.

In the Introduction to this work, the characteristic map for ethane in Figure 1 was discussed. It was stated that solid films are produced in the region of this map characterized by low pressure and high flow rate. For a given reactor configuration and applied power, the characteristic map for ethylene would be of similar form. Since ethylene is more reactive in plasma polymerization, the region of powder formation extends to higher pressures

and the region of film formation is more limited. It was found that with reaction conditions of 50 watts and 2.0 torr, good films could be formed at reasonable deposition rates with both ethane and ethylene by adjusting the flow rates to 20 cm^3/min and 83 cm^3/min respectively. Under these conditions, the conversion of ethane to polymer is 1.8%, at a rate of 0.14 mg/hr-cm^2. Ethylene conversion is 0.5% and the rate of deposition is 0.18 mg/hr-cm^2. Thus, similar products can be formed with ethane and ethylene at low conversions with equal powers and pressures.

It is also important that the effects of changing flow rate, pressure, and power be similar for the two monomers. As mentioned before, R_p increases with increasing flow rate or pressure at low values of flow rate and pressure, but is a decreasing function of each at high values of flow rate and pressure. As the applied power is increased from a very low value, R_p is a strong function of power but at high power densities it becomes roughly independent of power. Trends in R_p as a function of flow rate, pressure, and power are indications of rate controlling factors. These rate controlling factors should be the same for each system, so that the effects of pulse variables can be compared. The effects of changing flow rate, pressure, and power, independently, on the rate of plasma polymerization of ethane are shown respectively in Figures 4, 5 and 6. At the previously stated reaction conditions, R_p decreases with increasing flow rate and pressure. Thus, R_p is residence time controlled, as opposed to monomer supply controlled. Furthermore, it is electron energy limited, as opposed to monomer concentration limited. R_p is a strong function

of power in this range. The effects of CW variables on ethylene's rate of deposition are shown in Figures 7, 8 and 9 for flow rate, pressure, and power, respectively. The trends in R_p for changes in these three variables are similar to those of ethane. This indicates that the rate limiting factors are the same. This similarity is important in rendering it possible to compare the effects of pulsed plasma variables (pulse width and pulse duty) on polymerization rates of ethane and ethylene.

A. Review of the Intermittent Illumination Method for Photo Polymerization

The rate of plasma polymerization as a function of pulse width and pulse duty was studied in an attempt to gain a better understanding of the reaction mechanism. The basis for this attempt is found in the method of intermittent illumination for photochemical chain polymerization. This method was developed in 1926 (28) to determine the average lifetime of growing chains (τ_s) and has since been dealt with in several texts (29-32). This method is commonly referred to as the rotating sector technique, because in photo polymerization a rotating disk with a sector cut out is placed between the light source and the reaction vessel to pulse the light.

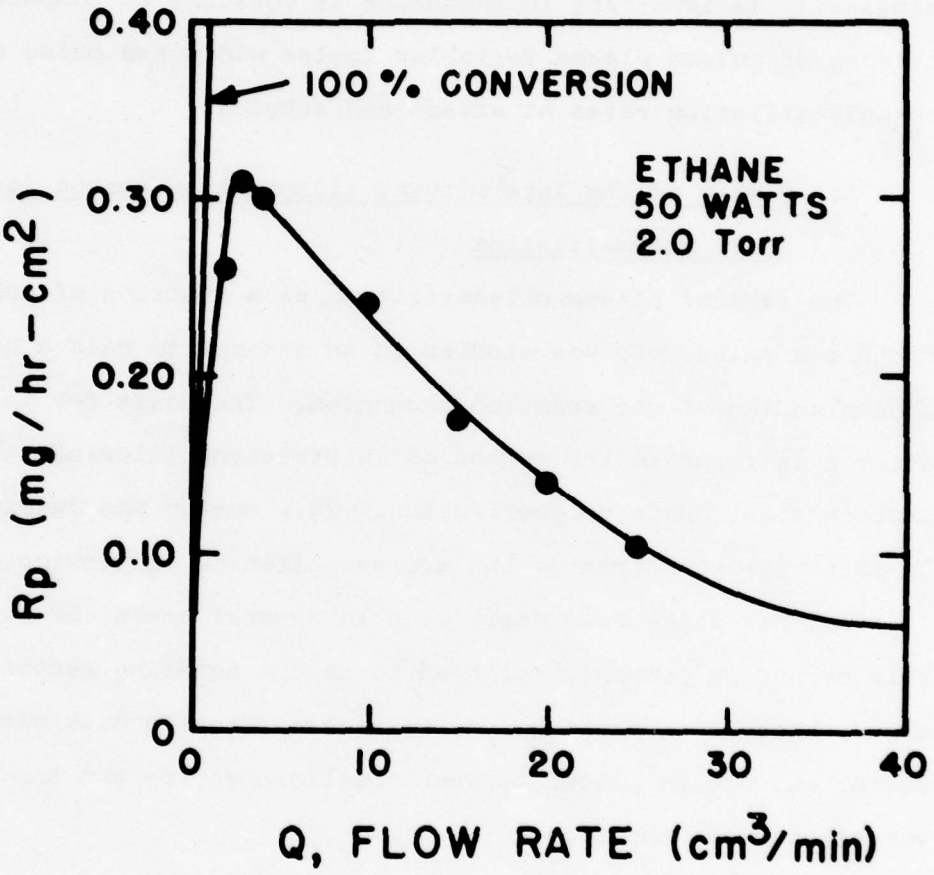


Figure 4. Effect of monomer flow rate on deposition rate of ethane.

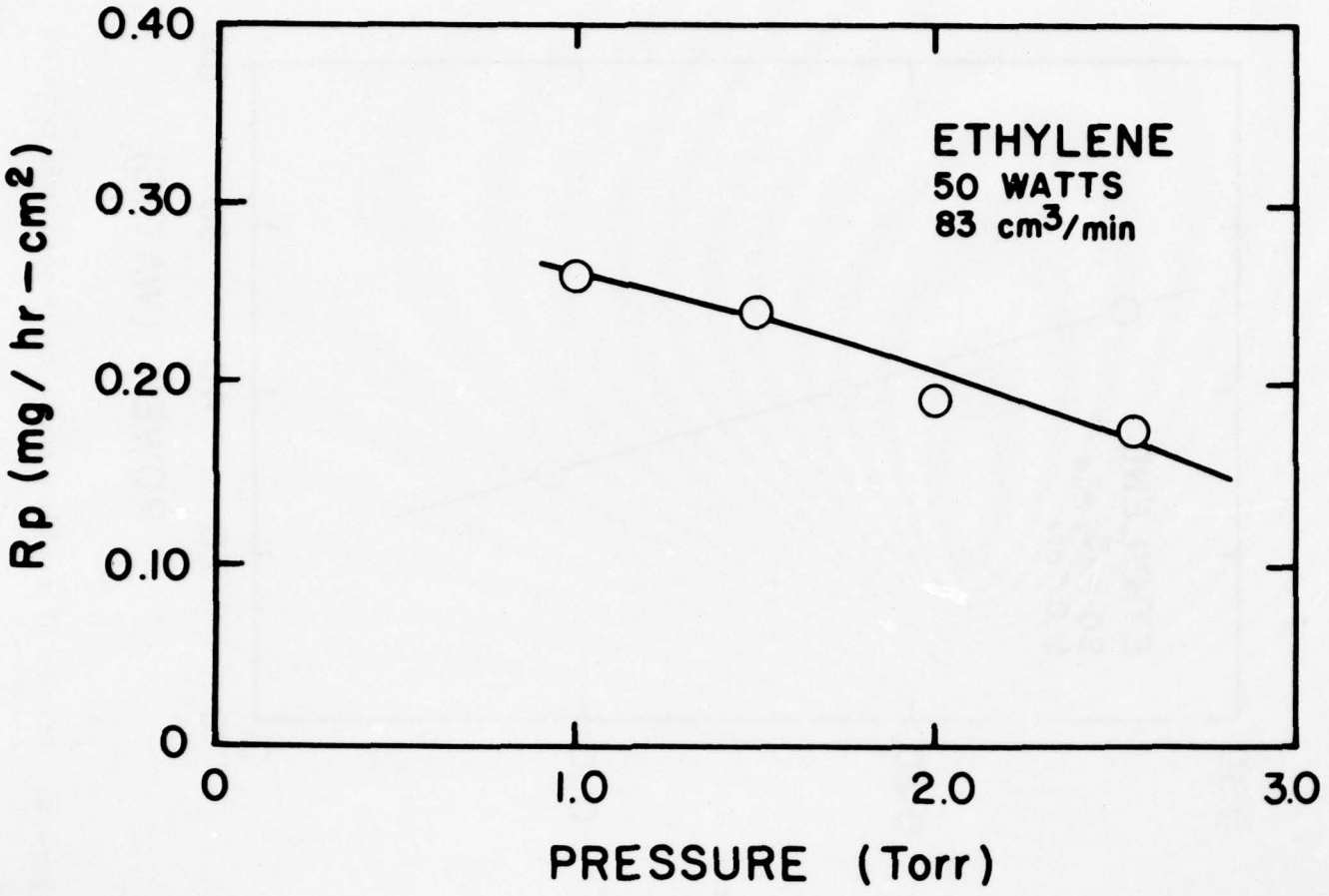


Figure 5. Effect of system pressure on deposition rate of ethane.

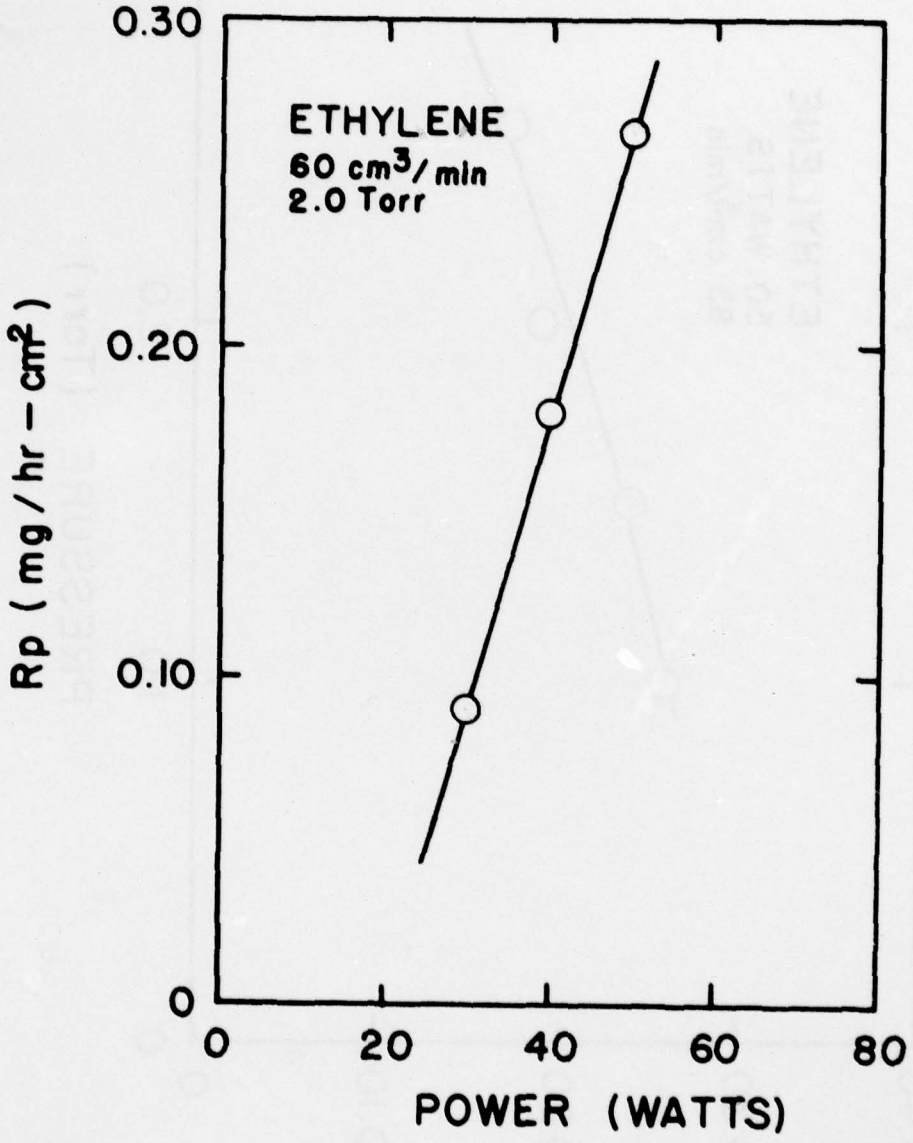


Figure 6. Effect of applied power on deposition rate of ethane.

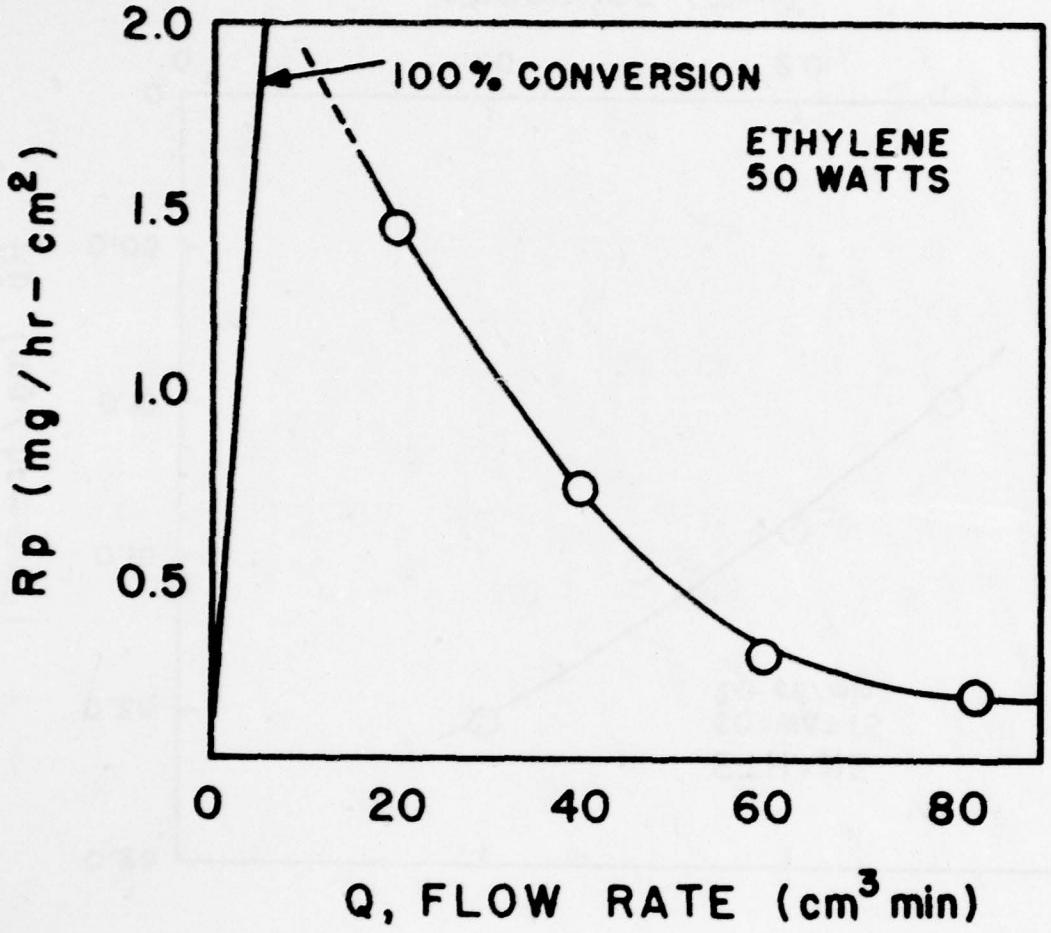


Figure 7. Effect of monomer flow rate on deposition rate of ethylene.

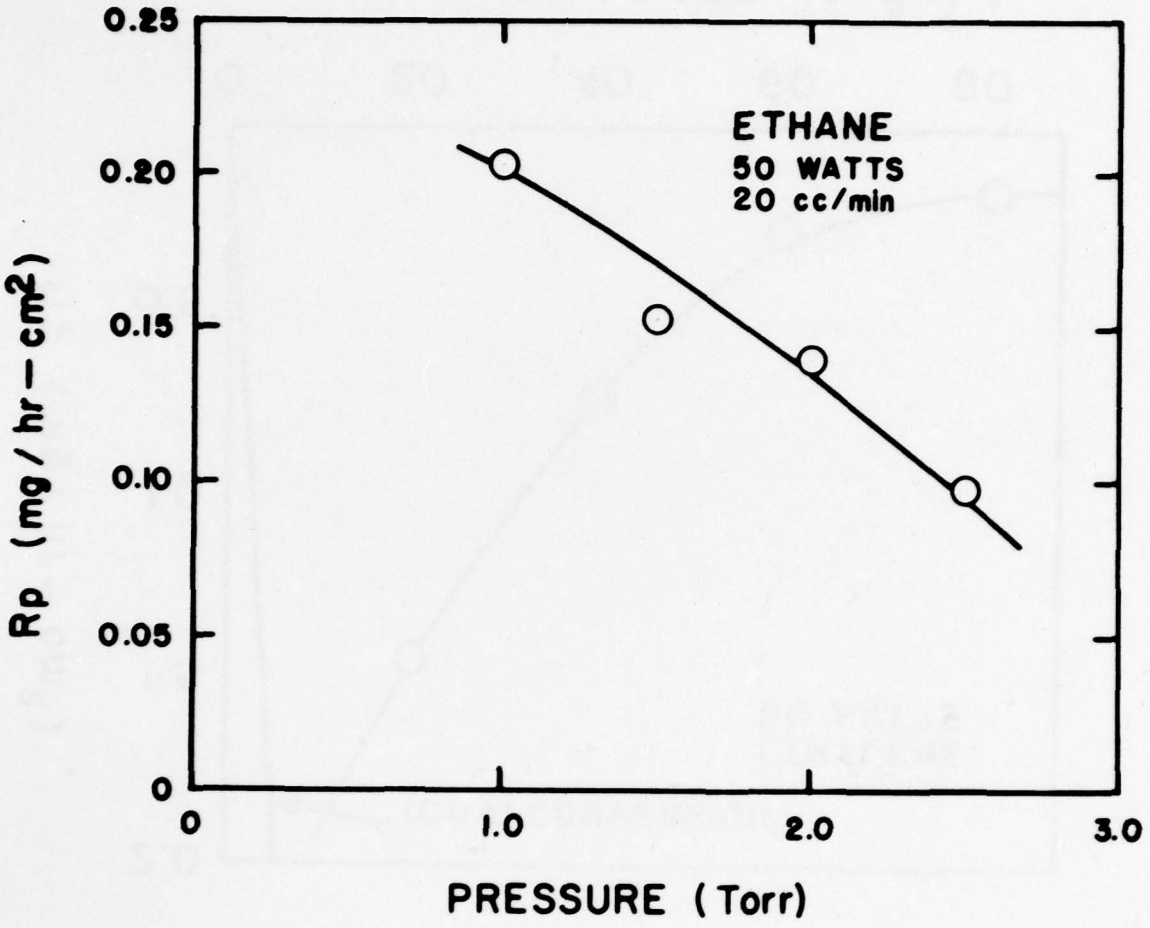


Figure 8. Effect of system pressure on deposition rate of ethylene.

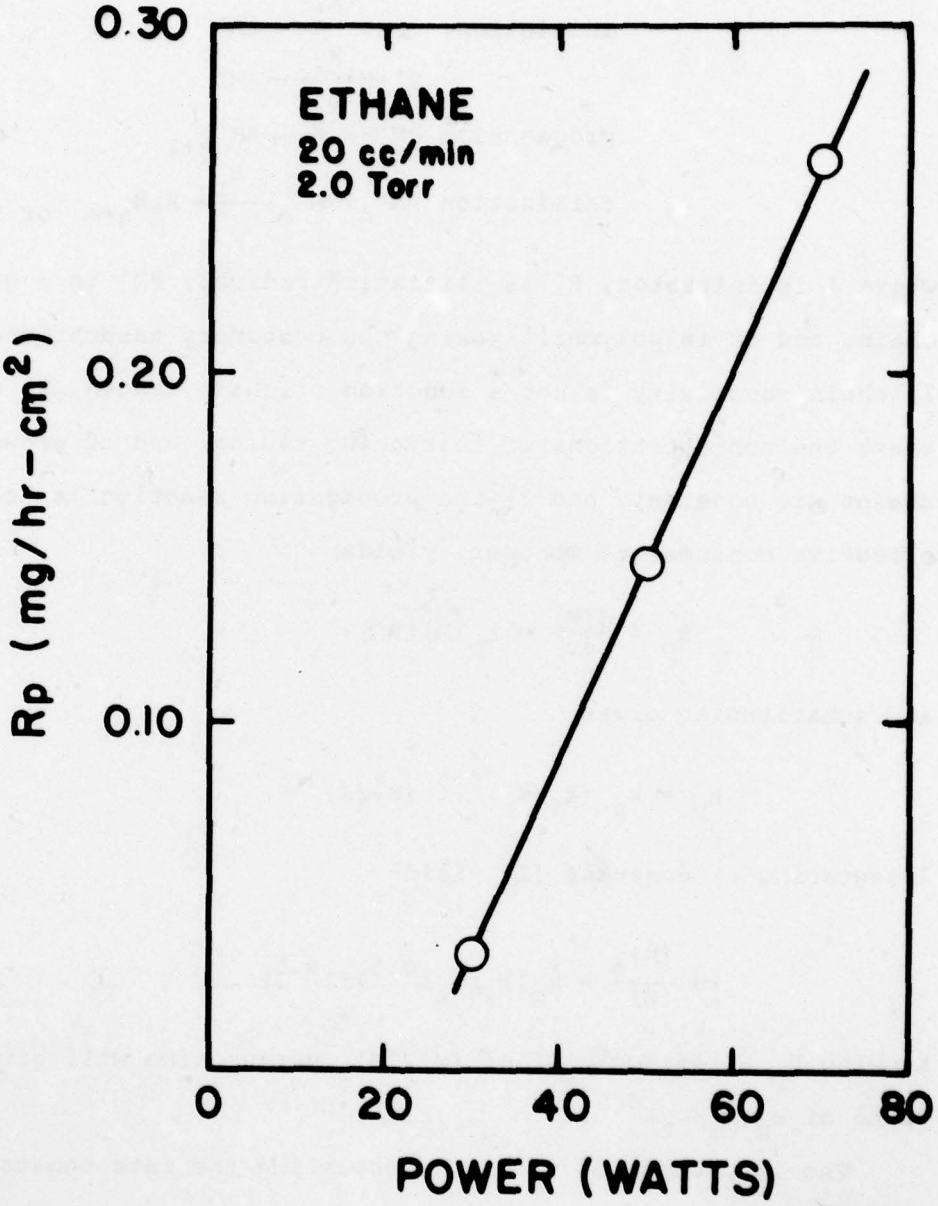


Figure 9. Effect of applied power on deposition rate of ethylene.

In photoinitiated polymerization the kinetics can be represented by

$$\text{initiation:} \quad I \xrightarrow{k_i} 2R^{\cdot}$$

$$R^{\cdot} + M \xrightarrow{k_2} RM^{\cdot}$$

$$\text{propagation} \quad RM^{\cdot}_x \xrightarrow{k_p} RM^{\cdot}_{x+1}$$

$$\text{termination} \quad RM^{\cdot}_n + RM^{\cdot}_m \xrightarrow{k_t} R_2M_{n+m} \quad \text{or} \quad RM_n + RM_m$$

where I is initiator, $R^{\cdot}$ is initiating radical, $RM^{\cdot}$ is a growing chain, and RM is polymer. Making the customary assumptions: 1) chain reactivity is not a function of chain length, 2) at steady state the concentrations of initiating radical and of growing chains are constant, and 3) the propagation reaction is the only effective consumer of monomer, yields

$$R_p \equiv \frac{d[M]}{dt} = k_p[M][R^{\cdot}]$$

and substituting gives

$$R_p = k_p \, (k_i/k_t)^{0.5} \, [M][I]^{0.5} \quad .$$

Integrating at constant [I] yields

$$\ell n \, \frac{[M]_o}{[M]} = k_p(k_i/k_t)^{0.5}[I]^{0.5}t \quad .$$

Knowing R_p a semilog plot of $[M]/[M]_o$ versus time will give the value of $k_p(k_i/k_t)^{0.5}$.

The importance of τ_s is in decoupling the rate constants. k_i can be estimated from nonpolymerization studies of initiator decomposition. τ_s is defined as the ratio of the concentration

of growing chains to their rate of termination. Thus,

$$\tau_s \equiv \frac{[R^\cdot]}{2k_t[R^\cdot]^2} = \frac{k_p[M]}{2k_t R_p}$$

With the above equation, the absolute value of the three rate constants can now be found.

In developing the theory of intermittent illumination three extreme cases can be considered. First, if the light is steady a steady state concentration of radicals is produced. If the production of radicals is proportional to the amount of light absorbed (I) times a quantum yield (ϕ) the net production of radicals is

$$\frac{d[R^\cdot]}{dr} = 2\phi I - 2k_t[R^\cdot]^2$$

and, since at steady state this is equal to zero,

$$[R^\cdot]_s = (\frac{\phi I}{k_t})^{0.5}$$

If the sector is now rotated slowly so that the steady state concentration of radicals is held long enough to ignore the growth and decay parts of the process, the average concentration of radicals is simply proportional to the fraction of time during which the system is illuminated, times the steady state value. The third extreme is very rapid rotation. In this case, negligible growth and decay of radical concentration can occur and the effect is the same as changing the intensity of light from I to $I/(1+r)$. This gives $\overline{[R^\cdot]} = [R^\cdot]_s/(1+r)^{0.5}$.

Since the rate of reaction is proportional to radical concentration, these extremes can be used to define the limits of the rate of polymerization divided by the rate under steady

illumination (R_p^o). R_p/R_p^o is equal to $(4+1)^{-1}$ at very high values of t_{on}/τ_s and to $(r+1)^{-0.5}$ at very low values of t_{on}/τ_s. The equations that describe the transition are developed by integrating the expressions for radical concentrations during the light and dark periods to give (29-33)

$$\frac{\overline{[R^\cdot]}}{[R\cdot]_s} = (r+1)^{-1}\ 1+m^{-1}\ \ell n\ 1 + \frac{rm}{1+\frac{[R^\cdot]_s}{[R^\cdot]_2}}$$

where

$$\frac{[R^\cdot]_2}{[R\cdot]_s} = \frac{(rm)\ \tanh m + \left\{(rm)^2\ \tanh^2 m + (rm+\tanh m)\ \tanh m\right\}^{0.5}}{2(rm+\tanh m)}$$

and

$$m \equiv t_{on}/\tau_s \quad .$$

This gives $\overline{[R\cdot]}/[R\cdot]_s = R_p/R_p^o$ as a function only of m and r. Figure 10 is a plot of R_p/R_p^o versus $\log t_{on}/\tau_s$ for r = 1.0 from these equations. In order to evaluate τ_s, experimental data are plotted in the same manner. The plots are overlaid to give the best fit of data to the theoretical curve and the experimental value of t_{on} that coincides with $t_{on}/\tau_s = 1.0$ is τ_s for the system.

B. Kinetics of Pulsed Plasma Polymerization

The process of plasma polymerization is considerably more complicated than photo polymerization, but the results can be described by a free radical chain polymerization mechanism (34). In light of this, the method of intermittent illumination can be expected to yield some information about the mechanism of polymer formation in radio frequency plasmas.

Figure 11 is the normalized deposition rate (R_p/R_p^o) of plasma

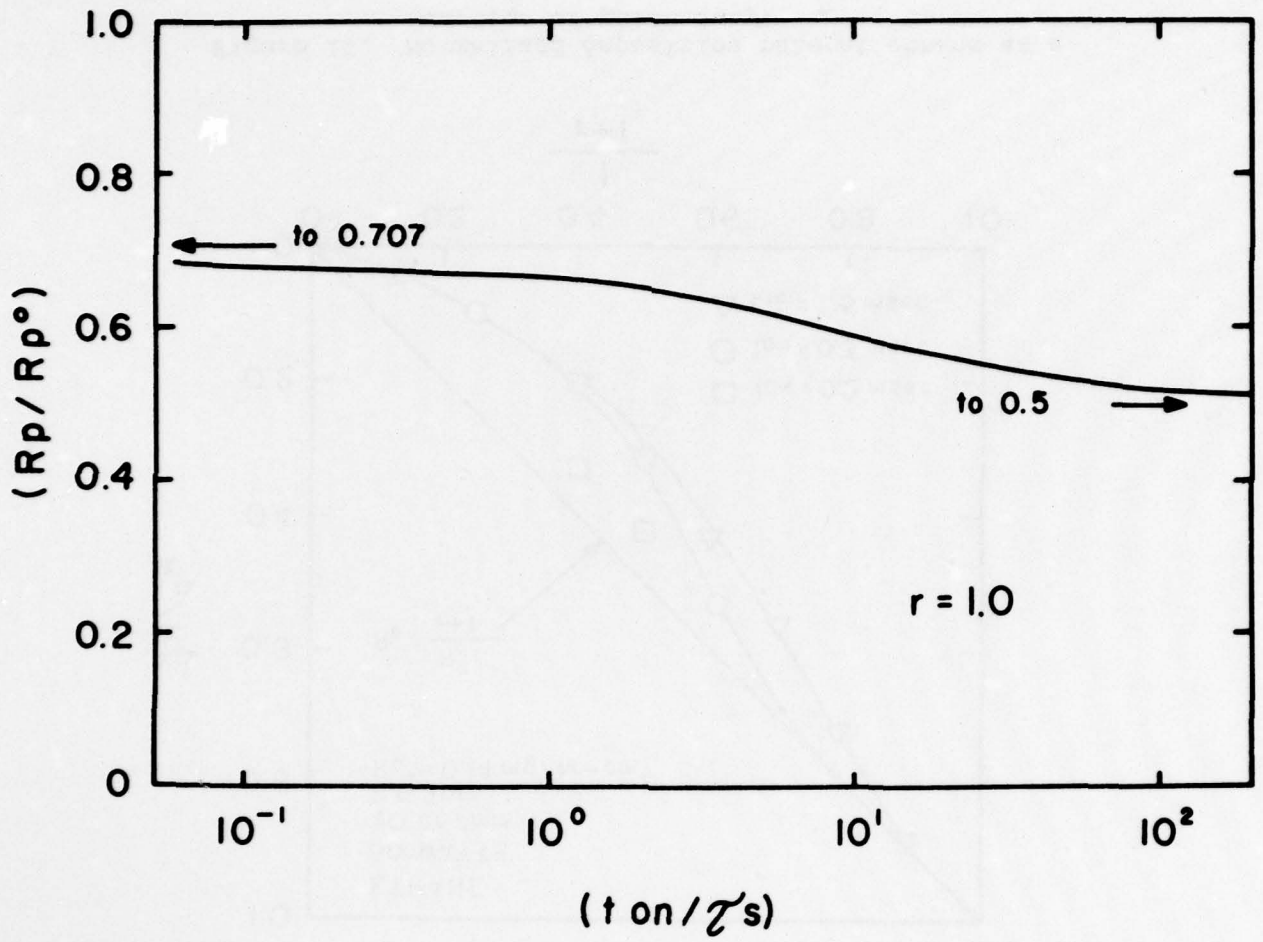


Figure 10. Theoretical dependence of polymerization rate on t_{on}.

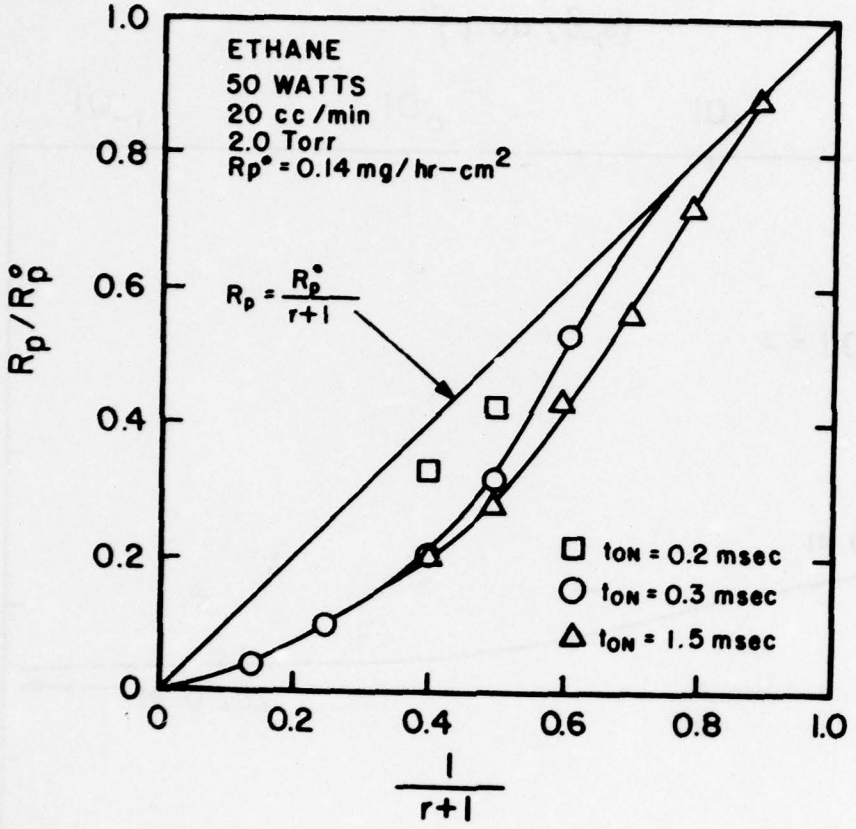


Figure 11. Normalized deposition rate of ethane as a function of pulse duty.

polymerized ethane as a function of pulse duty. The diagonal line represents the case of $R_p/R_p^o = 1/(r+1)$, the theoretical long t_{on} limit. In photo polymerization, the data would lie on or above this line. The data for plasma polymerization of ethane, however, all exhibit a negative deviation from theory. By comparing the measured values of R_p/R_p^o at long t_{on} ($t_{on} \geq 0.5$ msec) to the theoretical limit, Figure 12 was developed. This plot indicates that the negative deviation increases with decreasing duty cycle. The introduction of rest periods between pulses of initiator appears to have a net retarding effect on the rate of film formation.

Figure 13 shows the normalized rate of deposition as a function of log t_{on} with r = 1.0. A transition in R_p is seen to occur in the vicinity of t_{on} = 0.25 msec. The negative deviation can be noted in this figure at long t_{on}. Since 0.2 msec is the lower limit for the generator used in this work, it is not clear whether the short t_{on} limit has been reached. We know that $\tau_s \equiv k_p[M]/2k_t R_p$ for ideal chain polymerization. While plasma polymerization is not a simple chain reaction, similar trends in τ_s can still be expected. If the system pressure is increased to 2.5 torr, monomer concentration is increased and R_p^o is decreased to 0.11 mg/hr-cm^2. Thus, τ_s would be expected to increase.

The results of experiments with ethane at 2.5 torr to find R_p/R_p^o as a function of log t_{on} with r = 1 are presented in Figure 14. This figure shows that the transition is shifted from around 0.25 msec to 0.5 msec by a 0.5 torr increase in pressure. The magnitude of this shift is greater than expected, but it is in the anticipated direction . The long t_{on} value of R_p/R_p^o for both

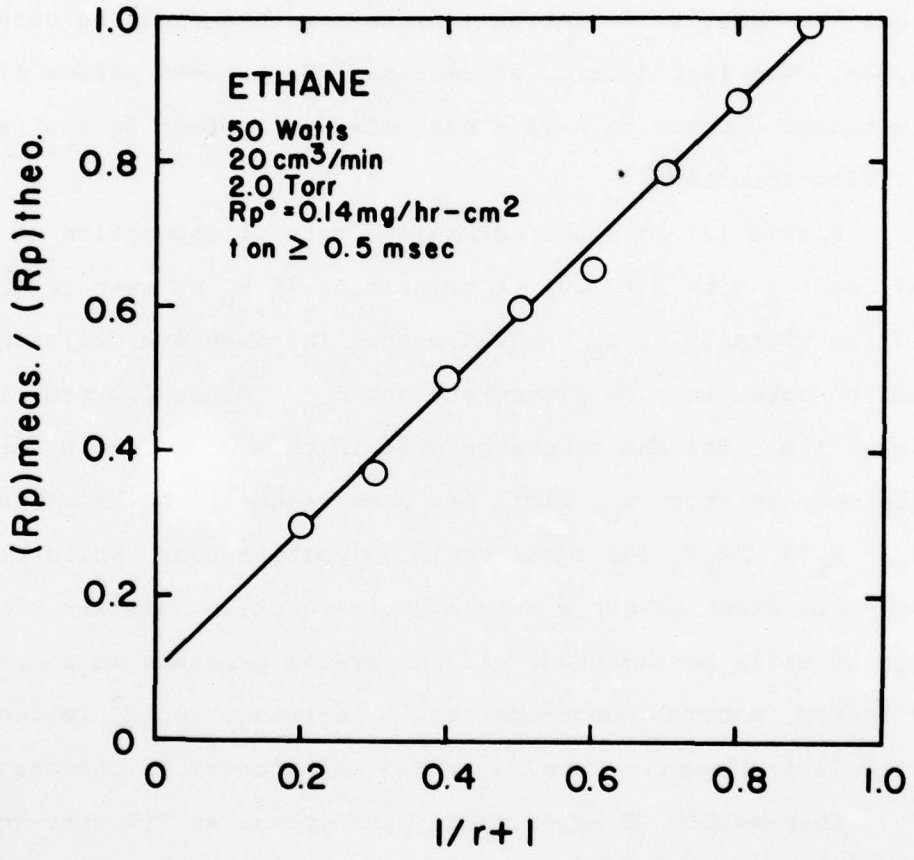


Figure 12. Deviation of R_p from theory as a function of pulse duty.

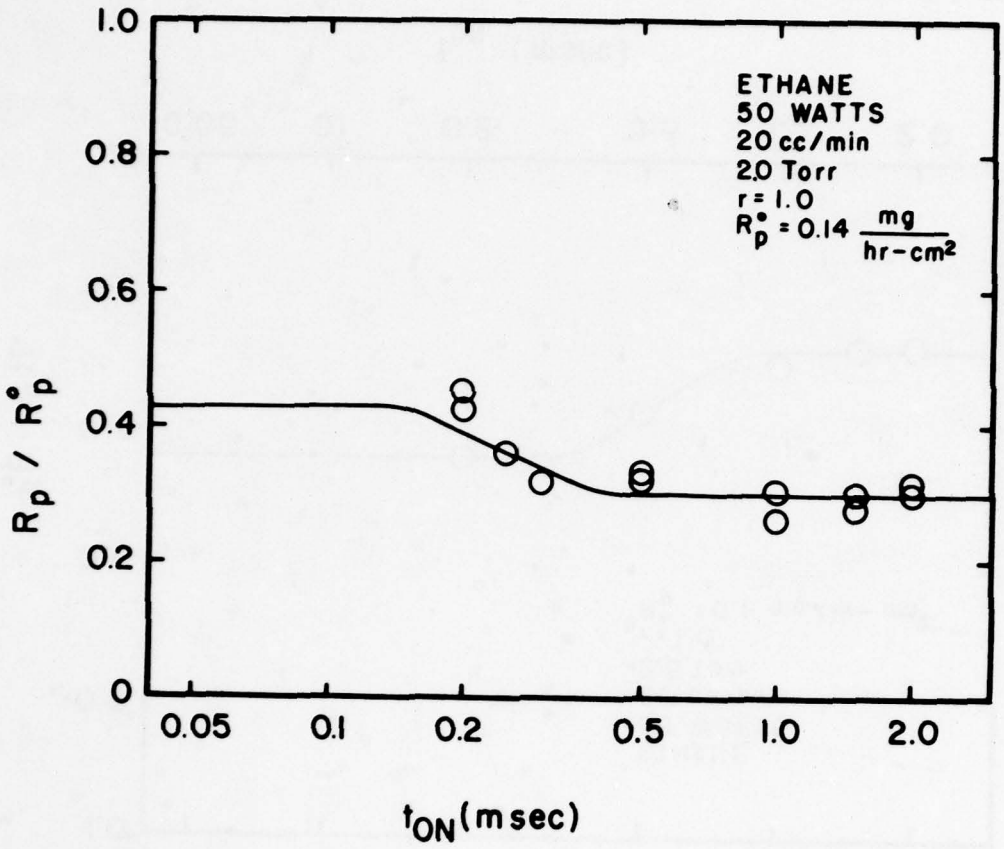


Figure 13. Normalized deposition rate of ethane at 2.0 torr as a function of t_{on}.

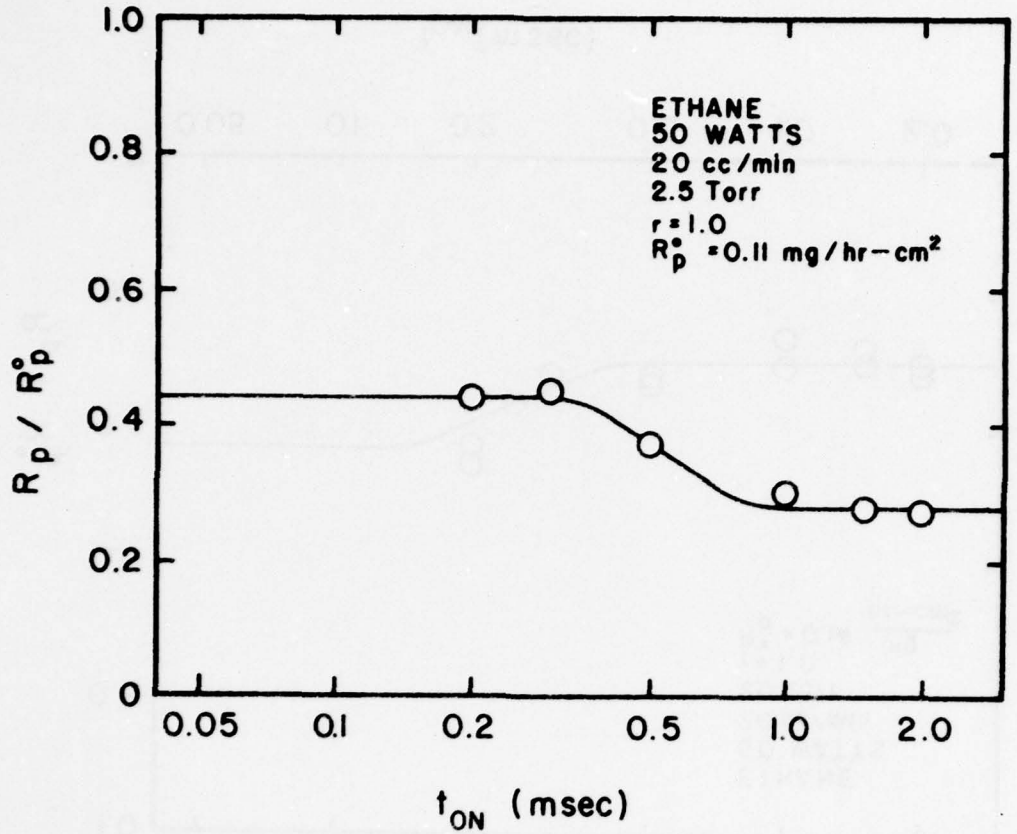


Figure 14. Normalized deposition rate of ethane at 2.5 torr as a function of t_{on}.

sets of experiments is near 0.30, and the short t_{on} value is near 0.42. The ratios of each of these extremes to the theoretical limit are approximately 0.6, indicating that the retardation is dependent only on pulse duty.

Figure 15 shows the effect of pulse duty on the deposition rate of plasma polymerized ethylene with t_{on} equal to 0.5 msec. These data exhibit a negative deviation similar to the long t_{on} data of ethane. Figure 16 is a plot of normalized deposition rate versus log t_{on} (r = 1.0) for ethylene. This figure shows that 0.5 msec can be considered a long t_{on} for this system. Comparison with ethane data in Figure 13 shows that the long and short t_{on} values of R_p/R_p^o are similar, and the transition occurs in the same region. Thus, even though the unsaturated monomer is much more reactive in the plasma system, it's characteristic time is the same as that for ethane under similar plasma conditions.

By comparing Figures 13, 14 and 16 to Figure 10, it can be seen that the transition in R_p/R_p^o for plasma polymerization is much sharper than would be expected for photo polymerization. This discrepancy and the previously described negative deviation are not surprising, considering the differences between the two systems. Intermittent illumination theory was developed for well defined, homogeneous, free radical chain polymerization. The plasma system contains other active species besides radicals, and is a mixture of homogeneous and heterogeneous reactions.

The process of plasma polymerization can be described as a molecular fragmentation and recombination rather than a straightforward chain polymerization. A general chain reaction scheme,

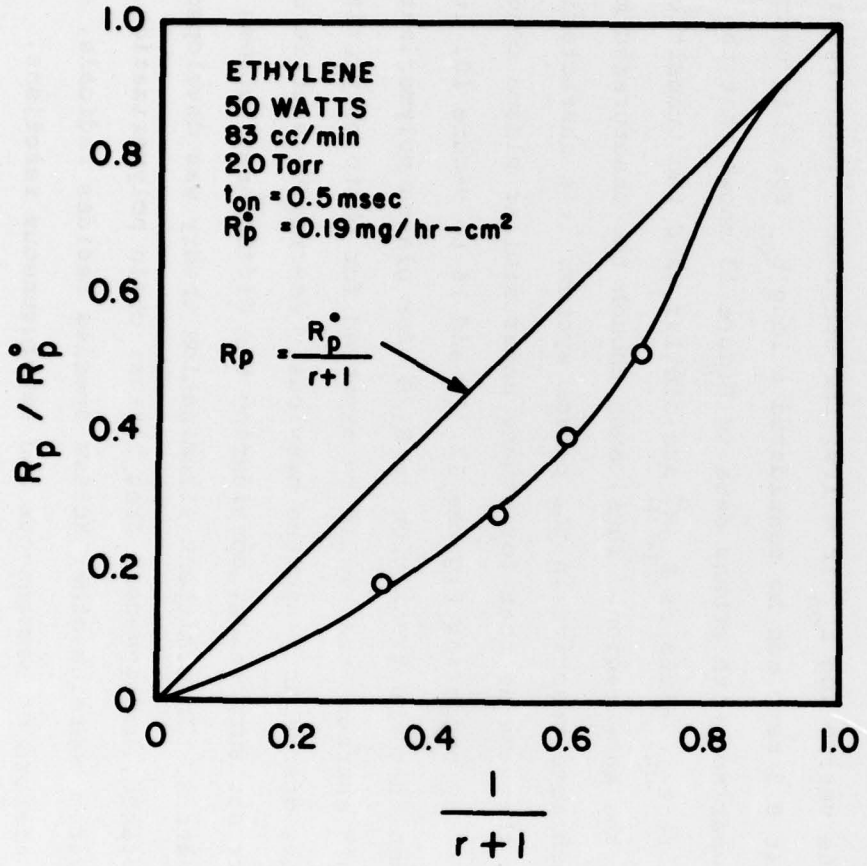


Figure 15. Normalized deposition rate of ethylene as a function of pulse duty.

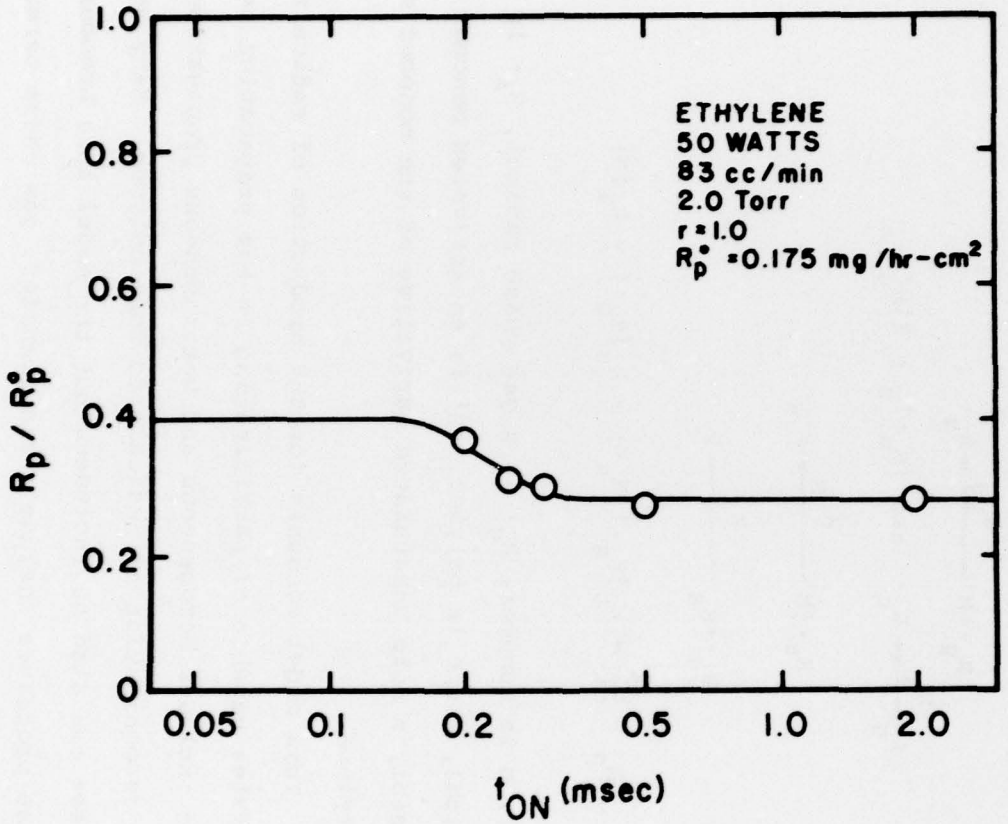


Figure 16. Normalized deposition rate of ethylene as a function of t_{on}.

while not rigorous, can be developed to describe the results of plasma polymerization. A simple version of such a model is

$$M \xrightarrow{k_i} 2\ R_g\cdot$$

$$M \xrightarrow{k_2} M'$$

$$R_g\cdot + M' \xrightarrow{k_{pg}} R_g\cdot$$

$$R_g \xrightarrow{k_a} R_s\cdot \quad \text{and} \quad [R_s\cdot]_s = K[R_g\cdot]_s$$

$$R_s\cdot + M' \xrightarrow{k_{ps}} R\cdot_s$$

$$R_g\cdot + R_s \xrightarrow{k_t} P$$

$$R_p \equiv \frac{dP}{dt} = k_t[R_g\cdot][R_s\cdot] = k_a[R_g\cdot] = k_i[M]$$

Here, M is monomer, $R_g\cdot$ is a gas phase radical, $R_s\cdot$ is a surface radical, and P is polymer. M' is an activated monomer molecule, possibly a more unsaturated derivative of the monomer such as acetylene.

This model accounts for the production of radicals and intermediates capable of participating in the propagation reaction. It also includes homogeneous and heterogeneous propagation reactions and recombination of radicals to form polymer. Many other processes can also be included, but the model then becomes unwieldly. These processes include chain transfer, gas phase termination, reinitiation of neutral species in the gas or on the surface, multiple initiations, ablation of radicals and polymer from the surface, and monomer adsorption.

In searching for an explanation of the net retarding effect of pulsing on plasma polymerization, reactions with retarding characteristics were included in the model. Degradative chain transfer can slow polymerization rates by forming resonance stabilized radicals. Gas phase termination could lead to the formation of dimers and other neutral species that are less reactive than the monomer. Ablation would cause a decrease in the final amount of polymer collected on the substrate. The retarding effects of impurities such as oxygen were also explored. However, none of these is capable of explaining the negative deviation without adjusting rate constants, because they are as apt to occur in CW as they are in pulsed plasma polymerization.

The major problem with these mechanisms is their failure to show that $[R\cdot]/[R\cdot]_s$ is not equal to $(r+1)^{-1}$ at very long pulse widths. This problem can be solved if it can be shown that the rate constants for ablation, chain transfer, and/or gas phase termination are increased during pulsed operation. An increase in these constants is not easily explainable. The negative deviation can also be explained by a decrease in the rate constants for initiation, propagation, heterogeneous termination, and/or adsorption.

Several possible reasons for such a reduction can be postulated. First, it is possible that by perturbing the system periodically with on-off cycles of RF, certain rate constants are affected (35). Widom (36) found that in systems where the reactants are not in equilibrium over their internal states, such as very rapid reactions, the rate constants are always lower than the equilibrium values.

Another possible source of deviations from theory is the difference in gas temperatures between pulsed and continuous wave operation. While no attempt was made to measure gas temperatures during this study, it was noted that under pulsed operation the reactor shell was cooler with decreasing duty cycle. This coincides with a decreasing ratio of measured deposition rate to predicted rate, with decreasing duty cycle. While adsorption was probably not affected because the electrode was water cooled, gas phase kinetic constants may have been affected. Since the effects of gas temperatures, independent of power, have not been studied, the effect on deposition rate is not known.

It was also noted that the glow in the reaction zone was much brighter within 3 or 4 mm of the electrode than in the bulk of the plasma. It is known that in DC plasmas most of the potential drop occurs near the cathode, in the vicinity of the negative glow. As the RF potential switches polarity, such an area of high voltage drop is set up alternately near each electrode. In these areas it is likely that the population of activated species is much higher than in the bulk. These layers of active species could disperse during the period between pulses and thus become less effective in film formation. This corresponds to a decrease in k_a.

One process that can explain the negative deviation without changing rate constants concerns the assumption that the growth and decay of radical concentration is very fast compared to long pulse widths. It is probable that the production and consumption of gas phase radicals is fast compared to long pulse widths, but

it is possible that the rise and fall of surface radical populations lags behind somewhat. Since $R_p = k_t[R\cdot_s][R\cdot_g]$ for this system a phase lag would cause the average product of $[R\cdot_s]$ and $[R\cdot_g]$ to be less than if they were in phase. This yields a net reduction in deposition rate without changing rate constants. Proof of this phenomenon requires further study.

Pulsed plasma provides another method of probing the phenomenon of plasma polymerization. The response of the reaction to changes in pulse variables is not altogether as expected, but nonetheless, well-behaved. The anomalies, on further inspection, may provide as much information about reaction mechanisms as the similarities to photo polymerization. Several routes of investigation into the deviations encountered have been suggested here, the most promising of which is probably the effect of gas temperature on deposition rates.

IV. PLASMA POLYMERIZED MATERIALS FOR ANTIREFLECTION COATINGS

The primary reasons for using antireflection coatings on infrared (IR) laser windows are to increase the total transmittance of the window and to protect the window from atmospheric damage. The requirements of these coatings are that they have low absorption at the wavelength of interest (usually 2.5 μm, 5.9 μm or 10.6 μm), good adherence to the window, be antireflective and moisture resistant. In the search for antireflection coatings for alkali halide IR laser windows plasma polymerized material represent a unique area of study. The vast majority of research is centered on inorganic materials (37). The applicability of plasma polymerized ethane as a material for AR coatings has been studied in this laboratory (25). Films of plasma polymerized ethane were found to adhere well to alkali halide windows and to provide reasonable moisture protection.

Figure 17 is a typical infrared spectrum of plasma polymerized ethane. The absorptions near 7 μm are due to C-H bending and wagging, and the absorption at 3.4 μm is due to C-H stretching in methyl and methylene groups. If the polymer was composed solely of saturated aliphatic chains the infrared absorption would be confined to these frequencies. Molecular fragmentation and isomerization in the plasma leads to the formation of multiple bonds and aromatic groups. These structures contribute to broad band absorptions in the regions of 5.0-6.2 μm, 10-11 μm and 14 μm. It has also been found that the large concentration of trapped free radicals formed in plasma polymerization oxidize rapidly on contact

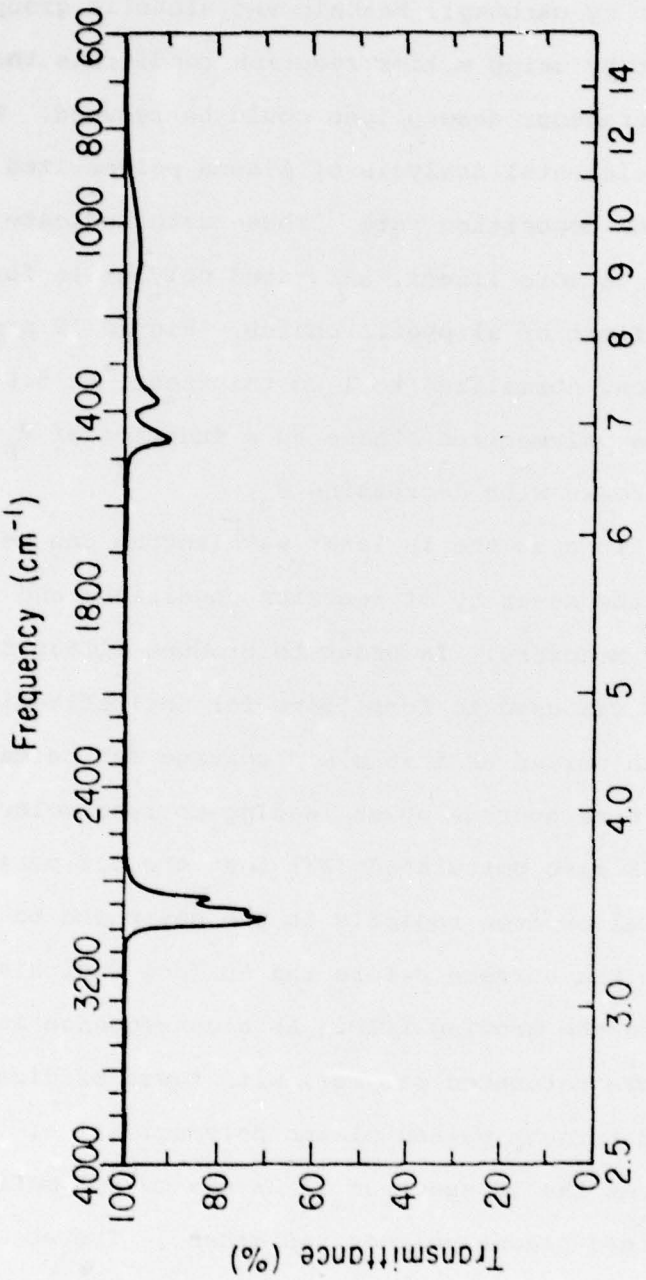


Figure 17. Infrared spectrum of plasma polymerized ethane.

with air. These sites lead to absorptions in the regions of 4-6.5 μm and 7.5-11 μm ny carboxyl, ketonic and alcholic groups.

It was found that by using milder reaction conditions the intensity of these extraneous absorptions could be reduced. Fig. 18 shows the results of elemental analysis of plasma polymerized ethane as a function of deposition rate. These data indicate that with decreased R_p a more linear, saturated polymer is formed, since H/C = 2 is the limit of aliphatic chains. Figure 19 presents the IR absorption, normalized to 1 μm thickness, at 5.9 μm and 10.6 μm for plasma polymerized ethane as a function of R_p. These absorptions decrease with decreasing R_p.

Thus, low absorptions at the IR laser wavelengths can be obtained by limiting the severity of reaction conditions and using mildly reactive monomers. In order to produce milder discharges pulsed plasma was used to form films for antireflection coating studies. With pulsed RF a stable discharge can be maintained at much lower time average power leading to less molecular rearrangement. It was also postulated (27) that the off periods between pulses would allow free radicals in the gas phase to combine with those on the surface before the surface radicals could be buried within the growing film. As a consequence it is expected that a more saturated polymer, with fewer oxidizable sites can be produced through pulsed plasma polymerization.

Figure 20 compares the IR spectrum of CW plasma polymerized ethane to that of pulsed plasma polymerized ethane. The absorption near 6 μm in the CW sample is due to C=C stretching. The absence of this peak in pulsed plasma polymerized sample is evidence of

decreased unsaturation. There is also decreased absorption in the ranges of 4-6 μm and 7.5-11 μm. Consistant with this are the results of elemental analysis as a function of pulse duty (Figure 21). As the duty cycle approaches zero the H/C ratio in the polymer approaches 2.0. This is the limit of linear, saturated chains.

Antireflection coatings range from single layer coatings limited to giving zero reflectance at one wavelength to multilayer systems having virtually zero reflectance over a range of wavelengths (38). A single layer coating is the simplest, both theoretically and experimentally.

In order to give zero reflectance the refractive index of the coating (n_1) must be the geometric mean of the refractive indices of the surrounding medium (n_o) and the substrate (n_s), i.e., $n_1^2 = n_o n_s$. The thickness of the film (d_1) must be equal to one quarter the wavelength of the incident beam or an odd multiple thereof. The deviation of these criteria is presented in detail in reference 28. Any material with a refractive index between that of the substrate and the incident medium will be antireflective but the minimum reflectance increases rapidly with deviation from the geometric mean.

Plasma polymerized ethane, with a refractive index of 1.51 (sodium d line) is antireflective for materials with refractive indices greater than 1.51 in air (n = 1.0). According to the geometric mean criterion, zero reflectance in air is possible for a window with a refractive index of 2.28 by applying a quarter wavelength layer of plasma polymerized ethane.

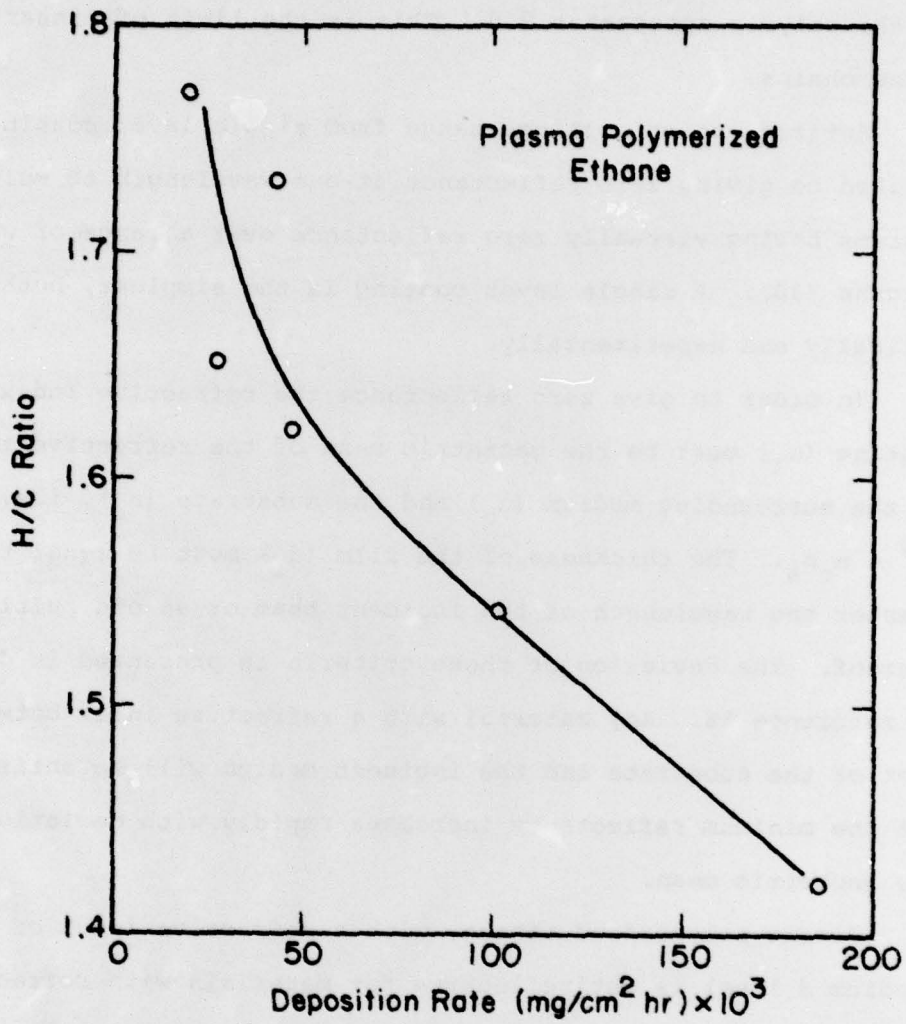


Figure 18. Hydrogen-carbon ratios in continuous wave plasma polymerized ethane.

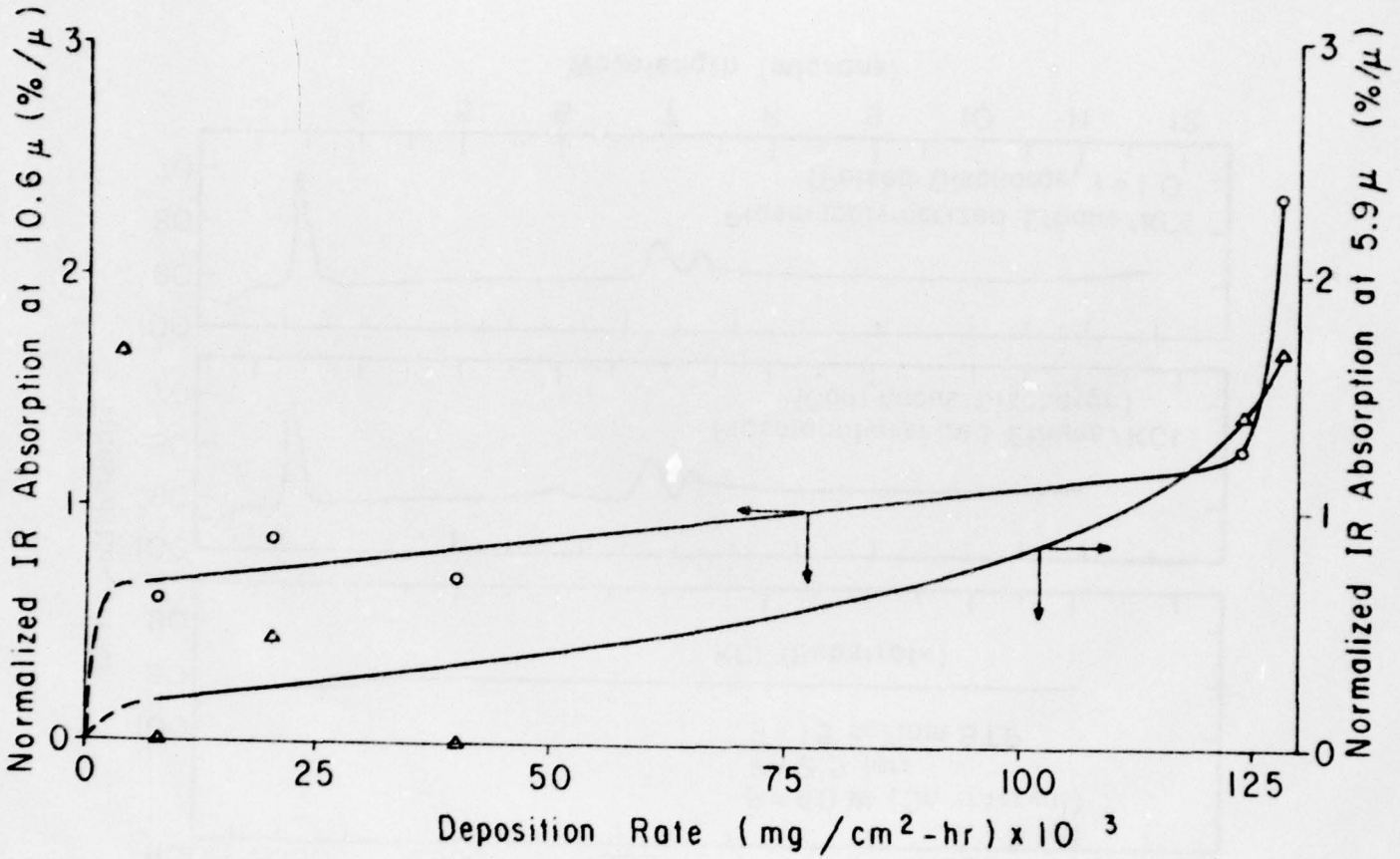


Figure 19. Enfrared absorptions at 10.6 μm and 5.9 μm in plasma polymerized ethane.

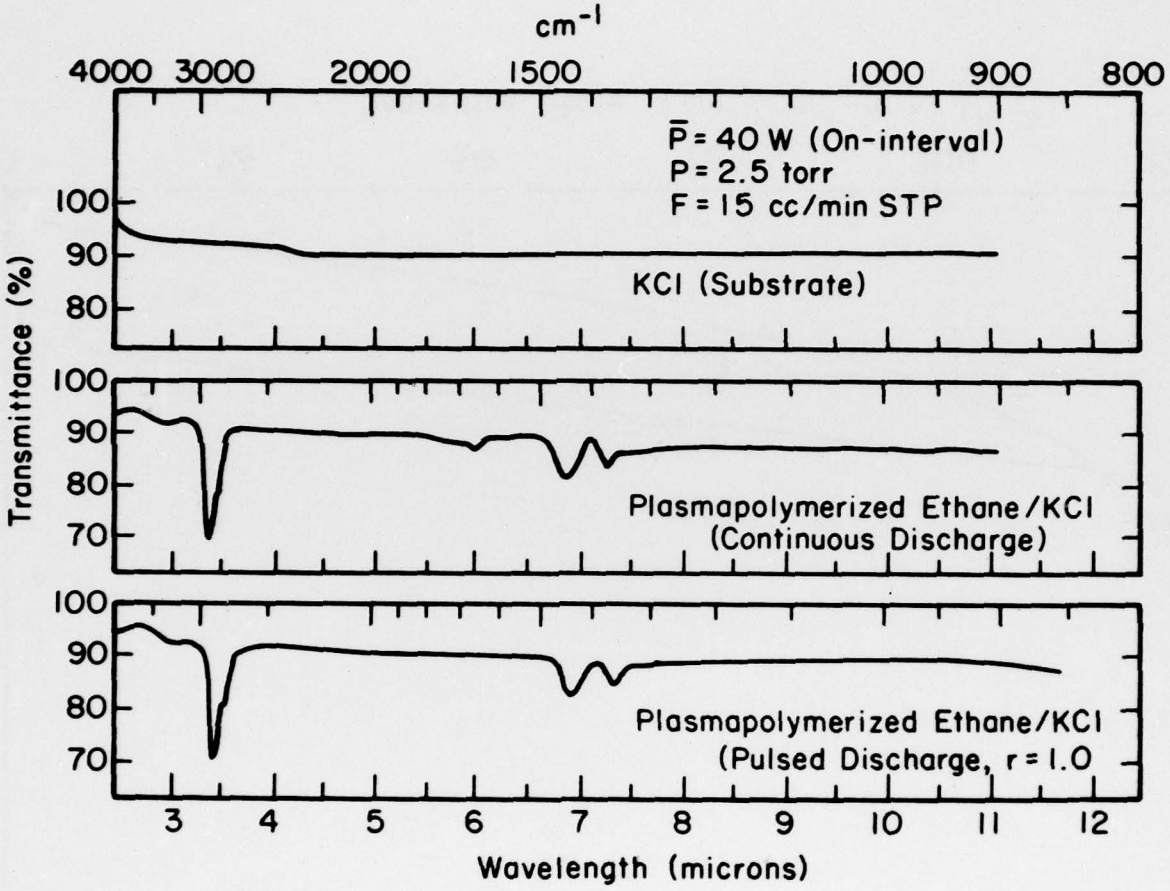


Figure 20. Effect of pulsed plasma on infrared spectra.

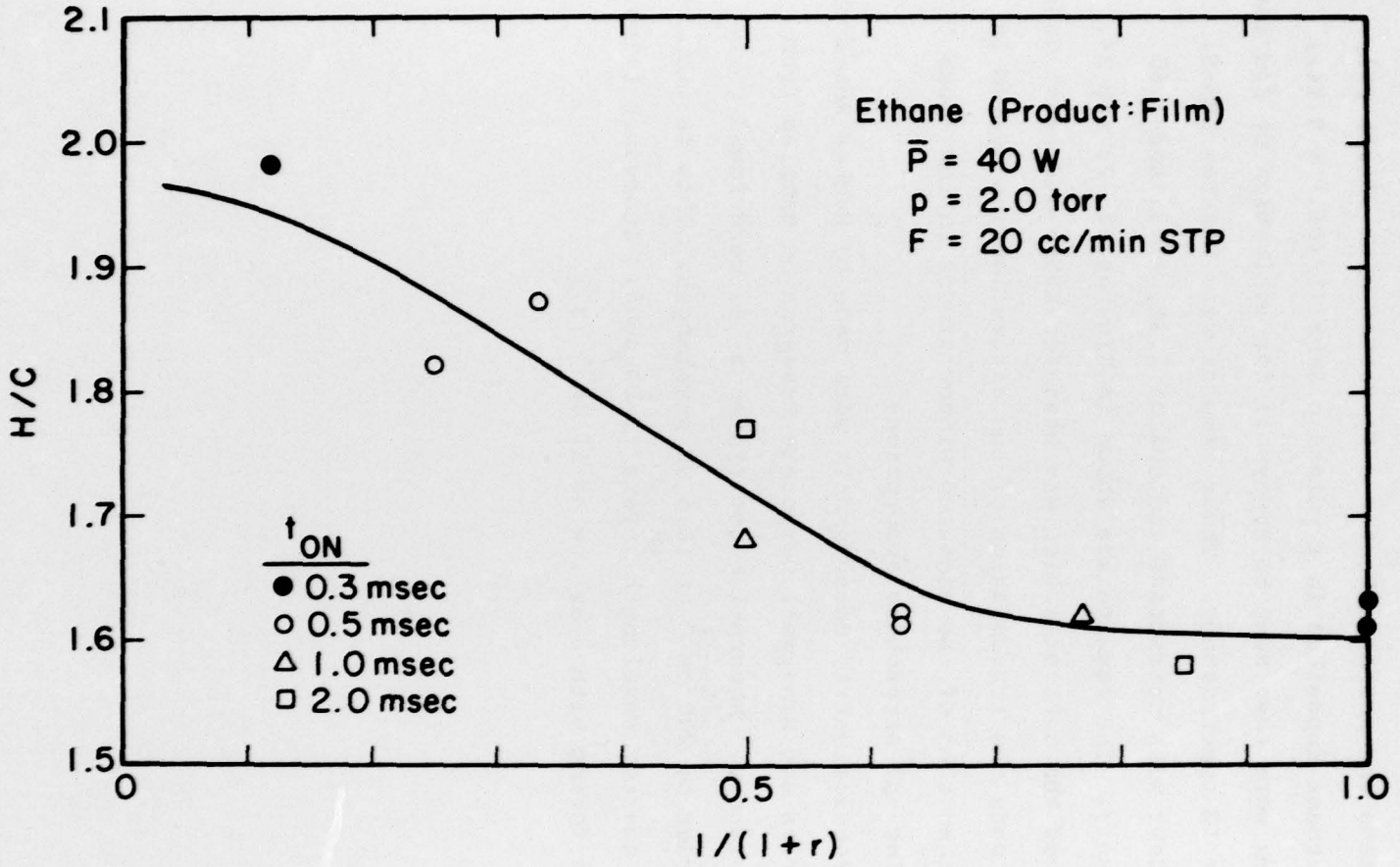


Figure 21. Hydrogen-carbon ratios in pulsed plasma polymerized ethane.

Samples of several alkali halide windows supplied by Honeywell Systems and Research Center were coated with plasma polymerized ethane deposited in a pulsed plasma ($1/(r+1) = 0.14$). This films were then sent to Honeywell for evaluation by fourier transform IR spectroscopy. These samples were Harshaw KRS-5, CsI and CsBr with refractive indices of 2.36, 1.73, and 1.65, respectively. The results are shown in Figures 22, 23 and 24. As expected the antireflection was best for KRS-5 and least CsBr. In every case the transmission of the antireflection system is greater than that of the uncoated window except in the areas of C-H bending and stretching absorptions .

Microcalorimetric measurements were made by Hughes Research Laboratories and Honeywell Corporate Research on samples from this laboratory. Absorption coefficients (β) were found to be on the order of 200 cm^{-1} at 10.6 μm wavelength. This is much too high for quarter wavelength layers to be used. Inorganic films have been formed with β as low as 10 cm^{-1} (37).

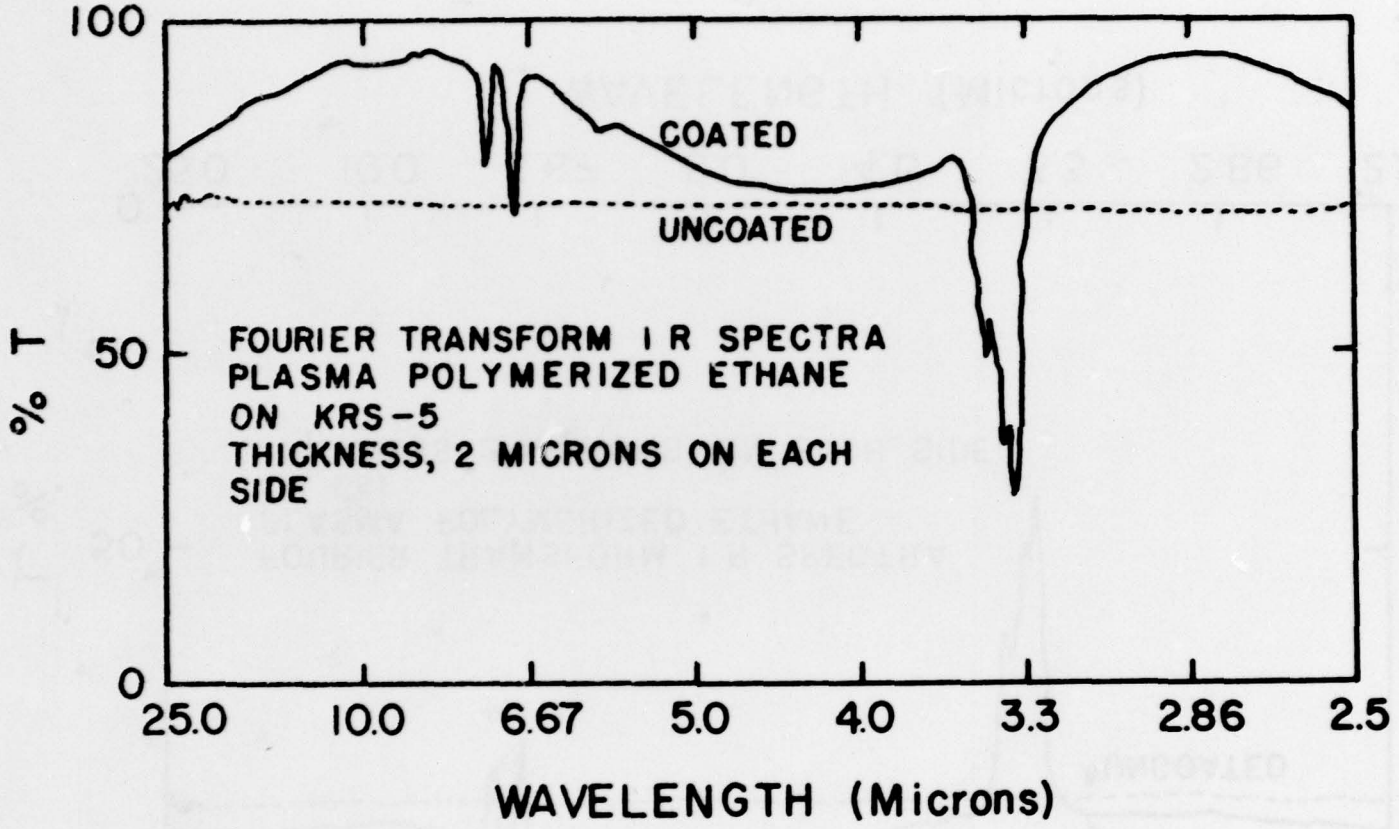


Figure 22. Fourier transform infrared spectrum of plasma polymerized ethane on KRS-5.

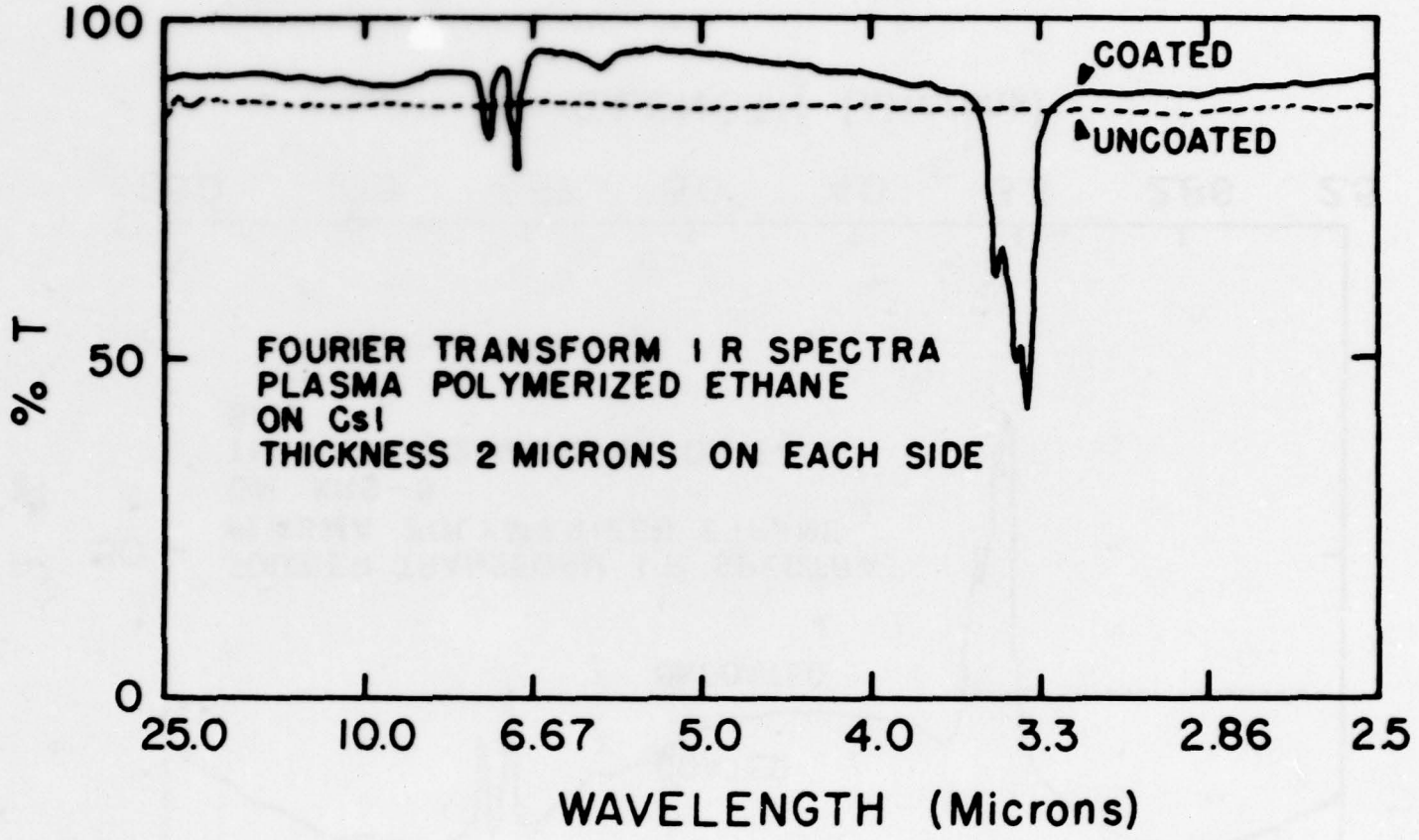


Figure 23. Fourier transform infrared spectrum of plasma polymerized ethane on CsI.

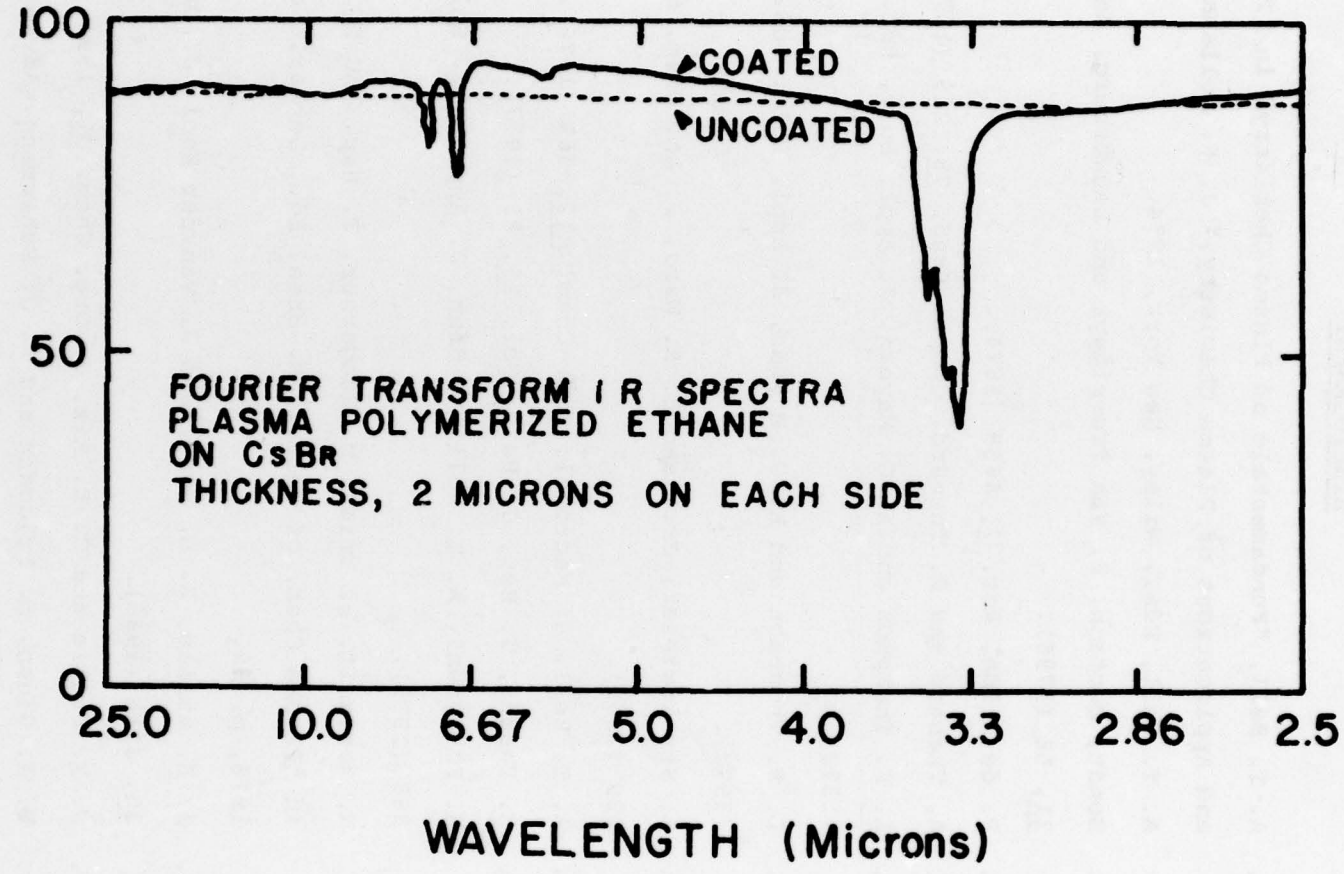


Figure 24. Fourier transform infrared spectrum of plasma polymerized ethane on CsBr.

BIBLIOGRAPHY

1. A. T. Bell, "Fundamentals of Plasma Chemistry" in "Techniques and Applications of Plasma Chemistry," J. R. Hollahan and A. T. Bell, Eds., Wiley, New York, 1974.
2. Bondt, Dermann, P. Van Troositwyk and Lauwerburg, Ann. Chim. 21, 58 (1796).
3. P. de Wilde, Ber. 7, 4658 (1874).
4. A. Thenard and P. Thenard, Compt. Rend. 78, 219 (1874).
5. L. F. Thompson and K. G. Mayhan, J. Appl. Poly. Sci. 16, 2317 (1972).
6. L. F. Thompson and K. G. Mayhan, J. Appl. Poly. Sci. 16, 2291 (1972).
7. A. Streitwieser, Jr., and H. R. Ward, J. Am. Chem. Soc. 85, 539 (1969).
8. A. T. Bell, J. Macromol. Sci.-Chem. A10, 369 (1976).
9. H. Yasuda, T. Hsu, J. Poly. Sci. 15, 81 (1977).
10. H. Kobayashi, A. T. Bell, M. Shen, J. App. Poly. Sci. 17, 885 (1973).
11. N. Morosoff, B. Crist, M. Bumgarner, T. Hsu, and H. Yasuda, in "Plasma Chem. of Poly.," M. Shen, Ed., Dekker, New York, 1976, p. 83.
12. J. K. Stille, R. L. Sung, and J. Van der Kooi, J. Org. Chem. 30, 3116 (1965).
13. J. K. Stille and C. E. Rix, J. Org. Chem. 31, 1591 (1966).
14. F. J. Dinan, S. Fridmann and P. J. Schirmann, Advan. Chem. Ser. 80, 289 (1969).
15. H. Sculer and M. Stockburger, Spectrochim. Acta 13, 841 (1959).

16. S. Walker and R. F. Barrow, Trans. Faraday Soc. 50, 541 (1954).

17. S. Walker and T. F. Bindley, Trans. Faraday Soc. 58, 217 (1962).

18. S. Walker, T. F. Bindley and A. T. Watts, Trans. Faraday Soc. 58, 849 (1962).

19. D. K. Lam, R. F. Baddour, and A. F. Stancell, in "Plasma Chem. of Polymers," M. Shen, Ed., Dekker, New York, 1976, p. 53.

20. T. Williams and M. W. Hayes, Nature 216, 614 (1967).

21. E. Nasser, "Fundamentals of Gaseous Ionization and Plasma Electronics," Wiley, New York, 1971, p. 191.

22. S. Morita, M. Shen and A. T. Bell, to be published in J. Appl. Poly. Sci.

23. J. M. Tibbitt, Ph.D. Thesis, University of California, Berkeley, California (1976).

24. P. V. Hinman, M.S. Thesis, University of California, Berkeley, California (1977).

25. T. A. Reis, H. Hiratsuka, A. T. Bell and M. Shen, NBS Special Publication No. 462, Washington, D.C., 1976, p. 230.

26. T. A. Reis, M.S. Thesis, University of California, Berkeley, California (1976).

27. H. Hiratsuka, J. W. Vinzant, A. T. Bell and M. Shen, "Proceedings of the High Power Laser Optical Components and Components Materials Meeting," Defense Advanced Research Projects Agency, Arlington, Virginia, 1977, p. 420.

28. D. L. Chapman, F. Briers and E. Walters, J. Chem. Soc. 129, 562 (1926).

29. G. M. Burnett, "Mechanism of Polymer Reactions," Interscience, New York, 1954.

30. W. A. Noyes and P. A. Leighton, "The Photochemistry of Gases," Reinhold Publishing, New York, 1941.

31. P. J. Flory, "Principles of Polymer Chemistry," Cornell University Press, Ithaca, New York, 1953.

32. F. Rodriguez, "Principles of Polymer Chemistry," McGraw-Hill New York, 1970.

33. M. Matheson, E. Auer, E. Bevilacqua and E. Hart, J. Am. Chem. Soc. 71, 497 (1949).

34. J. M. Tibbitt, R. Jenson, A. T. Bell, M. Shen, Macromolecules, 10, 647 (1977).

35. L. Polak, "Some Principles of Nonequilibrium Plasma-Chemical Reaction Kinetics," in "Reactions Under Plasma Conditions," M. Venugopalan, Ed., Wiley, New York, 1971.

36. B. Widom, J. Chem. Phys. 34, 2050 (1961).

37. M. Braunstein, A. I. Braunstein and J. Rudisill, "Conference on High Power Infrared Laser Window Materials," 2, Airforce Cambridge Research Labs. Bedford, Massachusetts, 1972, p. 777.

MISSION
of
Rome Air Development Center

RADC plans and executes research, development, test and selected acquisition programs in support of Command, Control Communications and Intelligence (C^3I) activities. Technical and engineering support within areas of technical competence is provided to ESD Program Offices (POs) and other ESD elements. The principal technical mission areas are communications, electromagnetic guidance and control, surveillance of ground and aerospace objects, intelligence data collection and handling, information system technology, ionospheric propagation, solid state sciences, microwave physics and electronic reliability, maintainability and compatibility.

Printed by
United States Air Force
Hanscom AFB, Mass. 01731